AGU PUBLICATIONS

Tectonics

RESEARCH ARTICLE

10.1002/2016TC004190

Key Points:
- Inner and Outer Carpathian domains have been balanced and restored
- Interplay between thick- and thin-skinned thrusting
- The Pieniny Unit was deposited in the Inner Carpathian foredeep basin

Correspondence to:
A. Castelluccio,
adacastelluccio@yahoo.it

Citation:
Castelluccio, A., S. Mazzoli, B. Andreucci, L. Jankowski, R. Szaniawski, and M. Zattin (2016), Building and exhumation of the Western Carpathians: New constraints from sequentially restored, balanced cross sections integrated with low-temperature thermochronometry, *Tectonics*, *35*, 2698–2733, doi:10.1002/2016TC004190.

Received 24 MAR 2016
Accepted 17 OCT 2016
Accepted article online 21 OCT 2016
Published online 26 NOV 2016

Building and exhumation of the Western Carpathians: New constraints from sequentially restored, balanced cross sections integrated with low-temperature thermochronometry

Ada Castelluccio[1], Stefano Mazzoli[2], Benedetta Andreucci[1], Leszek Jankowski[3], Rafał Szaniawski[4], and Massimiliano Zattin[1]

[1]Department of Geosciences, University of Padua, Padua, Italy, [2]Department of Earth Sciences, University of Naples "Federico II", Naples, Italy, [3]Polish Geological Institute-Carpathian Branch, Cracow, Poland, [4]Institute of Geophysics, Polish Academy of Science, Warsaw, Poland

Abstract Western Carpathian orogeny has been the subject of intense scientific debate due to the occurrence of enigmatic features, leading several authors to provide contrasting geological models. In this paper, a new interpretation for the tectonic evolution of the Western Carpathians is provided based on the following: (i) an analysis of the stratigraphy of the Mesozoic-Tertiary successions across the thrust belt domains, (ii) a reappraisal of the stratigraphy and sedimentology of the "tectonic mélange" (i.e., the so-called Pieniny Klippen Belt) marking the suture between the Inner and Outer Carpathians, and (iii) the construction of a series of balanced and restored cross sections, validated by 2-D forward modeling. Our analysis provides a robust correlation of the stratigraphy from the Outer to the Inner Carpathians, independently of the occurrence of oceanic lithosphere in the area, and allows for the reinterpretation of the tectonic relationships among the Inner Carpathians, the Outer Carpathians, and the Pieniny Klippen Belt and the exhumation mechanisms affecting this orogenic belt. In order to constrain the evolution during the last 20 Ma, our model also integrates previously published and new apatite fission track and apatite (U-Th-Sm)/He data. These latter indicate a middle-late Miocene exhumation of the Pieniny Klippen Belt. In this study, the recent regional uplift of the Pieniny Klippen Belt is described for the first time using a 2-D kinematic model for the tectonic evolution of the Western Carpathians.

1. Introduction

The development of arcuate mountain belts and associated back-arc basins in the Mediterranean-Carpathian area has been generally associated with the process of rollback of subducting oceanic lithosphere and trench retreat [e.g., *Maliverno and Ryan*, 1986; *Faccenna et al.*, 2004]. This process has led to seafloor spreading in, e.g., the Aegean back-arc basin, which developed since the early Miocene in the hinterland of the Hellenic orogen [e.g., *Jolivet*, 2001; *Meijer and Wortel*, 1997; *McClusky et al.*, 2000]. Ophiolite suites—including blueschist facies, metabasites, and metasediments—are well exposed along the Hellenic belt in the Axios/Vardar Unit [e.g., *Kiriakidis*, 1989], thus providing a clear record of the subduction of oceanic lithosphere predating continent-continent collision [e.g., *Stampfli and Hochard*, 2009]. Similar features characterize the Alboran domain in the western Mediterranean, where back-arc extension occurred in the hinterland of the ophiolite-bearing Betic Cordillera and Rif chains [e.g., *Faccenna et al.*, 1997; *Mazzoli and Algarra*, 2011, and references therein]. However, the rollback of subducting oceanic lithosphere has also been invoked in areas where high-pressure metamorphic rocks and ophiolitic nappes are completely lacking as any geophysical evidence for a continuous oceanic slab. For instance, the Western Carpathian orogeny is interpreted to be the result of the subduction of the oceanic lithosphere flooring the eastern branch of the Piemont-Liguria Ocean during the Late Cretaceous [e.g., *Birkenmajer*, 1986; *Oszczypko*, 2006; *Picha et al.*, 2006] and the later imbrication of the passive margin deposits belonging to the European Platform. The remnants of the former ocean are interpreted as being preserved in the so-called Pieniny Klippen Belt (PKB), a narrow, arcuate zone consisting of intensely sheared Mesozoic to Paleogene rocks. Traditionally, this belt is interpreted as a suture between the so-called Inner and Outer Carpathians, marking the original locus of the completely subducted eastern segment of the Piemont-Liguria Ocean (also known as the Vahic Ocean in the Western Carpathian region [*Mahel'*, 1981; *Plašienka*, 1995a, 2003]). Several stratigraphic [e.g., *Birkenmajer*, 1960, 1986] and tectonic studies [*Plašienka*, 2012, and references therein] have been carried out supporting this hypothesis, leading to the definition of the Pieniny Ocean. Geophysical evidences of cold and dense material stored at the base of the upper mantle, at depths between 400 and 650 km [*Wortel and Spakman*, 2000; *Ustaszewski et al*., 2008; *Handy et al*., 2010], have been interpreted as a result of partial break off of a previously continuous oceanic slab extending from the Western to the Eastern Carpathians [*Sperner et al*., 2002]. Other processes, such as gravitational collapse [*Houseman and Gemmer*, 2007] or mantle lithosphere delamination [e.g., *Göğüş et al*., 2011], have been proposed to explain the observed upper crustal features (e.g., surface uplift and subsidence, crustal extension and shortening, and migration of volcanism). These models can also explain the eastward younging of the end of thrusting along the Western Carpathian front. Although these hypotheses are fully compatible with the original occurrence—and subsequent subduction—of oceanic lithosphere in the Carpathian region, they do not rule out the possible occurrence of continental lithosphere subducting below the Western Carpathian belt. *Jurewicz* [2005] first put into doubt the original presence of oceanic lithosphere flooring the Pieniny Basin during the Early Cretaceous, suggesting instead the occurrence of thinned continental crust between the Outer and the Inner Polish Carpathians.

Independent of the undeterminable original occurrence and extent of oceanic lithosphere in the study area, a reappraisal of the stratigraphy and sedimentology of the PKB is integrated in this paper with the analysis of the tectonic and stratigraphic relationships between the Inner and Outer Carpathian successions using a series of balanced and restored cross sections. The proposed tectonic evolution, validated by applying suitable algorithms to a 2-D forward kinematic model, reproduces thick- and thin-skinned thrusting in the Western Carpathians from the Early Cretaceous to the present day. The restoration is carried out independently for the Inner and the Outer Carpathian domains, thereby taking into account the possibility of the original occurrence and later subduction of oceanic lithosphere between the two domains. To constrain the tectonic and thermal evolution during the last 20 Ma, our model also integrates new and previously published apatite fission track and apatite (U-Th-Sm)/He ages. In this way, erosion is effectively taken into account in the sequential restoration of balanced cross sections and related forward modeling, thus providing a comprehensive picture of the tectonic evolution of the area extending from the Inner Carpathians of Slovakia to the Outer Carpathian front in Poland.

2. Geological Setting

The Central Western Carpathians are part of a curved orogenic system extending from the Danube Valley in Austria to southern Romania (Figure 1). The origin of this chain is related to the collision between the European Platform and the Alps-Carpathians-Pannonia (ALCAPA) and Tisza-Dacia Mega Units belonging to the Adriatic paleogeographic domain [*Csontos and Vörös*, 2004]. The northeastward and eastward movements of these microplates are generally interpreted as being triggered by the interplay between lateral extrusion [*Ratschbacher et al*., 1991a, 1991b] and rollback of the subducting slab [*Sperner et al*., 2002]. The closure of the southern branch of the Alpine Tethys (in the sense of *Schmid et al*. [2008]) started in the late Early Cretaceous. It was due to the collision between the Tisza and Dacia Mega Units, associated with the onset of subduction in the Alpine Tethys Ceahlau-Severin area [*Schmid et al*., 2008]. The north and later northeastward movements of the ALCAPA unit, which shaped the Western Carpathians, started during the Late Cretaceous, with the shortening of the PKB and the more internal units, and lasted until the Neogene with the closure of the Carpathian embayment [*Săndulescu*, 1988; *Földvary*, 1988]. It led to the emplacement of the Western Carpathian accretionary wedge on top of the southern margin of the European Platform. The tectonic transport direction changed progressively from NW to NE [*Csontos and Vörös*, 2004, and references therein]. This was associated with a diachronous end of thrusting, from circa 15.5 Ma in the western Polish sector to 11.5 Ma in the Ukrainian region [*Nemčok et al*., 2006b]. Based on structural and stratigraphic evidences, the Western Carpathians are subdivided into two different tectonic domains [*Książkiewicz*, 1977a, 1977b]: the Inner Carpathians (IC) and the Outer Carpathians (OC). The former are made up of Variscan crystalline basement, including Paleozoic metamorphic rocks, and its Mesozoic sedimentary cover that was incorporated into a series of thick-skinned thrust sheets (in this paper, the so-called "Central Western Carpathian (CWC) domain" [e.g., *Froitzheim et al*., 2008] is included in the Inner Carpathians for the sake of simplicity). These thrust sheets are unconformably overlain by clastic deposits belonging to the Central Carpathian Paleogene Basin (CCPB). Early Alpine shortening involved the Inner

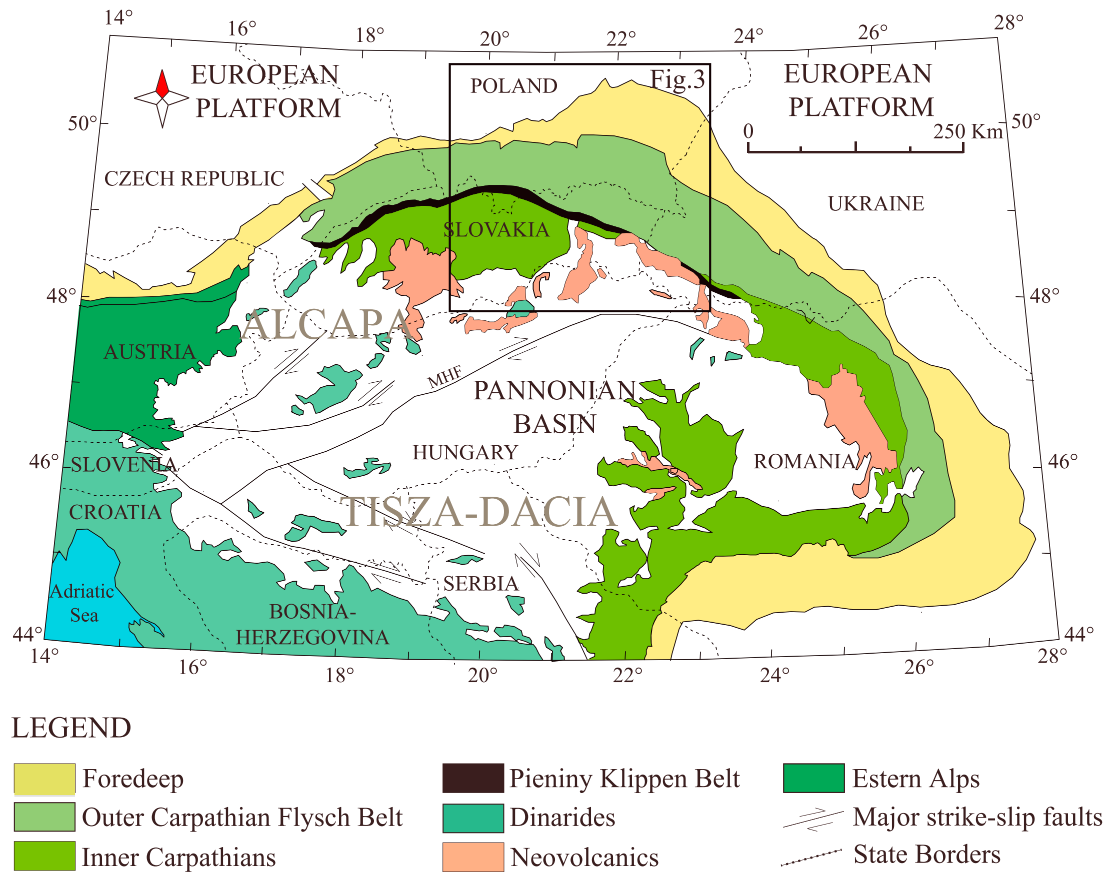

Figure 1. General tectonic map of the Carpathian-Pannonian region. Major tectonic domains include foredeep, Outer Carpathians, Pieniny Klippen Belt, Inner Carpathians, Dinarides, Eastern Alps, and areas of volcanic rocks. The Mid-Hungarian fault zone (MHF) separates the ALCAPA and Tiza-Dacia Mega Units of the Inner Carpathian domain.

Carpathian zone during the Late Cretaceous [*Mahel'*, 1986; *Plašienka*, 1999]. Thrusting caused the uplift of the Variscan crystalline basement and the imbrication and subsequent partial erosion of its Mesozoic cover [e.g., *Anczkiewicz et al.*, 2013, and references therein; *Janočko et al.*, 2006; *Roca et al.*, 1995]. The Late Cretaceous movement of the Inner Carpathian range toward the north and NE produced a flexure of the European Platform and the progressive migration of thrusting toward the north, thereby involving the successions deposited in the Outer Carpathian sedimentary basin. The Outer Carpathians consist of a fold and thrust belt formed mainly by siliciclastic turbiditic deposits of Upper Jurassic to lower Miocene age [*Książkiewicz*, 1962, 1977a, 1977b; *Bieda et al.*, 1963; *Mahel' and Buday*, 1968; *Koszarski and Ślączka*, 1976], which were deformed since Oligocene times. In the frontal part of the thrust belt, this siliciclastic succession is overlain by a regressive sequence made of middle-upper Miocene molassic deposits constituting the Subcarpathian Nappe extending from eastern Poland throughout the Ukrainian and Romanian foredeep [*Jankowski et al.*, 2004a, 2004b]. Stratigraphic investigations suggest a diachronous end of thrusting in the Western Carpathians, although generally ceasing within the middle Miocene [*Nemčok et al.*, 2006b], followed by upper Miocene out-of-sequence shortening and thick-skinned reactivation of basement normal faults, the latter tectonic phase being more pronounced in the eastern part of the Polish foreland [*Krzywiec*, 2001]. The Outer and Inner Carpathian realms are separated by a few hundreds of meters to 20 km wide zone called the Pieniny Klippen Belt [*Andrusov*, 1931, 1938, 1950, 1974; *Birkenmajer*, 1956, 1957, 1958, 1960, 1986; *Birkenmajer and Dudziak*, 1988; *Plašienka*, 1995a, 1995b; *Plašienka and Mikuš*, 2010; *Roca et al.*, 1995; *Uhlig*, 1890]. This belt runs from the Vienna Basin to northern Romania and consists of Mesozoic blocks of shallow to deepwater facies embedded in a less competent Upper Cretaceous to Paleocene matrix. Some papers suggest the occurrence of even younger deposits, such as the Oligocene Myjawa succession [*Oszczypko et al.*, 2005].

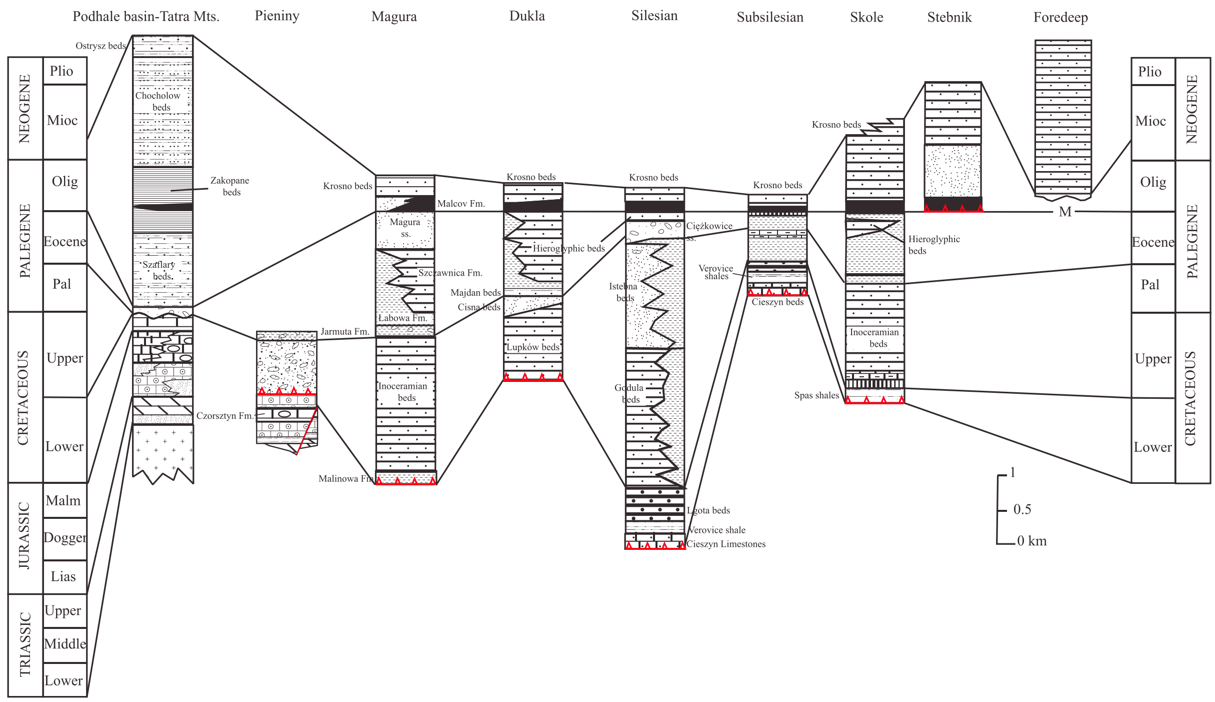

Figure 2. Chronostratigraphic chart of the main tectonic units of the Polish-Slovakian Carpathians. All stratigraphic columns are aligned to the same isochronous horizon, the Menilite Formation ("M"). Lithological description and average thickness of each formation are based on published data (see text for details). The Tatra stratigraphic column represents a simplification of the autochthonous succession [*Uchman*, 2004]. The Pieniny column was constructed accordingly to the Czorsztyn Unit description by *Voigt et al.* [2008]. All formations are grouped into horizons of similar age. This subdivision has been used in the construction of the geological cross sections.

3. Main Tectonostratigraphic Units of the Western Carpathians

3.1. Outer Carpathians

The Outer Carpathian accretionary wedge is built by a series of thrust sheets which are completely detached from their original substratum and involved in Oligocene-early Miocene thin-skinned thrusting [e.g., *Roure et al.*, 1993]. These thrust sheets are traditionally grouped, based on their stratigraphy (see below), into larger tectonic units. These groups of thrust sheets include, from the innermost to the outermost, (i) the Magura (originally belonging to the Alpine Tethys according to *Schmid et al.* [2008]), (ii) the Dukla, (iii) the Silesian, (iv) the Subsilesian, (v) the Skole, (vi) the Stebnik, and (vii) the Zglobice units (Figure 2). The latter unit is thrust on top of the middle Miocene foredeep deposits, consisting of shallow to deepwater siliciclastic sediments (sourced by the Carpathian chain), intercalated with lower to middle Miocene evaporitic layers. A general thickening (up to 2500 m) of the basin succession toward the south and southwest is recorded, mainly due to the flexure of the European Platform during the emplacement of the Carpathian accretionary wedge and related reactivation of the Tornquist-Teisseyre fault zone (TTZ) located north of the Carpathian foredeep [*Krzywiec*, 2001, and references therein]. The effects of this reactivation are more pronounced in the eastern Poland, whereas the western part, far from the TTZ, has a more regular flexural profile.

In the following, the main tectonostratigraphic units are indicated with reference to the hanging wall unit (e.g., the Magura Unit thrust is the fault carrying the Magura on top of the Dukla and further units).

3.1.1. Zglobice Unit

The Zglobice Unit is a very narrow belt cropping out along the Western Carpathian front (Figure 3). It is the outermost unit made of Badenian (i.e., Langhian to lower Serravallian) sediments thrusting on top of the middle Miocene foredeep deposits.

3.1.2. Stebnik Unit

The Stebnik Unit, together with the Zglobice Unit and its laterally equivalent narrow belt of the Borislav-Pokuttia Unit cropping out in Ukraine, is part of the Neogene allochthonous molasse (Figure 2) belonging to the Subcarpathian Nappe [*Jankowski et al.*, 2004a, 2004b]. These units comprise mainly early to middle

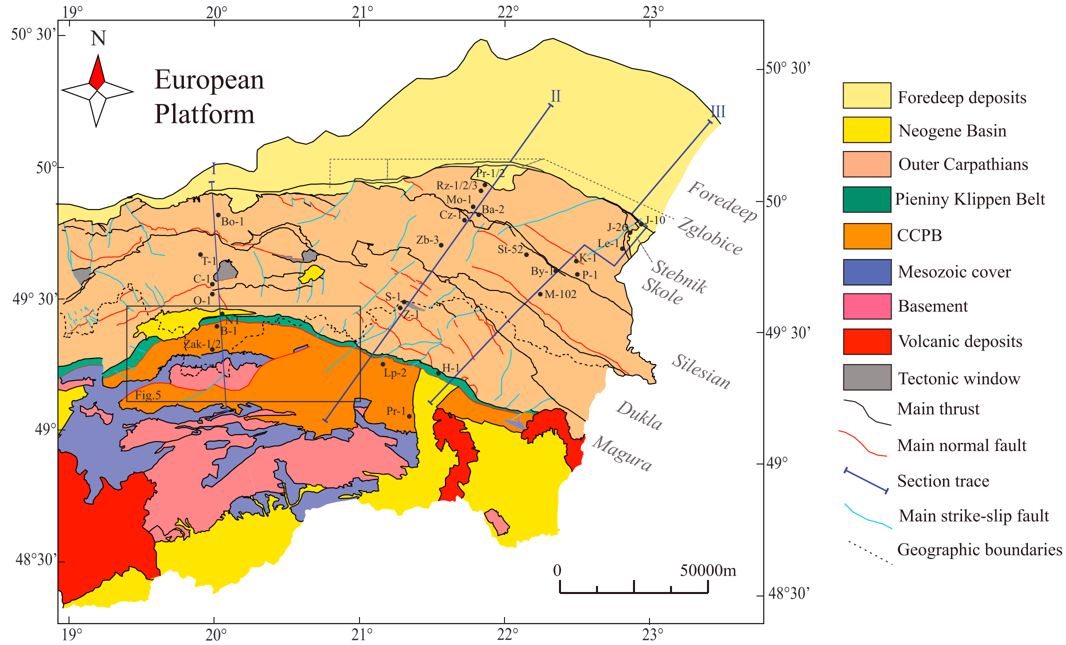

Figure 3. Schematic map of the Polish-Slovakian Carpathians showing the main tectonic units, the location of the section traces, and the key wells (Bańska PIG-1 (B-1), Borzęta IG-1 (BO-1), Chabówka-1 (C-1), Obidowa IG-1 (O-1), Tokarnia IG-1 (T-1), Nowy Targ PGI-1 (NT), Zakopane IG-1 and IG-2 (Zak-1/2), Zborov-1 (Z-1), Lipany-2 (Lp-2), Smilno-1 (S-1), Jaksmanice-10 and 26 (J-10/26), Leszczyny-1 (Le-1), Bykowce-1 (By-1), Strachocina-52 (St-52), Mokre-102 (M-102), Hanušovce-1 (H-1), Kuźmina-1 (K-1), Paszowa-1 (P-1), and Prešov-1 (Pr-1)). Profile III has been offset into two segments in line with the availability of borehole data. Tectonic windows (in grey) are exposures of the Dukla Units (cropping out extensively more to the southwest).

Miocene deposits, the oldest being ascribed to the Upper Oligocene Menilite Formation which was drilled by the Jaksmanice-10 well [*Wdowiarz et al.*, 1974; *Zieliński*, 1963]. The latter behaves as the main detachment level, allowing the formation of several ramp anticlines.

3.1.3. Skole Unit

The Skole Unit (Figure 2) extends from the Eastern Polish Carpathians along the whole western Ukraine (Figure 3). This succession starts with the Spas Shales, a Lower Cretaceous anoxic black shale formation interbedded with thin, laminated siltstones [*Kotlarczyk*, 1985; *Kruglov*, 2001] that represent the main décollement level for this unit. These deposits are followed by a thin level of red radiolaritic shales, passing upward to the 1500 m thick siliciclastic turbiditic formation named Inoceramian beds [*Kotlarczyk*, 1978]. The oldest deposits of this formation are Upper Cretaceous-Paleocene in age and are overlain by green clayey shales intercalated with the thin-bedded sandstones of the Hieroglyphic beds (late Paleocene-middle Eocene). The Eocene part of the succession terminates with the Globigerina marls and is overlain by approximately 250 m of Oligocene bituminous shales belonging to the Menilite Formation. The youngest formation (upper Oligocene-lower Miocene) of the Skole Unit is the Krosno Formation, which consists of thick-bedded calcareous sandstones, reaching a maximum thickness of approximately 2400 m [*Ślączka et al.*, 2006].

3.1.4. Subsilesian Unit

The Subsilesian Unit (Figure 2) is not continuous across the region, being exposed only in a series of tectonic windows (Figure 3). In the western sector of the Polish Carpathians, its external part is formed by a mélange, in which Miocene rocks are mixed together with other units (such as the Subsilesian Unit). In the eastern sector this unit is known as Węglówka unit, which is interposed between the Silesian and Skole Units. The oldest deposits of Subsilesian Unit consist of Lower Cretaceous euxinic shales intercalated, in the upper part, with turbiditic limestones and marls (Cieszyn beds). The Upper Cretaceous-Paleocene succession starts with a thin level of green radiolarian shales and radiolarites, becoming more marly and sandy upward. The occurrence of about 700 m of green marls and variegated shales characterizes the Eocene succession. The uppermost deposits, as for the adjacent unit, consist of the Oligocene bituminous shales of the Menillite Formation passing upward to the more calcareous sandstones and marly shales of the Krosno Formation.

3.1.5. Silesian Unit

The oldest deposits belonging to this unit are the Cieszyn Limestones (Tithonian-Berriasian) [*Matyszkiewicz and Słomka*, 1994], which only crop out in a few small areas of the Western Carpathians (Figure 2). This 250 m thick calcareous flysch [*Książkiewicz*, 1960; *Peszat*, 1967] passes upward to Lower Cretaceous sandy deposits (Grodziszcze ss.) and, higher up, to more shaly ones (Verovice shales, followed by Lgota beds). During the Upper Cretaceous to Paleocene, the deposition of up to 2000 m thick flysch deposits of Godula beds in the inner part of the Silesian Unit is intercalated with the deposition of variegate shales. The youngest deposits of the Paleocene succession consist in thick-bedded sandstones (Istebna beds). The Eocene sediments are characterized by thick variegate shales intercalated with sandstones (Ciężkowice Formation) the latter being more calcareous in the upper part of the succession (Hieroglyphic beds). The whole sequence is closed by the Globigerina marls and the Oligocene Menilite Formation, as it occurs in the neighbor unit. For this reason, both formations represent a useful marker for lithostratigraphic correlations. Younger deposits also occur in the Silesian Unit and belong to the Oligocene-lower Miocene Krosno beds, whose lithology is quite similar to the outer units [*Ślączka et al.*, 2006].

3.1.6. Dukla Unit

In the Polish region, the base of the succession consists of Upper Cretaceous shaly deposits known as Lupków beds (Figure 2) [*Leško and Samuel*, 1968; *Ślączka*, 1971; *Korab and Durkovic*, 1978], followed by calcareous and/or micaceous Paleocene sandstones (Cisna beds). A 1000 m sequence of thick-bedded sandstones (Hieroglyphic beds), locally intercalated with variegate shales, characterizes the Eocene sedimentation. As for the previously described units, the Globigerina marls are the uppermost deposits of the Eocene sequence, followed by dark bituminous shales belonging to the Menilite Formation and the Cergowa sandstones. This succession passes gradually upward to the lower Oligocene Krosno Formation, whose maximum thickness reaches approximately 1000 m [*Ślączka et al.*, 2006].

3.2. Alpine Tethys Successions in the ALCAPA Unit

3.2.1. Magura Unit

The Magura Unit (Figure 2) is the uppermost thrust sheet of the OC, being bounded by a continuous thrust running from the Western to the Eastern Carpathians, across the Czech Republic, Slovakia, Poland, Ukraine, and north Romania (Figure 3). The Magura Unit is detached along Aptian-Cenomanian black and green radiolarian shales, which are the oldest deposits of the unit. Higher up, Upper Cretaceous variegate shales pass to the Inoceramian beds, a thin to massive sandstones and turbiditic succession, that is interbedded with dark shales containing submarine slumping and intensely deformed layers [*Cieszkowski et al.*, 1987]. These deposits become rich of exotic carbonate blocks in their upper part (Jarmuta Formation; Paleocene) [*Burtan et al.*, 1984]. Sedimentation during middle and upper Eocene changes gradually to shale-rich deposits (Łabowa Formation). These are interpreted by some authors [e.g., *Oszczypko*, 1991] as deposited below the calcite compensation depth. The youngest deposits are represented by the Globigerina marls (Oligocene) and then by the Menilite and Malcov Formation, consisting of black bituminous shales and thick calcareous sandstone and shales, respectively [*Oszczypko-Clowes*, 2001].

3.2.2. Pieniny Klippen Belt

The Pieniny Klippen Belt (PKB) is a narrow and arcuate structure separating the OC and the IC tectonic domains (Figure 3). Several publications on the geology of the PKB came out in the past 50 years, which described the belt as either a tectonic mélange [e.g., *Roca et al.*, 1995] or as a "wildflysch" [*Nemčok*, 1980]. A more recent study published by *Plašienka and Mikuš* [2010] described the PKB as a Meso-Alpine fold-nappe system formed by several tectonic events that took place from the Late Cretaceous to the Pliocene. From bottom to top, four tectonic units are recognized within the PKB: the Magura Nappe, the Biele Karpaty Superunit, the Oravic Superunit (PKB s.s.), and elements of the Fatric Nappe belonging to the IC [*Plašienka*, 2011]. Basing on its internal structure, the PKB is subdivided into three structural elements: (i) "blocky klippen," characterized by block-in-matrix structures; (ii) "ribbon klippe," in which the competence contrast among different formations are less pronounced; and (iii) "klippen matrix," made of the less competent deposits (see *Plašienka* [2012] for details).

The PKB includes rocks from the Triassic to the lower Eocene (Figure 2). Triassic deposits, although not very common within the PKB, have been found as megablocks in the Pieniny Mountains (Haligowce Series) and in the western part of Slovakian PKB [*Andrusov*, 1950]. They consist mainly of dolomites and dolomitic limestones. Jurassic sediments include clastic (partly conglomeratic) deposits, passing upward to a more deep-water facies. Crinodal limestones followed by red radiolarian cherts and nodular limestones characterized the depositional environment from the Middle to the Late Jurassic [*Birkenmajer*, 1960]. Triassic and Jurassic deposits together with Lower Cretaceous marls, flysch sediments (see *Birkenmajer* [1986] for details), and, locally, cherty limestones occur in the PKB as megablocks (Milpoš Breccia) [*Plašienka and Mikuš*, 2010]. These Mesozoic olistoliths are surrounded by an intensely deformed matrix consisting of Upper Cretaceous-Paleogene shales, sandstones, and marls (also known as Klippen mantle [*Birkenmajer*, 1960]). Sedimentological investigations highlight the occurrence of syntectonic submarine slumping in this less competent matrix [*Plašienka et al*., 2012]. The syntectonic clastic deposits are interpreted as being related to two distinct phases: (i) opening of the Vahic Ocean during the Jurassic (closed by Late Cretaceous subduction) and (ii) Maastrichtian collision of the lower plate (i.e., the Oravic continent) with the Austroalpine margin [*Plašienka*, 2012]. The youngest synorogenic deposits recorded in the Pieniny succession are represented by the clastic sediments of the Jarmuta Formation that can be correlated with the Upper Cretaceous to Paleocene flysch deposits of the Magura Unit [*Ślączka et al*., 2006].

3.3. Adria-Derived Nappes in the ALCAPA Unit (Inner Carpathians and Central Western Carpathians)

South of the PKB (Figure 3), the IC (here including the so-called "Central Western Carpathians") represents the inner zone of the study area (Figure 2). Shortening in the IC started during the Early Cretaceous [*Voigt et al*., 2008], involving the IC s.s. (Tatra Mountains and Podhale regions) during the Late Cretaceous [*Săndulescu*, 1988; *Rakús et al*., 1990]. This early Alpine phase led to the imbrication of several nappes made up of Variscan basement rocks and Permian to Turonian deposits [*Roca et al*., 1995]. These nappes are unconformably overlain by the Paleogene deposits of the Central Carpathian Paleogene Basin (CCPB), later affected by late Miocene extensional tectonics [*Royden*, 1993].

3.3.1. Central Carpathian Paleogene Basin

This basin extends throughout the western part of the Inner Carpathian realm (Figure 3), being filled by Paleogene flysch-like deposits (Figure 2). It is composed of several minor basins, such as the Orava Basin, the Podhale and Liptov Basins, and the Poprad Depression, all of them characterized by a similar sedimentary infill. The regional unconformity defining the bottom of this basin is overlain by Eocene to Oligocene [*Gross et al*., 1993; *Samuel and Fusan*, 1992] or even early Miocene deposits [*Olszewska and Wieczorek*, 1998; *Soták*, 1998a, 1998b]. The lowermost succession consists of conglomerates, sandstones, and breccias [*Filo and Siranova*, 1998] that are overlain by the Szaflary beds (facies equivalent to the "Nummulite Eocene" transgression). The hemipelagic Globigerina marls lie on top of this transgressive sequence, which is covered by the lower member of the Zakopane beds (Huty Formation in the sense of *Gross et al*. [1984]). These beds are predominantly characterized by thin-bedded claystones and mudstones intercalated with thin-bedded sandstones and "Menilite-type" shales. The sandy component increases upward into the lower Oligocene Chochołow beds and becomes relevant in the upper part of this formation, where thin tuff layers also occur. The upper Oligocene-lower Miocene Ostrysz beds are the youngest deposits of the CCPB and are made up of thick-bedded sandstones intercalated with mudstones and claystones. These lithologies reflect several changes of the relative sea level, the more prominent being controlled by tectonics. These include a late Eocene tectonic subsidence, marked by basin formation related to gravitational collapse [*Wagreich*, 1995], and a more localized differentiated subsidence due to retroarc flexural loading associated with late Oligocene back thrusting in the eastern CCPB [*Soták et al*., 2001].

3.3.2. The Variscan Basement and Its Cover

Pre-Paleogene successions crop out in the northern Inner Carpathian domain as isolated mountain massifs within the widespread Paleogene succession belonging to the CCPB (Figure 2). Several boreholes and seismic lines revealed the occurrence of both sedimentary cover and basement-cored nappes below the CCPB deposits. From south to north, three distinct Paleozoic-Mesozoic tectonic realms can be recognized basing on basement structure and lithology: Gemer, Vepor, and Tatra units (indicated as Basement Unit in Figures 3 and 4). The Eo-Alpine Cretaceous convergence caused the imbrication of these nappes. North directed Cretaceous thrusting was later overprinted by south verging structures associated with right-lateral movement along the main tectonic contacts (i.e., Supra-Tatra and Vepor unit boundary) and, during the Late Cretaceous-early Paleogene, by ESE directed extensional and gravity sliding [*Putiš*, 1994, and references therein]. The structurally uppermost Gemer Unit consists of basement, lower Paleozoic Variscan-metamorphosed volcano-sedimentary successions and Carboniferous-Permian continental and marine cover sediments [*Vozárová and Vozár*, 1988; *Faryad*, 1991; *Soták et al*., 1999]. The Vepor and Tatra units are formed by a basement including high-grade gneisses and granitoid rocks, overlain by Permian to Lower Cretaceous

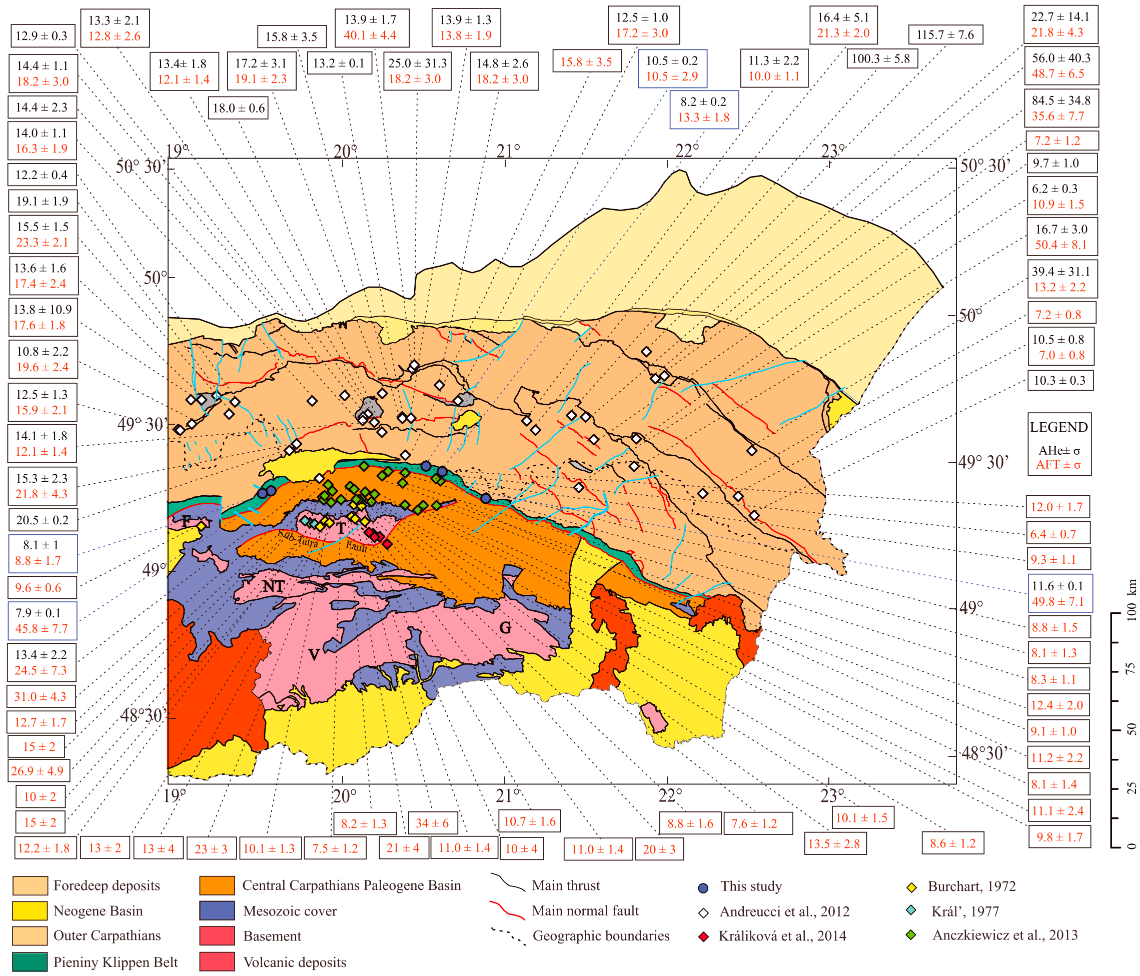

Figure 4. Schematic map of the Polish-Slovakian Carpathians showing the spatial distribution of new and published thermochronometric data referred to the last cooling event. AFT central ages and AHe weighted mean ages are indicated for each sample. Abbreviations indicate the locations of samples with older cooling ages (see text for detailed explanation): F = Fatra Mountains, G = Gemer Unit, NT = Nízke Tatry Mountains, V = Vepor Unit.

sedimentary successions. In the Tatra region, the Mesozoic cover consists of Lower Triassic clastic continental deposits [*Roniewicz*, 1959; *Dżułyński and Gradziński*, 1960], followed by Middle Triassic sabkha and shallow-water limestones intercalated with dolomitized layers [*Jaglarz and Szulc*, 2003]. The Triassic succession ends with variegated shales and evaporites intercalated with dolomite and sandstone beds of the Keuper Formation [*Prokešová et al.*, 2012], which has similar facies to those outcropping as megablocks in the PKB [*Andrusov*, 1931, 1938]. Higher up in the succession, the Jurassic section starts with sandy crinoidal limestone that passes upward into silicified radiolarian limestone and radiolarian cherts of Middle Jurassic age. A thin layer of limestone and gray marls closes the Upper Jurassic section, which is overlain by Lower Cretaceous marls and cherty limestones. The clastic supply increased during the Late Cretaceous, the related formations being characterized by sandstones and claystones [*Janočko et al.*, 2006]. The above described (so-called "High-Tatra") Mesozoic autochthonous sedimentary cover of the Tatra basement is tectonically overlain by the Sub-Tatra nappes (Križna and Choč nappes) [*Kotański*, 1963]. The sedimentary succession of the Sub-Tatra nappes, which were thrust northward during the Late Cretaceous orogenic event, differs from the autochthonous cover and represents, in general, more basinal facies.

4. Structural Modeling

Several balanced and restored cross sections have been constructed across the Western Carpathians [*Behrmann et al.*, 2000; *Gągala et al.*, 2012; *Morley*, 1996; *Nemčok et al.*, 1999, 2000, 2001, 2006a; *Roca et al.*, 1995; *Roure et al*., 1993] in order to provide a geometrically valid interpretation for the structures building the mountain belt. Most of them [*Behrmann et al*., 2000; *Gągala et al*., 2012; *Morley*, 1996; *Nemčok et al*., 1999, 2000, 2001, 2006a] only include the Outer Carpathians in the restoration and, except for *Gągala et al*. [2012], *Roca et al*. [1995], and *Roure et al*. [1993], do not include a 2-D kinematic model validating the balanced cross sections and explaining the related structural evolution.

In this study, three balanced and sequentially restored geological sections were constructed across the Western Carpathians (Figure 3) using Move, a software developed by Midland Valley Exploration Ltd. and dedicated to cross-section building and restoration.

Our own field data integrated with published data sets and geological maps allowed us to constrain the surface geology and the geometry of deep structures. Flexural-slip restoration coupled with 2-D forward kinematic modeling was performed in order to check the geometries of the tectonic structures and then validate the cross sections and the tectonic scenario. Syntectonic and posttectonic erosion has been simulated, taking into account published low-temperature thermochronometric data including apatite fission track and apatite and zircon (U-Th-Sm)/He ages integrated with new cooling ages from the PKB.

The balanced sections have been constructed across the Polish and Slovakian Carpathians from the foreland basin across the Outer Carpathian accretionary wedge and the PKB, to the Inner Carpathian range. Surface data come from 1:200,000 scale geological maps [*Nemčok and Poprawa*, 1988–1989; *Jankowski et al*., 2004a; *Polák*, 2008], 1:50,000 scale geological maps [*Nemčok et al*., 1994], and our own fieldwork, which allowed us to increase the number of dip data and reinterpret some tectonic contacts [see also *Mazzoli et al*., 2010]. The thickness of the successions is well constrained by geological maps, where both stratigraphic contacts and dip data are shown, boreholes (Bańska PIG-1, Borzęta IG-1 [*Marciniec and Zimnal*, 2006], Chabówka-1, Obidowa IG-1, Tokarnia IG-1 [*Wójcika et al*., 2006], Nowy Targ PGI-1 [*Paul and Poprawa*, 1992], Zakopane IG-1 [*Sokołowski*, 1973], and IG-2 for profile I; Przybyszówka-1 and 2, Rzeszow-1, 2, and 3, Mogielnice-1, Babica-1, Czarnorzeki-1, Zboiska 3 interpreted by *Nemčok et al*. [2006a], Zborov-1 interpreted by *Nemčok et al*. [2000], Lipany-2 from *Soták et al*. [2001], and Smilno-1 [*Behrmann et al*., 2000] for profile II; and Jaksmanice-10 and 26, Leszczyny-1, Bykowce-1, Strachocina-52, Mokre-102 [from *Gągala et al*., 2012, and references therein], Hanušovce-1 [*Behrmann et al*., 2000], Kuźmina-1 [*Malata and Żytko*, 2006], Paszowa-1 [*Semyrka*, 2009], and Prešov-1 [*Čverčko*, 1975] for profile III) and published information [*Ludwiniak*, 2010; *Janočko et al*., 2006; *Nemčok et al*., 2000; *Oszczypko et al*., 2006; *Ślączka et al*., 2006]. The geometries of the main tectonic structures have been constrained using seismic lines already interpreted in previous works [e.g., *Dziadzio et al*., 2006; *Dziadzio*, 2006; *Gągala et al*., 2012, and references therein; *Hrušecký et al*., 2006; *Krzywiec*, 2001; *Oszczypko et al*., 2006]. These data will be described later for each cross section. The deep architecture of the basement has been traced taking into account the magnetotelluric survey carried out by *Stefaniuk* [2006]. Basement morphology is generally controlled by ENE-WSW trending normal faults downthrowing to the south in the western part of the study area and NW-SE trending normal faults generally lowering the basement to the southwest in the eastern region. Strike-slip faults, constrained by the interpretation of electrical conductivity anomaly integrated with seismic reflection [see *Oszczypko et al*., 2006; *Żytko*, 1997], offset the main basement structures forming a framework in which isolated highs are surrounded by structural depressions. Evidence for reverse-slip reactivation of inherited basement normal faults has been documented in some geologic cross sections and seismic lines where Jurassic deposits lay on top of Cretaceous sediments (see geological section in Figure 6 of *Oszczypko et al*. [2006] where inversion of basement normal faults has been detected below the Ukrainian Carpathian foredeep). The occurrence of inversion anticlines [*Hayward and Graham*, 1989] in Miocene deposits overlying these normal faults suggest a late inversion affecting the basement, which could correlate with the emplacement of the Carpathian thrust and fold belt [*Oszczypko et al*., 2006]. The depth and geometry of the sole thrust below the Outer Carpathians is constrained by published geological sections [e.g., *Nemčok et al*., 2000, 2006a; *Gągala et al*., 2012; *Golonka et al*., 2011; *Oszczypko*, 2006] integrating borehole data and commercial seismic lines.

Concerning the deep structures of the IC, magnetotelluric studies indicate that the Tatra crystalline basement is detached and underlain by a layer of low-resistivity sedimentary rocks [e.g., *Ernst et al*., 1997]. This is consistent with the interpretation of the Tatra block as a detached basement slice transported over sedimentary successions occurring in its footwall [e.g., *Roca et al*., 1995].

Table 1. Overview of the AFT and AHe Age

Sample	Latitude	Longitude	Elevation (m)	Depositional Age	AHe Weighted Mean Age ± 1σ (Ma)	AFT Central Age ± 1σ (Ma)	Mean Confined Track Length ± SD (μm)
PL 72	*49.32298*	*19.53182*	*586*	Late Cretaceous-Paleocene	7.95 ± 0.14	45.80 ± 7.70	10.21 ± 2.58
PL 75	*49.31235*	*19.48207*	*570*	Late Cretaceous-Paleocene	8.11 ± 0.09	8.80 ± 1.70	
PL 82	*49.30322*	*20.79382*	*608*	Late Cretaceous	11.63 ± 0.11	49.80 ± 7.10	10.15 ± 1.85
PL 86	*49.42570*	*20.44130*	*423*	Eocene	10.50 ± 0.12	10.50 ± 2.90	
PL 87	*49.40512*	*20.53657*	*569*	Late Cretaceous-Eocene	8.62 ± 0.15	13.30 ± 1.80	

We applied the equal area calculation [*Chamberlin*, 1910, 1919] in order to obtain the depth of the décollement surface where it is not constrained.

Several lithostratighraphic units, having different formation names, were recognized within the Magura, Dukla, Silesian, Subsilesian, and Skole units. They are interpreted as belonging to different preshortening sedimentary basins [e.g., *Picha et al*., 2006; *Golonka et al*., 2011]. However, they are characterized by comparable lithologies with variable sandstone/shale ratio. For the purpose of this work, we group in the same layer all those lithostratigraphic units deposited during the same time interval. The Upper Cretaceous-Paleocene layer has been used as regional datum for the restoration because it is one of the best constrained horizons and can be restored to an almost flat datum, since it represents the top of the oldest deposits before the onset of the shortening.

Once the cross sections were constructed, flexural-slip restoration was performed. This restoration is based on minimum shortening and area conservation assumptions. Each thrust sheet has been unfolded individually using the flexural-slip algorithm. The pin line has been placed parallel to the axial plane of the folds. The unfolded thrust sheets have been positioned next to each other in order to verify whether the current geometry produced some gaps and/or overlaps between them. After minimizing such gaps/overlaps, they have been refolded back to their original geometry using the Upper Cretaceous-Paleocene horizon as a template. Finally, the modified thrust sheets have been inserted in their original position in the cross section. This procedure allowed us to fix the geometric inconsistencies in the cross sections and prepare them for the sequential restoration.

4.1. Sequential Restoration and 2-D Forward Modeling

Flexural-slip restoration has been performed in order to prepare the sections for sequential restoration. Each section has been separated into different fault blocks. Each fault block has been unfolded individually using the flexural-slip unfolding algorithm and then fit back together with the adjacent ones to minimize gaps and overlaps between blocks

Subsequently, the structures have been restored taking into account the timing of deformation provided by stratigraphic studies of syntectonic deposits and the relationships among the tectonic structures (sequential restoration). We applied a vertical simple shear algorithm for listric normal fault restoration in order to deform back the hanging wall along faults with a well-constrained geometry. On the other hand, the fault-parallel flow algorithm is best suitable for reverse fault restoration in shortening settings. Both these algorithms preserve bed area and length. The flexural-slip algorithm was also applied to simulate the flexure of the downgoing plate. The application of the bed area preservation principle does not allow one to simulate the loss of material from the lower crust due to deep geodynamic processes (such as delamination). Thus, the crust below the IC resulting from the sequential restoration is more than 30 km thick, the latter being the real crustal thickness values coming from deep seismic profiles published by, e.g., *Bielik et al*. [2004].

The undeformed section resulting from the sequential restoration has then been deformed forward in time (from the Early Cretaceous to the present day) in order to validate our structural interpretation and define the structure of the eroded successions. Constraints on the maximum burial and exhumation history have been obtained by thermal modeling based on low-temperature thermochronometric data (apatite fission track and apatite and zircon (U-Th-Sm)/He ages) including both new (Table 1) and published data [*Anczkiewicz et al*., 2013; *Andreucci et al*., 2013; *Zattin et al*., 2011, and reference therein].

5. Low-Temperature Thermochronometric Data

Several low-T themochronometric data sets are available for this study area [*Anczkiewicz*, 2005; *Anczkiewicz et al.*, 2005, 2013; *Andreucci et al.*, 2013; *Burchart*, 1972; *Danišik et al.*, 2010; *Kráľ*, 1977; *Králiková et al.*, 2014a, 2014b; *Struzik et al.*, 2002; *Śmigielski et al.*, 2012, and data herein]. The oldest ages have been detected by the $^{40}Ar/^{39}Ar$ system [*Hók et al.*, 2000; *Putiš et al.*, 2009] in the Lúčanská Fatra Mountains (IC) (see Figure 4 for location). These yield cooling ages, ranging between 345 and 248 Ma, are associated to post-Variscan cooling, erosion, and uplift of the basement. Lower temperature thermochronometers, such as zircon fission tracks (ZFT), approximately in the same area (indicated as F in Figure 4) [*Danišìk et al.*, 2010; *Králiková et al.*, 2014a, 2014b], show younger—i.e., Early Cretaceous (144–135 Ma) and Eocene (70–45 Ma)—cooling ages. The Early Cretaceous ages have been interpreted as a post-Jurassic rifting thermal event and the Eocene ages as cooling following Eo-Alpine nappe stacking. The combination of four thermochronometers, including zircon and apatite fission tracks (ZFT and AFT) and zircon and apatite (U-Th)/He (ZHe and AHe) methods, has been applied to the basement of the Tatra Unit (Nízke Tatra Mountains—location indicated as T in Figure 4) west of the Fatra Mountains [*Danišìk et al.*, 2011], confirming the occurrence of an Eocene cooling event due to erosion or basement exhumation related to the collapse of the Carpathian belt. Younger cooling ages have been detected by the AFT and AHe thermochronometers in the basement rocks. Regionally, the IC region shows a general younging of the AFT ages going from south to north. In fact, the Vepor (indicated as V in Figure 4), shows Cretaceous-Paleogene cooling ages, whereas the Tatra units are characterized by exhumation ages ranging between 10 and 15 Ma (for details, see *Danišik et al.* [2010, and references therein]). For the IC s.s., apatite fission track (AFT) and apatite (U-Th)/He (AHe) data suggest that the last cooling event is not older than 20 Ma for both the crystalline massifs and the Paleogene deposits of the CCPB [*Anczkiewicz*, 2005; *Anczkiewicz et al.*, 2005, 2013; *Danišìk et al.*, 2010, 2012a, 2012b, and references therein; *Śmigielski et al.*, 2012, 2016]. This feature has been interpreted by *Danišik et al.* [2010] as a shifting of the depocenter toward the Pieniny/Tatra boundary during the Tertiary, before the rapid middle-upper Miocene (or even younger) last cooling event, accompanied by the subsidence of the Paleogene-Neogene intramountain basins. This event has been associated to the lateral extrusion tectonic model [*Ratschbacher et al.*, 1991a, 1991b; *Sperner et al.*, 2002] and subsequently to the collision of the Adria Plate with the southern margin of the European Platform. AFT cooling ages lower than 9 Ma have been also recorded from basement samples in the Fatra Mountains and associated to the latest Miocene-Pliocene inversion of the Pannonian back-arc basin [*Králiková et al.*, 2014a].

Still debatable is the role of the magmatic activity in the heating process of the IC rocks. *Danišík et al.* [2011] pointed out that the early Miocene cooling ages detected by the AHe in some totally reset samples collected south of Tatra Mountains could be associated to the cooling after the Oligo-Miocene sedimentary burial or magmatism or increased heat flow. A more recent study focused on the Ukrainian Carpathians and their relationship with the Pannonian Basin [*Andreucci et al.*, 2015] suggested that magmatism had no significant impact on the thermal field of the inner part of the Ukrainian accretionary wedge and therefore on the thermal history of the analyzed rocks. Similar to the Ukrainian Carpathians, also, the thermal field of the Slovak IC is unlikely to have been perturbated by such magmatic activity.

In the Tatra Mountains, another possible explanation for the Middle/early late Miocene exhumation could be the activation of the Sub-Tatra fault, whose kinematics is still poorly known due to the occurrence of thick Quaternary cover. This fault has been either interpreted as south dipping normal fault [*Hrušecký et al.*, 2002; *Jurewicz*, 2005] or as north dipping reverse fault [*Sperner*, 1996; *Śmigielski et al.*, 2016]. *Králiková et al.* [2014a] suggest a change of kinematics over time. In this paper, we support the former hypothesis. Interpreting the Sub-Tatra fault as normal/transtensional fault, we honor not only the geometry coming from the interpretation of a seismic line published by *Hrušecký et al.* [2002] but also the fault kinematics recorded by mineral shear fibers (quartz, epidote, and carbonates) and striae on slickenside surfaces [*Jurewicz and Bagiński*, 2005]. In addition, the low-T thermochronometric data predicted by the tectonothermal modeling performed on a regional geological section across this area shows a good match with the real low-T thermochronometric ages [*Castelluccio et al.*, 2015].

A similar middle-late Miocene cooling event has been recorded also in the eastern Polish region of the OC belt, where the tectonic unroofing, triggered by low-angle normal faults, is the main cause of the young (<10 Myr) exhumation [*Andreucci et al.*, 2013]. This event is not recorded in the western Polish part of the

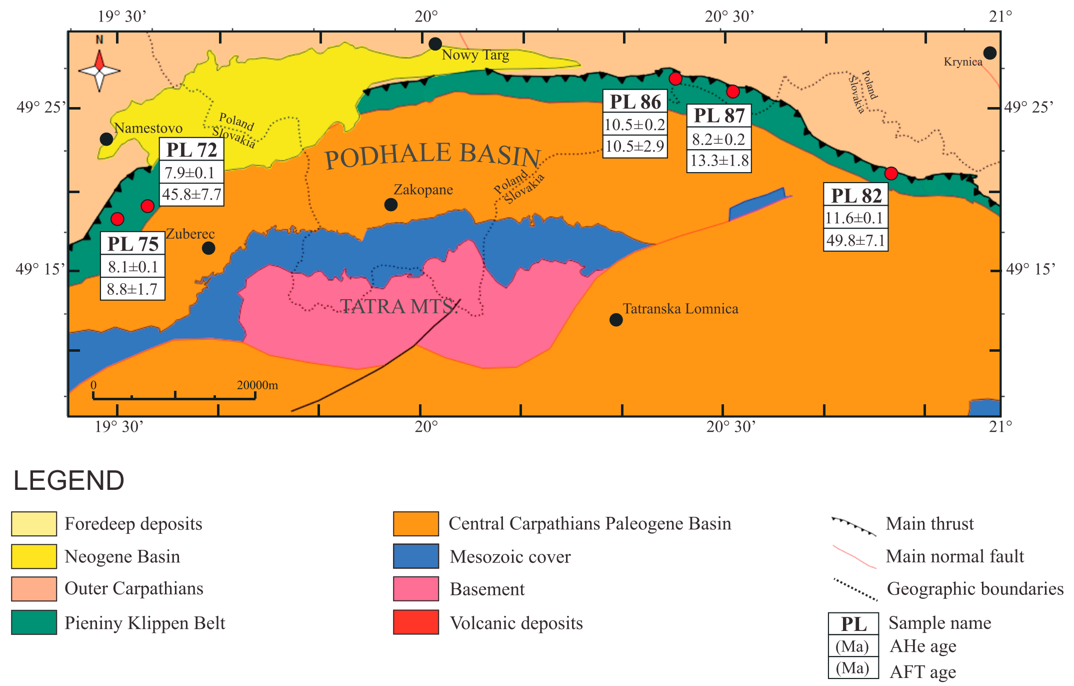

Figure 5. Schematic geological map of the Podhale-Tatra region showing the location of the sampling area along the Pieniny Klippen Belt.

OC, where 20–15 Myr cooling ages have been obtained and interpreted as associated with thrust-related uplift and coeval erosion [*Andreucci et al*., 2013].

To complete the framework of cooling ages, we provide new low-temperature thermochronometric data from the PKB, thus constraining the timing of exhumation of these deposits. The AFT and AHe data sets available for the study area, integrated with our new data from the PKB, are represented in Figure 4.

5.1. New Thermochronometric Data From the PKB

New AHe and AFT analyses were applied to five samples collected from siliciclastic sandstones and siltstones of the PKB (Figure 5). AHe analysis was performed at the Radiogenic Helium Dating Laboratory of the University of Arizona (Tucson), using the procedures described in *Reiners et al*. [2004]. Intact, euhedral, inclusions and coating-free apatite crystals, with the smallest dimension ≥60 μm, were preferably selected, handpicked, and measured for alpha-ejection correction using the methods described in *Farley* [2002]. In several cases no apatite crystal meeting the criteria listed above was found and slightly abraded, slightly coated or small-inclusion-bearing crystals had to be picked. However, no major effect on AHe dates is expected from small inclusions [*Vermeesch et al*., 2007], and it is, in general, possible to detect and limit the contingent effect of abrasion and coating [*Spiegel et al*., 2009; *Andreucci et al*., 2013]. Therefore, slightly flawed crystals were analyzed relying on their minor and/or detectable and interpretable impact on dates.

Single crystals were loaded into 0.8 mm Nb tubes and degassed under vacuum by heating with a Nd-YAG laser. The concentration of ^{4}He was determined by ^{3}He isotope dilution and measurement of the ^{4}He/^{3}He ratio through a quadrupole mass spectrometer. U, Th, and Sm concentrations were obtained by isotope dilution using an inductively coupled plasma mass spectrometer.

AFT analysis was performed at the FT laboratory of the University of Padua. A CN5 glass was used to monitor neutron fluence during irradiation at the Oregon State University Triga Reactor (Corvallis, USA). Central age calculation [*Galbraith and Laslett*, 1993] was performed with the Radial Plotter software [*Vermeesch*, 2009]. Chi-square (χ^2) testing assessed the homogeneity of age populations: a population is considered homogeneous for P(χ^2) higher than 5%. Mean Dpar of single crystals was measured and used as a kinetic parameter. For each sample track densities and length were measured from 20 grains (where possible).

10.1002/2016TC004190

Table 2. Apatite (U-Th-Sm)/He Analytical Data[a]

Sample	Replicate	Th/U	Raw Date (Ma)	1 s ± Date (Ma)	Ft (^{238}U)	Ft (^{235}U)	Ft (^{232}Th)	Ft (^{147}Sm)	Rs (um)	Corr Date (Ma)	1 s ± Date (Ma)	1 s ± Date %	W.m.a. (Ma)	W.m.a. err. (Ma)	eU (ppm)	eU w/ Sm (ppm)	U (ppm)	dU (ppm)	Th (ppm)	dTh (ppm)	Sm (ppm)	dSm (ppm)	^{4}He/g (nmol)	d^{4}He/g (ppm)
PL 72	**13A156_AC_PL72_Ap1**	4.19	6.63	0.35	0.66	0.62	0.62	0.89	41.40	**10.32**	**0.54**	5.22			44.83	45.65	22.87	0.34	93.42	1.35	195.52	2.84	1.62	0.08
	13A157_AC_PL72_Ap2	8.02	4.98	0.10	0.67	0.63	0.63	0.89	42.38	**7.74**	**0.16**	2.07	**7.95**	**0.14**	27.32	27.62	9.62	0.15	75.29	1.07	81.16	1.23	0.74	0.01
	13A158_AC_PL72_Ap3	*2.73*	*10.58*	*0.24*	*0.73*	*0.69*	*0.69*	*0.91*	*52.66*	***14.78***[b]	***0.34***[b]	*2.28*			*0.10*	*0.10*	*0.06*	*0.00*	*0.16*	*0.00*	*0.41*	*0.01*	*0.01*	*0.00*
	13A159_AC_PL72_Ap4	*1.49*	*40.16*	*0.63*	*0.61*	*0.56*	*0.56*	*0.87*	*35.27*	***66.76***[b]	***1.06***[b]	*1.59*			*127.83*	*130.98*	*95.35*	*1.37*	*138.21*	*2.01*	*698.47*	*10.22*	*27.99*	*0.32*
	13A160_AC_PL72_Ap5	*1.04*	*17.23*	*0.33*	*0.65*	*0.61*	*0.61*	*0.89*	*40.01*	***26.71***[b]	***0.51***[b]	*1.91*			*109.20*	*111.19*	*88.20*	*1.26*	*89.39*	*1.29*	*441.43*	*6.37*	*10.22*	*0.16*
PL 75	***13A161_AC_PL75_Ap1***	*2.63*	*8.18*	*0.19*	*0.90*	*0.89*	*0.89*	*0.97*	*153.40*	***9.12***	***0.22***	*2.36*			*1.61*	*1.64*	*1.00*	*0.01*	*2.58*	*0.04*	*7.36*	*0.11*	*0.07*	*0.00*
	13A162_AC_PL75_Ap2	6.82	7.88	0.14	0.72	0.69	0.69	0.91	51.38	**11.24**	**0.20**	1.79			67.95	69.09	26.51	0.38	176.33	2.51	280.91	4.06	2.92	0.04
	13A163_AC_PL75_Ap3	7.53	4.59	0.11	0.66	0.61	0.61	0.89	40.48	**7.27**	**0.17**	2.32	**8.11**	**0.09**	50.64	53.00	18.59	0.27	136.40	1.94	530.84	7.63	1.28	0.03
	13A164_AC_PL75_Ap4	14.36	4.92	0.22	0.68	0.63	0.63	0.89	43.07	**7.65**	**0.33**	4.38			52.98	53.58	12.35	0.18	172.90	2.48	165.29	2.48	1.42	0.06
	12A165_AC_PL75_Ap5	11.44	4.47	0.10	0.66	0.62	0.62	0.89	40.99	**7.08**	**0.15**	2.16			46.54	48.20	12.86	0.18	143.33	2.05	383.06	5.51	1.14	0.02
PL 82	**13A166_AC_PL82_Ap1**	16.00	8.30	0.15	0.75	0.72	0.72	0.92	58.38	**11.36**	**0.21**	1.83			29.46	31.33	6.31	0.09	98.50	1.41	418.65	6.08	1.35	0.02
	13A167_AC_PL82_Ap2	2.80	6.82	0.30	0.60	0.55	0.55	0.87	33.65	**11.76**	**0.52**	4.40			42.21	44.60	25.71	0.37	70.24	1.02	523.69	8.02	1.58	0.07
	13A168_AC_PL82_Ap3	5.82	5.18	0.12	0.58	0.53	0.53	0.86	32.53	**9.31**	**0.21**	2.24	**11.63**	**0.11**	45.67	47.30	19.57	0.29	111.08	1.60	370.20	5.40	1.30	0.03
	13A169_AC_PL82_Ap4	2.01	36.57	0.63	0.75	0.71	0.71	0.92	56.40	**49.60**[b]	**0.85**[b]	1.72			13.82	14.49	9.46	0.14	18.53	0.26	147.49	2.18	2.77	0.04
	13A170_AC_PL82_Ap5	1.40	8.38	0.13	0.71	0.67	0.67	0.91	49.39	**11.86**	**0.19**	1.58			64.32	68.40	48.70	0.69	66.49	0.95	880.74	12.80	2.96	0.03
PL 86	**13A176_AC_PL86_Ap1**	2.88	7.20	0.42	0.66	0.62	0.62	0.89	41.52	**11.12**	**0.65**	5.86			56.58	58.16	34.10	0.49	95.65	1.37	356.40	5.13	2.22	0.13
	13A177_AC_PL86_Ap2	14.52	8.05	0.23	0.70	0.66	0.66	0.90	47.49	**11.97**	**0.34**	2.80			59.34	60.08	13.72	0.20	194.15	2.79	199.16	2.88	2.61	0.07
	13A178_AC_PL86_Ap3	41.56	6.82	0.11	0.70	0.66	0.66	0.90	46.77	**10.29**	**0.17**	1.62	**10.50**	**0.12**	92.04	92.75	8.75	0.13	354.44	5.04	225.99	3.33	3.42	0.04
	13A179_AC_PL86_Ap4	27.64	4.97	0.17	0.67	0.63	0.63	0.89	42.20	**7.85**	**0.27**	3.38			39.94	40.54	5.45	0.10	146.78	2.09	158.06	2.28	1.08	0.03
	13A180_AC_PL86_Ap5	*4.01*	*10.00*	*0.27*	*0.60*	*0.54*	*0.54*	*0.87*	*33.55*	***17.52***[b]	***0.48***[b]	*2.74*			*125.88*	*126.92*	*65.62*	*0.95*	*256.43*	*3.67*	*274.70*	*4.12*	*6.84*	*0.17*
PL 87	**13A181_AC_PL87_Ap1**	5.14	5.98	0.17	0.71	0.67	0.67	0.91	48.54	**8.67**	**0.24**	2.79			19.24	19.90	8.83	0.13	44.27	0.64	151.16	2.20	0.63	0.02
	13A182_AC_PL87_Ap2	6.16	12.26	0.44	0.69	0.65	0.65	0.90	45.31	**18.36**[b]	**0.66**[b]	3.61			29.23	30.44	12.12	0.17	72.83	1.06	272.48	4.04	1.97	0.07
	13A183_AC_PL87_Ap3	7.60	4.39	0.27	0.75	0.72	0.72	0.92	58.07	**6.00**	**0.36**	6.04	**8.62**	**0.15**	6.19	6.32	2.26	0.04	16.74	0.24	29.14	0.49	0.15	0.01
	13A184_AC_PL87_Ap4	2.10	5.84	0.18	0.74	0.71	0.71	0.92	55.83	**7.97**	**0.25**	3.10			23.94	24.50	16.16	0.23	33.12	0.48	126.13	1.88	0.76	0.02
	13A185_AC_PL87_Ap5	7.84	8.28	0.44	0.75	0.71	0.71	0.92	56.64	**11.42**	**0.61**	5.35			16.35	16.63	5.84	0.08	44.68	0.64	69.90	1.04	0.74	0.04

[a]Italics indicate crystals that were considered not reliable and therefore discarded. See the text for details on the reasons for discarding crystals. W.m.a. stands for weighted mean dates: this was calculated using only the youngest crystals (<12 Ma). Boldface are used to highlight the name of the samples and the corresponding corrected date for an easier visualization.
[b]The corrected dates that were not involved in the calculation of this parameter are indicate.

Table 3. Apatite Fission Track Analytical Data[a]

		Spontaneous		Induced			Dosimeter						
Sample	No. of Crystals	r_s	N_s	r_i	N_i	$P(\chi)^2$ (%)	r_d	N_d	Age ± SE (Ma)	Mean Dpar ± SD (μm)	Minimum age ± SE (Ma)	No. of Confined Tracks	Mean Confined Track Length ± SD (μm)
PL 72	20	2.28	167	12.36	906	0.2	11.15	4798	45.8 ± 7.7	1.19 ± 0.10	38.1 ± 4.7	16	10.21 ± 2.58
PL 75	7	1.18	32	31.09	839	64.4	11.69	4798	8.8 ± 1.7	1.25 ± 0.19			
PL 82	20	5.76	432	25.42	1906	0.0	11.73	4798	49.8 ± 7.1	1.34 ± 0.18	16.6 ± 6.9	31	10.15 ± 1.85
PL 86	8	0.59	15	12.15	311	51.0	11.07	4798	10.5 ± 2.9	1.25 ± 0.47			
PL 87	20	1.65	160	30.02	2917	11.4	11.86	4798	13.3 ± 1.8	1.49 ± 0.18			

[a]Central ages calculated using dosimeter glass CN5 and z-CN5 = 396.08 ± 2.9 and the software TrackKey version 4.2 [*Dunkl*, 2002]. rs: spontaneous track densities (× 105 cm^{-2}) measured in internal mineral surfaces; Ns: total number of spontaneous tracks; ri and rd: induced and dosimeter track densities (× 106 cm^{-2}) on external mica detectors (g = 0.5); Ni and Nd: total numbers of tracks; $P(\chi^2)$: probability of obtaining χ^2 value for n degrees of freedom (where n = number of crystals-1); a probability >5% is indicative of an homogenous population. Minimum age is the peak age of the youngest age population obtained for partially reset samples using the BINOMFIT software [*Brandon*, 1992]. Sample preparation: Apatite grains were separated using heavy liquids and magnetic separation techniques. Mounts of apatite in epoxy were polished and then etched with 5 *M* HNO_3 at 20°C for 20 s to reveal spontaneous fission tracks. Samples were then irradiated with a CN5 dosimeter in the reactor at the Radiation Center of Oregon State University with a nominal neutron fluence of 9 × 1015 *n* cm^{-2}. After irradiation induced fission tracks in the low-U muscovite detector were revealed by etching with 40% HF at 20°C for 45 min. Samples were analyzed with a Zeiss Axioskop microscope equipped with a digitizing tablet and drawing tube and controlled by the program FTStage 3.11 [*Dumitru*, 1993]. FT ages were calculated using the external-detector and the zeta-calibration methods with IUGS age standards and a value of 0.5 for geometry correction factor. χ^2 test was used to detect whether the data sets contained any extra-Poissonian error.

AHe and AFT dates and AFT length data were used to model, for each sample, envelopes of admissible time-temperature paths, using the HeFTy software [*Ketcham*, 2005]. Timing and rates of cooling obtained by thermal modeling were used, in turn, to constrain the structural model in the last 20 Myr.

5.1.1. AHe Results

Five replicates were dated for each sample, as shown in Table 2.

Corrected ages range between 6.0 and 49.6 Ma, most of them clustering around 12 and 6 Ma, being younger than depositional ages. The data dispersion among single crystal dates of the same sample is comprised between 20 and 91%. Each sample has minimum ages of 6–9 Ma (one to three over five grains per sample), well matching the AFT central ages, being 2–4 Myr older. This data set indicates a very high degree of reset, although incomplete, as shown by the old outlier ages recorded by some crystals.

Analytical data are, in general, acceptable. However, four grains with suspiciously old dates (with respect to both the overall minimum ages and the weighted mean sample ages) and critically high or low analytical values (He < 1 mol/g and U < 5 ppm) were not accounted for the discussion and are indicated in Table 2 with Italic letters (PL 72_3, PL 72_4, PL 72_5, and PL86_5).

One crystal belonging to sample PL 75, with exceptionally low He content (<0.1 nmol), was also discarded, in spite of the acceptable crystal features and the age falling within the range of minimum and mean ages (PL 75_1).

5.1.2. AFT Results

The results of AFT dating are presented in Table 3 and in the radial plots of Figure 6.

Up to 20 grains per sample could be analyzed; the chi-square test indicates a variable spread (dispersion of 0 to 40%) of single-grain ages, ranging between 245 and 3 Ma. The average Dpar (diameter of etch figures parallel to the crystallographic *c* axis [*Ketcham et al.*, 1999]) of the samples ranged between 1.19 and 1.49 μm. Measurement of track lengths was possible on samples PL 72 and PL 82 (16 and 31 tracks per sample, respectively). Of the five analyzed samples, PL 72 and PL 82 show a partial reset of the AFT system after sedimentation (part of the single-grain ages older or as old as sedimentary age, high age dispersion); PL 87 shows an almost complete reset (all the dates are younger than the sedimentary age, but the age dispersion is still elevated, 20%); PL 75 and PL 86 show a complete reset

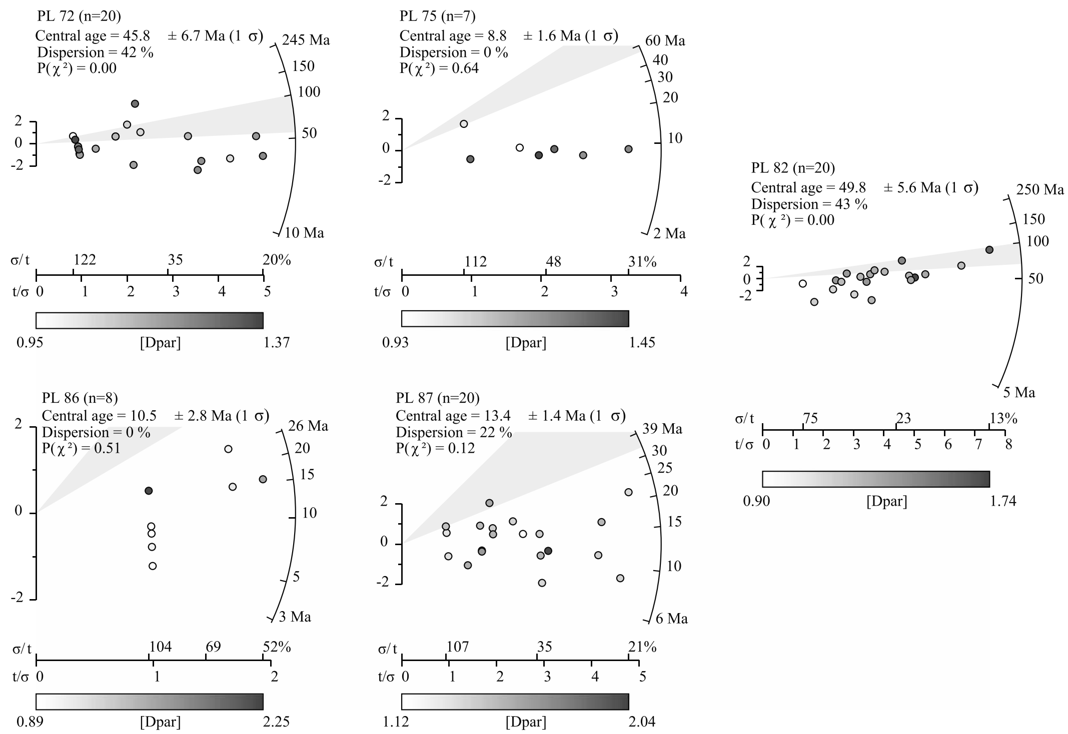

Figure 6. Radial plots for AFT samples whose depositional age is indicated by grey area. Standard deviation in single-grain age and standard error are indicated in horizontal and vertical axis, respectively. The RadialPlotter software [*Vermeesch*, 2009] has been used to determine the central age.

(very reproducible single-grain dates, all younger than the sedimentary age). However, we point out that in these last samples very few grains could be used for track counting due to the low spontaneous track density. The central ages of reset samples (included PL 87) range between circa 9 and 13 Ma.

5.2. Thermal Modeling

Using the AFT and AHe single-grain ages and AFT track lengths, where available, thermal modeling was performed by means of the HeFTy software [*Ketcham*, 2005] (Figure 7). Due to AHe age dispersion, due to incomplete, although very high degree of reset, only the youngest AHe dates (minimum age) were used for modeling (one to three crystals per sample). All Tt paths in Figure 7 show thermal histories characterized by a last cooling event starting at 10 Ma. No maximum values for cooling rates were imposed. Thermal models point out a prolonged (tens of Myr) stay in the AFT and AHe Partial Retention Zones, cooling down at an average rate of 25°C/Myr between circa 10 Ma and the present day. Details on the parameters used for modeling can be found in the caption of Figure 7.

6. Balanced Cross Sections

The section traces have been chosen to be roughly parallel to the tectonic transport direction, defined by the orientation of the major thrust ramps. This choice is aimed to avoid major out-of-plane movement that cannot be restored in 2-D. The main issue with this assumption (no out-of-plane movement) is represented by the evidence for a strike-slip component of displacement along the northern boundary of the PKB [e.g., *Birkenmajer*, 1983]. This strike-slip motion, roughly normal to the main thrust transport direction, implies the occurrence, along the PKB, of a lateral discontinuity in our balanced and restored profiles. Contrasting lateral shear senses have been documented along the PKB, which was first described as sinistral by *Birkenmajer* [1986] and later as dextral by *Jurewicz* [2000a, 2000b]. The occurrence of contrasting kinematic indicators is consistent with heterogeneous strain produced by shortening and general northward thrusting of the block-in-matrix assemblage constituting the arcuate PKB, rather than large-scale rotation of the Inner Carpathian plate which would be implied by a major, consistent strike-slip motion along the strike of the mountain belt.

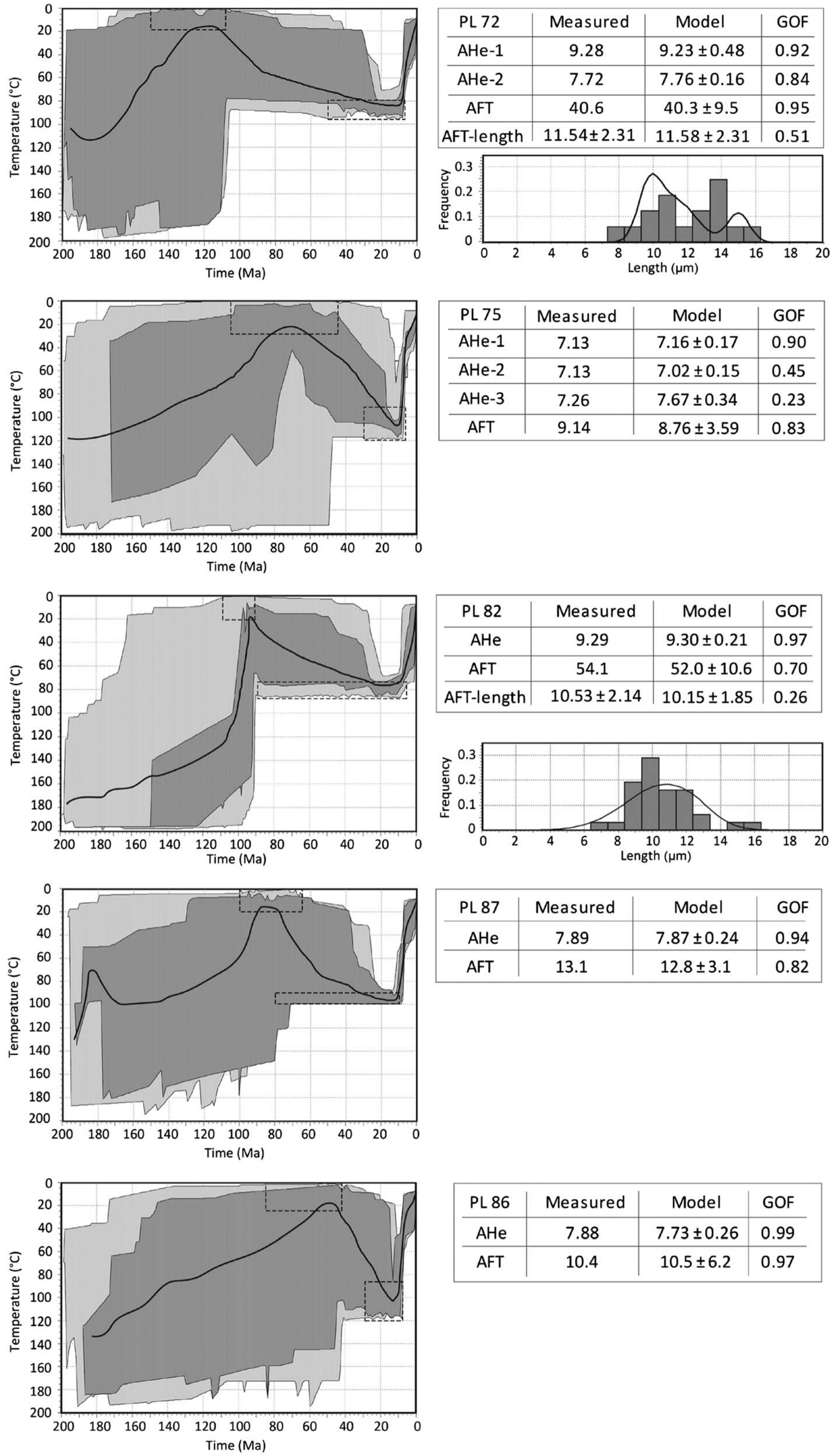

PL 72	Measured	Model	GOF
AHe-1	9.28	9.23 ± 0.48	0.92
AHe-2	7.72	7.76 ± 0.16	0.84
AFT	40.6	40.3 ± 9.5	0.95
AFT-length	11.54 ± 2.31	11.58 ± 2.31	0.51

PL 75	Measured	Model	GOF
AHe-1	7.13	7.16 ± 0.17	0.90
AHe-2	7.13	7.02 ± 0.15	0.45
AHe-3	7.26	7.67 ± 0.34	0.23
AFT	9.14	8.76 ± 3.59	0.83

PL 82	Measured	Model	GOF
AHe	9.29	9.30 ± 0.21	0.97
AFT	54.1	52.0 ± 10.6	0.70
AFT-length	10.53 ± 2.14	10.15 ± 1.85	0.26

PL 87	Measured	Model	GOF
AHe	7.89	7.87 ± 0.24	0.94
AFT	13.1	12.8 ± 3.1	0.82

PL 86	Measured	Model	GOF
AHe	7.88	7.73 ± 0.26	0.99
AFT	10.4	10.5 ± 6.2	0.97

Figure 7. Thermal modeling showing the evolution of the Pieniny deposits. The black line is the best fitting path, and the light and dark gray areas indicate the good path envelope and the acceptable path envelope. Modeling has been performed with the HeFTy software [*Ketcham*, 2005]. Temperatures between 0 and 20°C were applied during the period corresponding to the stratigraphic age interval.

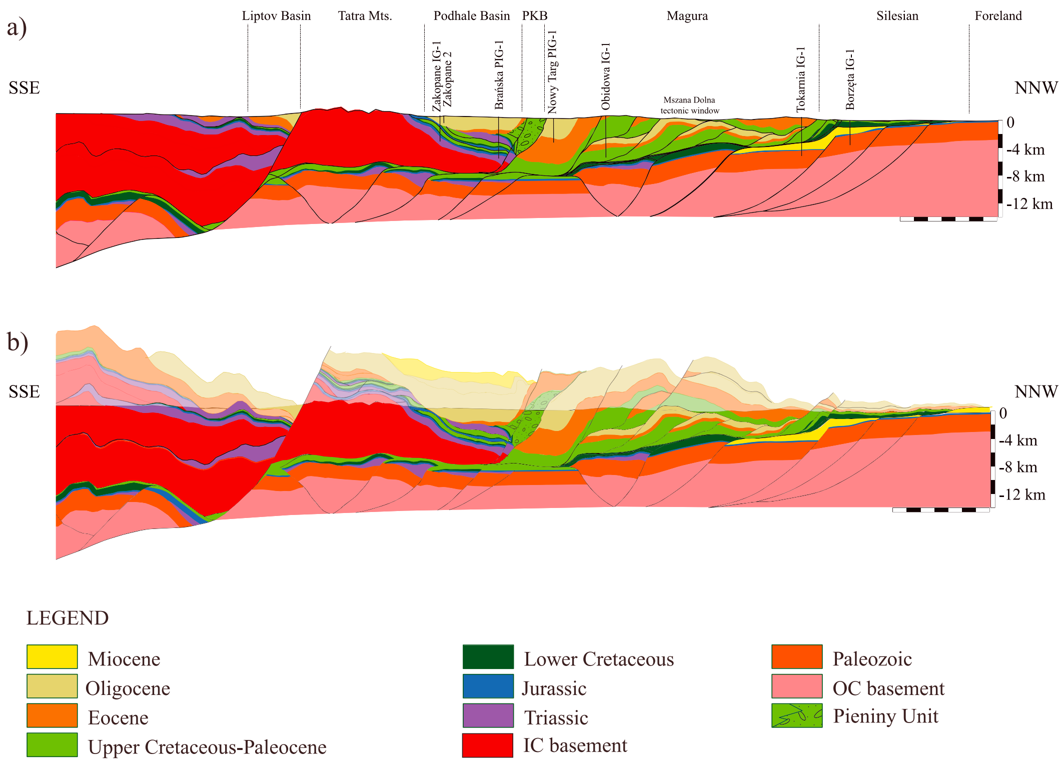

Figure 8. (a) Balanced geological section (Profile I) across the Western Polish Carpathians (located in Figure 3). The horizontal scale equals the vertical scale. (b) Thickness of the eroded strata reconstructed above the present-day topographic line represents the minimum value estimated from low-temperature thermochronometric data [*Andreucci et al.*, 2013]. The geometry of the eroded successions is obtained from the forward modeling shown in Figure 13.

It is worth noting that the arcuate shape of the PKB follows that of the whole Western Outer Carpathian belt, which has been documented by paleomagnetic studies [*Szaniawski et al.*, 2013] as having suffered only moderate tectonic rotations (approximately 20°) around a vertical axis (therefore, it did not result by bending of a formerly rectilinear belt [*Grabowski*, 1995, 1997; *Szaniawski et al.*, 2012]). More to the south, variable—mostly counterclockwise—rotations have been documented by paleomagnetic analyses performed on the allochthonous nappes of the CWC basement [*Grabowski*, 2005; *Grabowski and Nemčok*, 1999; *Grabowski et al.*, 2009, 2010; *Krs et al.*, 1996; *Kruczyk et al.*, 1992]. These rotations could be related to the multistage deformation history experienced by these nappes, rather than a regional geodynamic process. On the other hand, the counterclockwise rotations suggested by *Márton and Márton* [1996] and *Márton et al.* [1999, 2009], *Túnyi and Marton* [1996], and *Márton et al.* [2013] cannot be documented to have been accommodated by lateral shear along the PKB and do not contradict our interpretation due to the ALCAPA alignment and thrusting over the foreland.

The balanced cross-section lines are located in Figure 3 and shown in Figures 8, 10, and 11.

6.1. Profile I

Profile I (Figure 8a) extends across the Western Polish Carpathians to Slovakia, from Krakow to the Liptov Basin, south of the Sub-Tatra fault. It is almost N-S oriented and normal to the main tectonic structures. The deep architecture of the basement is characterized by several semigrabens bounded by south dipping Mesozoic normal faults. The structure of the basement is rather well constrained by magnetotelluric data [*Stefaniuk*, 2006] in the area beneath the foredeep deposits and the frontal part of the Magura Unit. The uncertainties in the interpretation of these structures increase with depth, where the position and the orientation of the tectonic structures involving the basement derive from the restoration of the younger successions in their original preshortening position. In the outer sector, the Jurassic deposits covering the basement are unconformably overlain by the Miocene foredeep sediments. This unconformity is the result

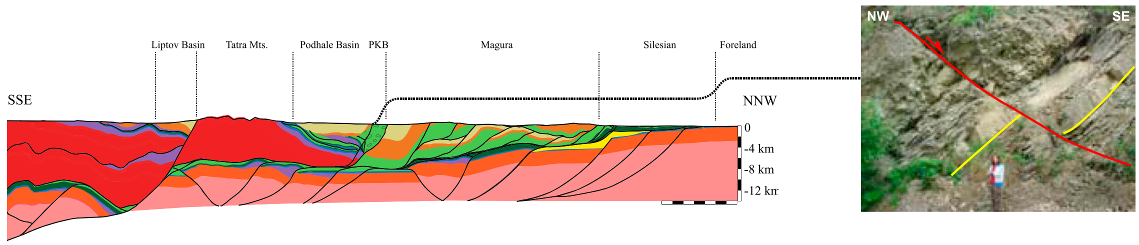

Figure 9. An example of field observation of normal faulting at the southern border of the PKB. The pictures (latitude 49°13,308′, longitude 19°22,139′) show a dip-slip normal fault plane, whose dip azimuth/dip is 152/32.

of the Late Cretaceous-Paleogene orogenic phase (so-called "Laramian" inversion in the Carpathian literature [*Roure et al*., 1993]), which led to the erosion of the Cretaceous sedimentary cover of the basement and the exposure of the underlying Jurassic deposits. The Neogene molasse has been penetrated by several wells (i.e., Tokarnia IG-1 [*Wójcika et al*., 2006]) more than 20 km south of the Carpathian thrust front, confirming the large displacement along the leading thrust of the Carpathian belt during the early Miocene. The "sigmoid" structure of the Carpathian front, especially in the area of Profile III, is related to the movement of the Skole and Stebnik thrusts on preexisting NE-SW trending basement faults. The inherited extensional structure controlled the development of lateral and oblique ramps within the overlying detachment planes during their subsequent shortening. The S-shaped Skole Unit resulted from a dramatic lateral variation of accommodation space, minimum in the western area and maximum in the eastern area, where the Stebnik basin developed [*Szaniawski et al*., 2013].

Basement-involved thrust sheets [*Froitzheim et al*., 2008; *Plašienka et al*., 1997] characterize the innermost sector of the IC (Figure 8b). On the other hand, the Outer Carpathians are a thrust and fold belt characterized by a thin-skinned style of shortening, with the sole thrust located along shaly layers intercalated within the Cretaceous succession. The present-day geometry is the result of in-sequence stacking of thrust sheets, which become wider southward. Starting from the foreland, the Silesian Unit consists of a hinterland-dipping duplex, with displacement of individual thrust faults ranging between 200 m and more than 3000 m. The Silesian Unit is also exposed in the Mszana Dolna tectonic window, in the footwall of the surrounding Magura Unit. The Magura Unit is a roof sequence that moved on top of the Silesian duplex for more than 36 km. This displacement value is obtained from the structural model used for the reconstruction of the eroded strata, since the location of the present-day Magura front is controlled by erosion. As already suggested by *Roca et al*. [1995], the deformation of the underlying Silesian Unit occurred after the emplacement of the Magura nappes on top of it, leading to folding of the Magura Unit sole thrust. Both Magura and Silesian Units were affected by normal faults that offset the previously formed thrust and fold structures. These faults mainly reactivate or detach along older thrusts at depth, such as that reactivating the Magura Unit thrust south of the Mszana Dolna tectonic window [*Mazzoli et al*., 2010]. The Magura Unit-Pieniny tectonic contact is dominantly steeply dipping, as suggested by several boreholes drilled across it (i.e., Hanusovce-1 well [*Leško et al*., 1985]). Nevertheless, its deep structure and kinematics are still a matter of debate, since subsurface data cannot be unambiguously interpreted. In this work, consistently with *Roca et al*. [1995], we interpret this contact as a reverse fault thrusting the Pieniny succession over the Magura Unit; the reverse fault was steepened by footwall imbrication and later strike-slip deformation. However, alternative interpretations exist, which invoke major left-lateral strike-slip faulting and back thrusting along the northern boundary of the PKB [*Birkenmajer*, 1983, 1985; *Picha et al*., 2006; *Zuchiewicz and Oszczypko*, 2008]. The strike-slip reworking of the PKB is evident at the outcrop scale, although likely minor in terms of absolute displacements. Back thrusting along a north dipping fault is inconsistent with both the northward convex trend of the tectonic contact and borehole observations, both indicating clearly a south dipping fault zone (i.e., Maruszyna IG-1 well [*Birkenmajer and Gedl*, 2012]). For these reasons we reject the back thrusting hypothesis. Different interpretations have been provided even for the contact bordering the PKB to the south. Our own field mapping (Figure 9) indicates the occurrence of a high-angle normal fault putting into contact the Paleogene deposits of the Podhale basin with the Pieniny succession at this location. The Podhale substratum is characterized by four tectonic units produced by the thick-skinned reactivation of basement normal faults as reverse faults. The structural high produced by the imbrication of these basement units is offset by the major Sub-Tatra fault in its southern sector. This structure has been interpreted as a reverse fault by several authors, including *Kotański* [1961], *Birkenmajer* [1986, 2003], *Sperner* [1996], and *Sperner et al*. [2002]. However, this interpretation has been questioned by many authors [*Mahel'*, 1986; *Bac-Moszaszwili*, 1993; *Kohút and Sherlock*, 2003; *Petrik et al*., 2003], who point out a normal dip-slip component for the Sub-Tatra fault based on the interpretation of a clear reflector visible in the seismic profile 753/92 [*Hrušecký et al*., 2002]—see interpretation in *Kohút and Sherlock* [2003]—and on kinematic indicators provided by mineral shear fibers (quartz, epidote, and carbonates) and striae on slickenside surfaces [*Jurewicz and Bagiński*, 2005]. This extensional dip-slip component of displacement is consistent with previously proposed interpretations for this structure (e.g., regional cross section accompanying the geologic map by *Lexa et al*. [2000]) and is adopted in this study.

6.1.1. Restoration of the Preorogenic Tectonic Setting (Early Cretaceous)

In order to restore Profile I to its preshortening tectonic setting, the Upper Cretaceous-Paleocene layer is considered the regional datum since it is the best constrained in the Outer Carpathian domain. In addition, this layer can be easily correlated with the Upper Cretaceous horizon representing the youngest deposit of the Inner Carpathian domain. Although the structure of the allochthonous accretionary wedge is well constrained by surface and subsurface data, there are some uncertainties about the extent of the Miocene molasse in the footwall to the Outer Carpathian sole thrust. Some authors suggest a scenario in which Miocene deposits occur beneath the whole Outer Carpathian wedge, although there are no constraints for such an interpretation [i.e., *Nemčok et al*., 2000; *Oszczypko*, 2006; *Ślączka et al*., 2006]. Here we apply a more conservative criterion, based on the data from the Tokarnia IG-1 well [*Wójcika et al*., 2006]. We extend the molasse deposits 8 km south of the above mentioned well, in order to be consistent with the sequential restoration based on minimum shortening. According to this assumption, the Carpathian thrust front attains a displacement of about 19 km, considerably less than the approximately 60 km obtained applying the alternative models proposed by *Nemčok et al*. [2000], *Oszczypko* [2006], and *Ślączka et al*. [2006]. By comparing the present-day geometry of this regional section and the undeformed Early Cretaceous sedimentary basin (Figure 12a), the amount of shortening can be obtained. It reaches a value of approximately 57 km (46%) for the IC and 73 km (54%) for the OC, without taking into account the middle Miocene reactivation of the deep basement normal faults causing mild inversion and shortening of the foreland basin substratum. The amount of shortening obtained in this study is less than that calculated by *Nemčok et al*. [2000] for almost the same transect across the Outer Carpathians. Our shortening value, although conjectural, is based on a conservative model that allows us to explain the geometric relationships between the IC, the PKB, and the neighboring Magura Unit. The sequential restoration provides a 125 km wide IC basin and a 135 km wide OC basin, in which the thickness of the postrift deposits is mainly controlled by the deep basement architecture.

6.2. Profile II

This NE-SW oriented section crosses the eastern sector of the Polish-Slovakian Carpathians, from the foreland basin to the Levoca Basin, one of the minor depressions belonging to the CCPB (Figure 10a). The European Platform underlying the Carpathian belt/foreland system is affected by SW dipping normal faults constrained by the interpretation of magnetotelluric data [*Stefaniuk*, 2006]. Here we represent only the major faults that are recognized from magnetotelluric sounding, seismic lines interpreted by *Nemčok et al*. [2006a], and boreholes [see *Nemčok et al*., 2006a]. The overall architecture of the cross section is similar to that shown in the previous profile, with the Jurassic deposits representing the youngest part of the succession on top of the foreland basement being sealed by the Neogene foredeep deposits in the frontal part of the thrust belt. The uncertainties in the interpretation increase at depth, beneath the Magura Unit. The deep basement architecture suggested in this section comes from the sequential restoration that allows us to restore the detached units that built the accretionary wedge to their original position and construct the basement beneath them. The Neogene molasse forms a wedge-shaped body with southwestward increasing thickness due to the flexure of the lower plate. Directly thrusted on top of it, the Skole Unit is made up of upright, mainly horizontal open folds (according with the fold classification published by *Fleuty* [1964]) produced by detachment folding, a mechanism described by *Homza and Wallace* [1994]. While the Oligocene and Eocene parts of the succession maintain a roughly similar thickness along the section, the Upper Cretaceous-Paleocene succession becomes thicker to the southwest.

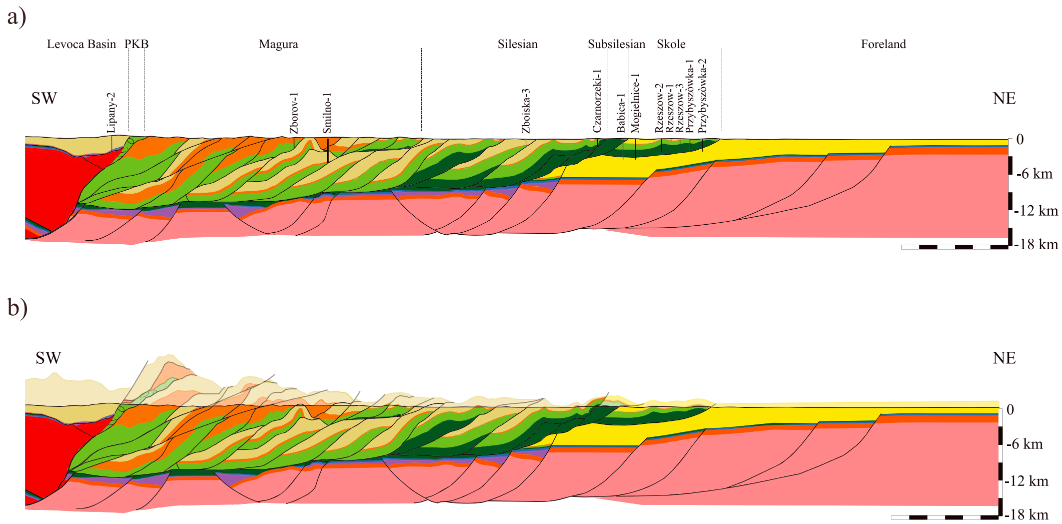

Figure 10. (a) Balanced geological section (Profile II) across the Eastern Polish-Slovakian Carpathians (located in Figure 3). The horizontal scale equals the vertical scale. (b) Thickness of the eroded strata reconstructed above present-day topography represents the minimum value estimated from low-temperature thermochronometric data [*Andreucci et al.*, 2013]. The geometry of the eroded successions comes from the forward modeling we performed in order to validate this section.

This is the only profile that intersects the Subsilesian Unit, which crops out as a narrow belt between the Skole and the Silesian Units. The Subsilesian Unit is deformed by thrust splays showing relatively limited displacement (each showing approximately 400 m of dip separation). These involve Lower Cretaceous sediments in the inner sector and younger deposits in the external part.

The Silesian Unit is characterized by broad open folds constructed using formation boundaries obtained from the geologic map [*Jankowski et al.*, 2004a] and bedding data collected in the field. These folds are mainly associated with thrusting involving Lower Cretaceous to Oligocene deposits. This unit consists of a hinterland-dipping duplex in which individual thrust splays show dip separation values ranging between a few hundreds of meters and 11 km. These values result from the sequential restoration of this profile, taking into account the constraints coming from Smilno-1, Zboiska-1, and Czarnorzeki-1 wells, and the detailed profiles published by *Nemčok et al.* [2006a]. Also for the Silesian Unit, the Upper Cretaceous and the Oligocene deposits become thicker southwestward.

The structure of the inner part of the Outer Carpathians is characterized by the thrust of the Magura Unit on top of the Dukla Unit, which is exposed in the Smilno tectonic window. The number of horses deforming the Dukla Unit has been inferred from the deformation they produced in the hanging wall rocks of the Magura Unit, since the quality of the seismic imaging of the subsurface structures is poor. The displacement ranges between approximately 1.6 km for the trailing thrust of the Dukla Unit and 18 km for the duplex cropping out in the Smilno area. A noteworthy thickening of the Eocene succession is recorded from the Silesian Unit (approximately 270 m), to the Dukla Unit (approximately 470 m), to the innermost sector where it locally exceeds 3 km. These deposits are affected by low-angle normal faults unraveled by the reinterpretation of some tectonic contacts portrayed in published 1:200,000 geological maps [*Jankowski et al.*, 2004a]. This reinterpretation comes from field observations [*Mazzoli et al.*, 2010] and the critical analysis of tectonic contacts, some of them mapped as reverse faults but displaying younger deposits at the hanging wall and older formations at the footwall. In addition, AFT and AHe dating methods applied to samples collected at the footwall of these faults reveal a very high cooling rate likely associated to tectonic unroofing [*Andreucci et al.*, 2013].

The trailing edge of the Magura Unit is characterized by the high-angle thrust of the PKB. Although *Hrušecký et al.* [2006] interpreted the PKB as flower structure, for the reasons explained in section 6.1, its southern contact is best interpreted as a high-angle SW dipping normal fault, downthrowing the Paleogene and Miocene deposits of the CCPB southward. In this section, the maximum thickness of the accretionary wedge is recorded in the Pieniny area where it reaches almost 20 km (Figure 10b). This value is consistent with paleothermal and thermochronological constraints described in section 4.

6.2.1. Restoration of the Preorogenic Tectonic Setting (Late Cretaceous)

The sequential restoration of Profile II has been performed by applying the same assumptions as for Profile I. We used the Upper Cretaceous-Paleocene horizon as a regional datum and, in addition, the available constraints on the position of footwall cutoffs beneath the Skole Unit thrust. Boreholes located along this profile [*Myśliwiec et al*., 2006] indicate a lack of Upper Cretaceous sediments in the footwall of the sole thrust approximately 5 km southwest of the Carpathian front. This makes the estimate of the displacement of the frontal thrust very difficult. Further wells, located southeast of the section trace, indicate the presence of the Skole Unit thrust at a maximum depth of approximately 3 km, gently dipping to the south, and the autochthonous Paleozoic deposits of the European platform directly in its footwall approximately 25 km southwest of the emerging Skole Unit thrust [*Nemčok et al*., 2006a]. Although these constraints did not allow us to infer the position of the Upper Cretaceous footwall cutoff without uncertainties, a conservative solution has been adopted that is consistent with the available subsurface information. Such a solution involved placing the cutoff of the Upper Cretaceous strata approximately 30 km SW of the Carpathian thrust front, in order to avoid huge displacements along the leading thrust. Each thrust sheet building up the Carpathian accretionary wedge has been sequentially restored from the foreland to the hinterland. Some thrusts, such as the trailing thrust of the Magura Unit, seem to not follow the general rule of the upsection propagating ramp, as it cuts downsection into the Upper Cretaceous succession. This apparent downsection propagation is mainly due to the local deformation of the basement after the Inner Carpathian emplacement on top of the lower plate. According to the model proposed in this paper and described later on in section 8, the IC tectonic load caused the lowering of the lower plate and the propagation of the subsequent thrust apparently downsection. The initial width of the restored Outer and Inner Carpathian basins is of 270 km and 38 km, respectively (Figure 12b), therefore considerably less than the 389 km wide basin proposed by *Nemčok et al*. [2006a] for almost the same section. The value of the shortening is about 169 km (63%) for the OC and 10 km (26%) for the IC successions.

6.3. Profile III

Profile III (Figure 11a) crosses the easternmost part of the Polish-Slovakian Carpathians. We chose the same transect of *Gągala et al*. [2012] and reinterpreted by *Andreucci et al*. [2013] for the OC, extending it farther to the southwest in order to include the Pieniny wildflysch and the IC domain. Although several data have been used to constrain the subsurface geometry of the major thrusts and the thickness of the successions, there are uncertainties about the interpretation of the deep structures, as well as about the geometric relationships between the Magura Unit and the Pieniny Unit, and the internal structure of the Inner Carpathian Mesozoic nappes beneath the Miocene deposits of the Prešov Basin. While the Stebnik, Skole, and Silesian Units are well constrained by seismic profiles and well data (see *Gągala et al*. [2012] for further details), there are uncertainties about the number of horses deforming the internal part of the Dukla Unit in the footwall of the Magura Unit thrust. We propose an interpretation that allowed us to construct a balanced section consistent with Profiles I and II in terms of structural architecture and amount of shortening for both the IC and OC. The middle to upper Miocene fill of the foredeep basin is characterized by a remarkable southwestward thickening, due to flexure of the lower plate, locally exaggerated by extensional reactivation of the Teisseyre-Tonquist Zone. The maximum thickness, around 5 km, can be recorded in correspondence of the outermost graben controlled by normal faults in the basement. In this section, the Neogene deposits lay directly on top of the Devonian foredeep basement [*Oszczypko et al*., 2006], although Jurassic and Upper Cretaceous deposits are known to occur more to the north [*Oszczypko*, 2006]. Magnetotelluric [*Stefaniuk*, 2006] and not publicly available seismic profiles show a basement structural high buried by the Silesian thrust sheets, 15 km south of the Paszowa well 1. This morphology influences the geometry of the overlying Silesian Unit thrust, producing its apparent bending as shown in the seismic profiles interpreted by *Gągala et al*. [2012]. No constraints on the architecture of the basement underlying the Dukla and innermost parts of the Silesian Unit are available. The suggested geometry comes from the sequential restoration, as described for the previous two sections. Also in this instance, the OC wedge is characterized by in-sequence thrust propagation. In the outer sector, thrusting involves Miocene foredeep deposits of the Stebnik Unit, being detached along the bituminous shales of the Menilite Formation. The inner and tectonically higher Skole Unit forms a leading imbricate fan, whose thrust splays are characterized by variable spacing (from approximately 1000 to 6000 m). A SW dipping low-angle normal fault offsets the inner part of this unit, terminating against a major NE dipping extensional fault at a depth of approximately 6 km. The main low-angle normal fault, bordering the Silesian Unit to the south, is responsible for the bending

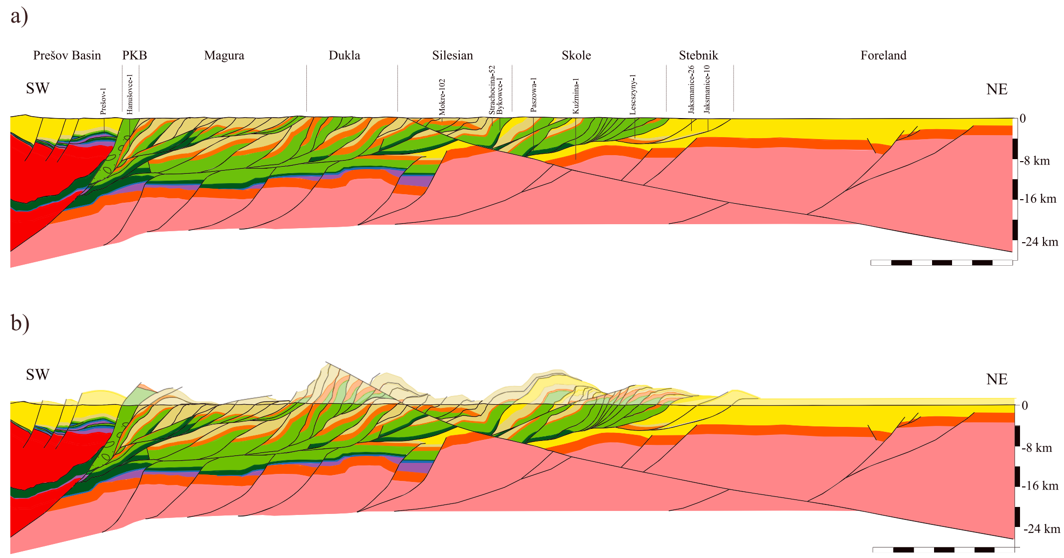

Figure 11. (a) Balanced geological section (Profile III) across the Eastern Polish-Slovakian Carpathians (modified after *Andreucci et al*. [2013]). For location see Figure 3. The horizontal scale equals the vertical scale. (b) Thickness of the eroded strata reconstructed above present-day topography represents the minimum value estimated from low-temperature thermochronometric data [*Andreucci et al*., 2013]. The geometry of the eroded successions comes from the forward modeling we performed in order to validate this section.

of the Silesian sole thrust and the basement high below it, as well as for significant late Miocene tectonic exhumation in this area [*Andreucci et al*., 2013]. This fault is a very pronounced morphologic feature, clearly visible in the field and delimiting the southern margin of the so-called Central Carpathian Depression [*Wdowiarz*, 1985]. It extends for more than 50 km along the Polish region. Data published in *Mazzoli et al*. [2010] show NE dipping fault planes with striae/shear fiber lineations indicating top to NE movement. A thick-skinned geometry has been suggested for this fault in order to honor the geometry of its hanging wall constructed using bedding data. This geometry is furthermore confirmed by the interpretation of the POLCRUST seismic profile published by *Probulski and Maksym* [2015], highlighting the occurrence of crustal NE dipping normal faults below the Central Carpathian Depression.

The neighboring Dukla Unit consists of several thrust sheets. Thrust spacing within this unit increases to the southwest, while dip-slip displacement of individual splays ranges between approximately 1.5 km and 8 km. The Dukla Unit is partially overridden by the high-displacement Magura Unit. The internal structure of the latter is characterized by the occurrence of several thrust splays whose dip angle increases toward the southwest. The dip separation values measured along each individual splay ranges from less than 4 km (for the outer thrust ramps) to approximately 19 km for the innermost one. The contact between the Pieniny deposits and the Magura Unit is a steep thrust producing the tectonic superposition of the former on top of the latter, as verified by the Hanušovce-1 borehole [*Behrmann et al*., 2000]. The southern boundary of the Pieniny wildflysch is a normal fault dipping to the southwest and following the general trend of the minor normal faults offsetting the Miocene fill of the IC basin. Constraints on the depth of the Oligocene horizon are provided by the Prešov-1 borehole and from available geological cross sections [*Milička et al*., 2011]. According to the adopted geological model and the results obtained from forward modeling integrated with paleothermal and low-temperature thermochronologic data, the thickness of the eroded strata has been estimated (see below). The maximum reconstructed thickness occurs in the central part of the OC, where the accretionary wedge reaches 19 km (measured without considering synorogenic erosion) (Figure 11b).

6.3.1. Restoration of the Preorogenic Tectonic Setting (Late Cretaceous)

The sequential restoration has been performed taking into account the same assumptions as for the previously described cross sections. Considering the uncertainties in the interpretation of basement geometry below the inner part of the allochthonous wedge, the footwall cutoff relative to foreland basin strata correlatable with coeval Stebnik Unit deposits has been placed 61 km south of the Carpathian thrust front, as already proposed by *Gągala et al*. [2012]. The resulting displacement estimated along the Carpathian frontal

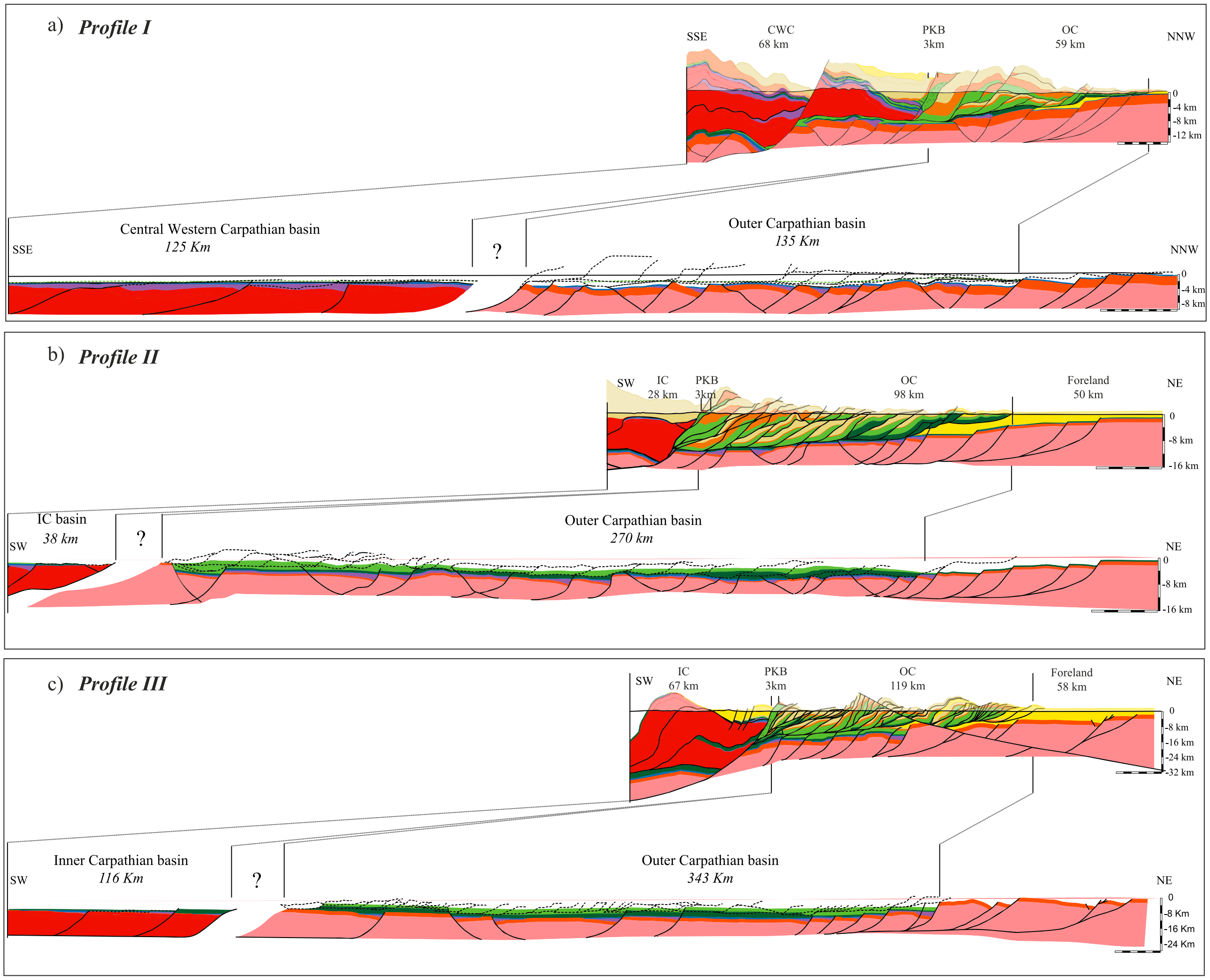

Figure 12. Restored cross sections. (a) Profile I at Early Cretaceous time. (b) Profile II and (c) Profile III at Late Cretaceous time. The sections have been sequentially restored based on the minimum shortening assumption. Black dashed lines show trajectories of future thrusts. In the southernmost part of Profile III the geometry of the eroded Variscan deposits corresponds partially to the outcropping successions, but it is in line with the general geological setting of the specific area.

thrust is of approximately 29 km. Additional displacement has been transferred to the Carpathian leading thrust by the reverse-slip reactivation of preexisting basement normal faults during the Neogene [*Oszczypko et al*., 2006]. A minor strike-slip reactivation of the foreland structures has been also detected by the occurrence of the pop-up structures in the Miocene siliciclastic deposits [*Krzywiec*, 2001] causing negligible out-of-plane moment along Profile III, in the foreland area.

Unfortunately, the correlation between the neighboring thrust sheets cannot be carried out without uncertainties, since the present-day position of all the emergent leading thrusts is controlled by erosion. We suggest a conservative scenario in order to minimize the shortening and be consistent with the estimate of burial given by the paleothermal and low-temperature thermochronometric indicators. Once restored to their initial configuration, the OC basin reaches a width of 343 km (Figure 12c). This value is considerably less than the approximately 600 km wide basin proposed by *Gągala et al*. [2012]. This discrepancy results essentially from a different interpretation of the deep structures, such as the number of the buried duplexes deforming the Dukla Unit. Since the number of the buried structures cannot be inferred without uncertainties, we propose an architecture, whose restoration provides shortening values comparable with the adjacent sections. The shortening value calculated for the OC successions is around 221 km (64%). On the other hand, the original length obtained for the Late Cretaceous IC basin is 116 km, subsequent shortening amounting to approximately 49 km (42%).

7. Controversy on the Interpretation of the PKB

The PKB is an independent domain separating the Austroalpine successions, included in the IC, from the OC basin belonging to the European Platform. Explaining its genesis and structure is still difficult due to the numerous and contradicting interpretations available in literature. The PKB is composed of no-metamorphic, erosion-resistant Mesozoic blocks surrounded by flysch, shaly, and marly matrix. These blocks are interpreted as part of a thrust stack [*Krobicki and Golonka*, 2008; *Pieńkowski et al*., 2008; *Schmid et al*., 2008], each of them correlated to distinct paleogeographic domains. On the other hand, many authors [e.g., *Nemčok*, 1980; *Cieszkowski et al*., 2009; *Golonka et al*., 2015] suggested the sedimentary origin of these units, describing the sedimentological and structural features of the olistoliths and olistostromes widely present in the PKB. *Golonka et al*. [2015] distinguished two parallel "olistostrome belts": the olistoliths and olistostrome of the southern belt derived from the IC Mesozoic cover, while the northern ones are related to the movement of the accretionary wedge during the Late Cretaceous. An opposite interpretation was provided by *Plašienka* [2012], who argued for an intrabasinal provenance of the olistoliths. According to the latter author, only minor exotic recycled pebbles (Klape Unit) come from the IC.

Most of Mesozoic paleogeographic reconstructions interpreted this "mèlange" as being the remnants of a sedimentary succession deposited in a wide oceanic basin, which represents the eastern branch of the Piemont-Ligurian Ocean (Vahic Ocean) [*Csontos and Vörös*, 2004; *Golonka et al*., 2006; *Plašienka*, 1995a, 2003]. *Göğüş et al*. [2016] argued that this ocean could not have been so wide.

The occurrence of different tectonic units within the PKB has been correlated to distinct preshortening paleogeographic domains. Simplifying, the shallow-water deposits have been associated to two distinct ridges: the Czorsztyn Ridge, originally separating the Magura Basin from the Pieniny Basin, and the Andrusov Ridge, originally located between the Pieniny Basin and the innermost Manín basin [*Birkenmajer*, 1986]. A progressive facies change occurs from the shallow-water to the Middle-Upper Jurassic deepwater deposits belonging to the basins originally interposed between the above mentioned ridges. The Jurassic succession is conformably overlain by Lower Cretaceous marls and Upper Cretaceous flysch deposits (see *Birkenmajer* [1986] for details). The youngest deposits are represented by the clastic Jarmuta Formation. Only the Pieniny Basin and the Czorsztyn Ridge (part of the Oravic Units) belong to the Vahic domain. The Manín Unit has sedimentological affinity with the IC nappes. For all these reasons the PKB has been regarded as marking the locus of an ancient plate boundary (oceanic suture) [*Uhlig*, 1907; *Andrusov*, 1931, 1938; *Birkenmajer*, 1953, 1960]. The closure of this ocean and the subsequent subduction of the oceanic slab started in the Late Cretaceous. Stacking of upper crustal thrust sheets propagated northward throughout the Paleocene-early Eocene and terminated with the continental collision of the ALCAPA and Tisza-Dacia microplates with the European Plate during the middle-late Miocene [*Săndulescu*, 1988; *Schmid et al*., 2008; *Matenco et al*., 2007]. At variance with the traditional interpretation, the occurrence of oceanic crust has been doubted upon by *Jurewicz* [2005] and *Roca et al*. [1995] who provided a tectonic model suggesting the presence of thinned continental crust flooring the Oravic and Vahic domains during the Mesozoic in the Polish region and a very narrow oceanic crust in the more western part of the Pieniny Basin.

In this paper we support the hypothesis that the PKB was deposited on thinned continental crust interposed between the IC and OC since the following:

i. Geophysical evidences indicate the absence of a continuous oceanic slab subducted beneath the Western Carpathians.
ii. No in situ ophiolites/high-pressure rocks occur in the PKB. High-pressure (blueschist facies) rocks have been found only as pebbles [*Schmid et al*., 2008]. The detritic ultramafic and anchi-metamophic rocks (Iňačovce-Krichevo Unit) drilled by five wells in the Eastern Slovakia and Ukraine [*Soták et al*., 1993] have been interpreted as belonging to a metamorphic core complex (made of units analogous to the Penninic Units of the Alps) buried under the Neogene deposits of the Pannonian Basin. They occur mostly as detritus in the Jurassic succession and are confined within the East Slovakian volcanic province. *Soták et al*. [1994, 2000] interpreted such rocks as pertaining to a pull-apart area made of ophiolite successions likely belonging to the Piemont-Ligurian Ocean [*Schmid et al*., 2008].
iii. The marked lateral lithofacies variations described by *Birkenmajer* [1986] are also typically recorded in successions deposited on rifted continental margins, as it has been documented, e.g., the Umbria-Marche successions in the northern Apennines [*Marchegiani et al*., 1999]. There, Lower Jurassic peritidal

carbonate platform facies (Calcari Massiccio Formation) and overlying condensed deposits pass laterally to basin sediments consisting of a complete succession including the Corniola, Rosso Ammonitico, Calcari e Marne a Posidonia, Calcari Diasprigni, and Maiolica formations [*Santantonio*, 1993, 1994]. These facies are straightforwardly comparable with the PKB successions, in which shallow-water deposits (ascribed to the "Czorsztyn Ridge") pass laterally to the pelagic sediments deposits of the Branisko Succession [*Birkenmajer*, 1986]. Therefore, it may be envisaged that successions with similar sedimentological composition, uplifted by thrusting and eroded in the IC, sourced the blocks included in the PKB. Thus, we interpret the region as a wide-rifted continental area during the Early Mesozoic, possibly with a narrow oceanic domain between the IC and OC margins, the wider ocean (i.e., the Meliata-Maliac domain) being located farther south.

8. Forward Modeling

Forward modeling is used in this study to validate the cross sections that were previously balanced and sequentially restored. The method requires as input parameters the displacement values obtained from the sequential restoration, the thickness of the undeformed successions, as well as the timing of deformation. The aim of the forward modeling is to produce a final deformed section that is as much as possible similar to the present-day tectonic setting. We present the 2-D kinematic modeling performed on Profile I (Figure 13) in order to show the geological scenario that holds for all the profiles. We model the evolution of the Carpathian basin from 145 Ma to the present day. The Early Cretaceous geological setting is the result of Permo-Triassic rifting and subsequent postrift Mesozoic sedimentation controlled by the faulted basement architecture (Figure 13a). This preshortening geometry comes from the sequential restoration. Shortening started during the Neocomian and involved the inner part of the CWC realm. Deformation then propagated northward, in the IC realm, producing the reverse-slip reactivation of preexisting normal faults and basin inversion (Figure 13b). The onset of thrusting in the IC is constrained by stratigraphic evidence, the youngest sediments preserved in the IC domain being Turonian in age [*Săndulescu*, 1988]. The inherited Mesozoic normal faults occurring in the crystalline basement were characterized by variable angles of dip. Their reactivation, during the Late Cretaceous-Paleocene inversion (Laramian inversion), caused their propagation into the overlying Mesozoic succession. The upward propagation into the Mesozoic succession involved a staircase trajectory of the thrusts, which propagated as flat segments along the Triassic evaporites. Thick-skinned deformation produced the imbrication of basement-involved thrust sheets. East of profile I, the Laramian inversion involved the Mesozoic normal faults of the European Platform [*Roure et al*., 1993], influencing the distribution of the black shales detachment horizon and, subsequently, the propagation of thrusting and its geometry in the OC basin. Quantifying the amount of shortening affecting the Pre-Eocene deposits of the OC basin is really difficult due to the multiple tectonic stages involving the basement faults (i.e., possible extension associated to the progressive emplacement of the accretionary wedge and Miocene inversion).

Subaerial exposure of the IC and associated erosion provided the sediment supply filling the Pieniny Basin, north of the IC front (Figure 13c). Provenance and sedimentological studies [e.g., *Birkenmajer*, 1956] document the southern provenance of the olistolithes and olistostromes included in the Pieniny succession, as well as their sedimentological similarity with the IC successions. The erosional event affecting the IC domain is marked by a regional unconformity; conglomerates together with poorly sorted sandstones and breccias overlain by the Eocene nummulitic trasgressive deposits [*Soták et al*., 2001] lay directly on top of the Mesozoic IC nappes. During the Late Cretaceous, the emplacement of the IC thrust sheets caused the flexure of the lower plate and the southward deepening of the OC basin, as recorded by the thickening of the Upper Cretaceous-Paleocene succession [*Nemčok et al*., 2000]. A change in tectonic style occurred during the Paleocene, switching from thick-skinned to thin-skinned thrusting. This change can be likely due to the occurrence of less competent deposits, more prone to behave as detachment levels for the future thrust planes, forming at the Late Cretaceous deformation front. Thus, the deposition of the thick Cretaceous shaly formation in the OC allowed subsequent thrusting to propagate at shallower depths instead of developing deeper in the basement. The deformation front reached the southern margin of the Magura paleogeographic realm during the middle Eocene [*Bromowicz*, 1999]. Shortening rates increased during the Oligocene, when thrusting propagated farther north into the OC paleogeographic realm. The southward thickening of the Eocene and Oligocene strata [*Nemčok et al*., 2000] suggests an increasing flexure of the lower plate due to the tectonic load provided by the advancing chain (Figure 13d). This remarkable change in thickness of

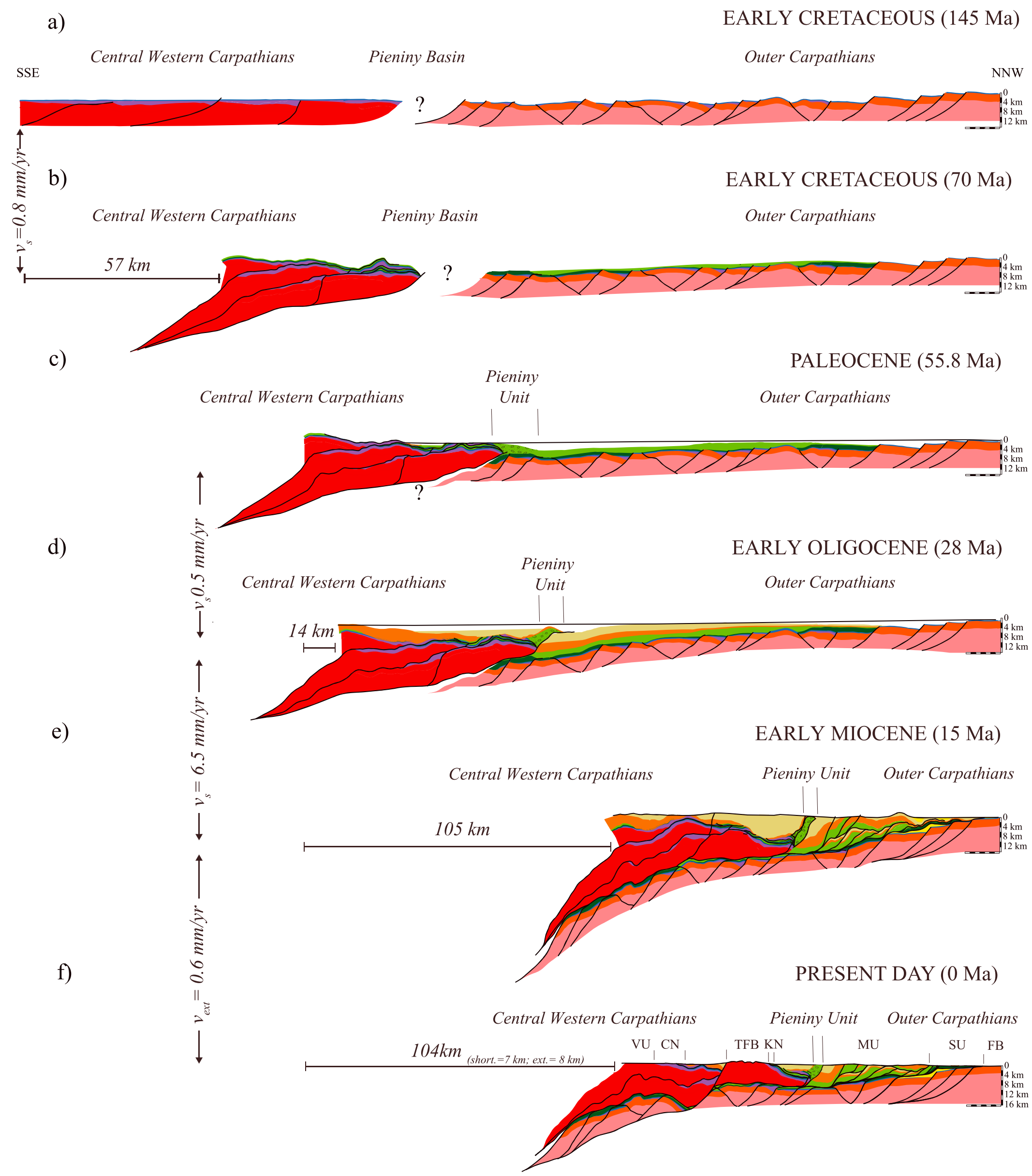

Figure 13. Forward modeling showing the evolution of the Carpathian region, from the Central Western Carpathians (CWC) to the foreland. (a) Initial stage at the beginning of the Early Cretaceous, before the deformation of the inner succession of the CWC (that will later produce the Veporic Unit). (b) Basement-involved thrusting in the CWC domain. (c) Thrusting and erosion of the Mesozoic sedimentary cover on top of the Tatricum crystalline basement and subsequent sedimentation in the Outer Carpathian foreland basin. Deposition of the Pieniny wildflysch in the frontal part of the Inner Carpathians. (d) Thrusting of the Pieniny wildflysch on top of the Outer Carpathian successions. (e) In-sequence thrust propagation in the Outer Carpathian domain. (f) Reverse-slip reactivation of Mesozoic normal faults in the basement and later normal faulting within the accretionary wedge. Erosion of the uppermost successions occurred during the middle-upper Miocene. VU: Vepor Unit; CN: Choč Nappe; KN: Križna nappe; TFB: Tatra-Fatra Belt; MU: Magura Unit; SU: Silesian Unit; and FB: foreland basin.

the OC Paleogene successions is also confirmed by low-T thermochronometric data [*Andreucci et al.*, 2013]. In-sequence, thin-skinned thrust propagation in the OC domain continued up to the early Miocene. It started with the emplacement of the far-traveled Magura thrust sheet on top of the Silesian deposits and then continued with the imbrication of the buried hinterland-dipping duplexes within the underlying Silesian Units (Figure 13e). Subsequently, shortening migrated at depth into the basement [*Oszczypko et al.*, 1998] producing localized uplift of the basement [*Oszczypko et al.*, 2006]. This downward migration of the deformation could be associated with the buttressing effect of preexisting high-angle normal faults that did not allow the Carpathian front to propagate into the Miocene foredeep deposits. Another possible reason could be change in the orientation of the maximum compressional stress, causing the rotation of the basement blocks and, consequently, Miocene activation of Mesozoic faults. The reactivation of preexisting basement normal faults in a reverse sense deformed the sole thrust of the accretionary wedge producing further shortening. During this stage, erosion started to involve the uppermost successions of the inner part of the OC thrust and fold belt. The gravitational instability of the wedge and its subsequent extensional collapse led to the development of normal faults [*Mazzoli et al*., 2010], some of them reactivating preexisting tectonic contacts. This tectonic event was coeval with rapid erosion during the late Miocene and was followed by a regional uplift localized in the CWC region (Figure 13f). Comparing the cooling ages obtained for the western sector of the OC [*Andreucci et al*., 2013] with the new thermochronometric data from the PKB presented in this paper (Figure 5), a remarkable difference in the timing of exhumation can be recognized. Cooling ages ranging between 20 and 15 Myr characterize the western Polish OC successions, whereas a more recent exhumation event (8–20 Myr) involves the PKB deposits. Cooling ages for the PKB are consistent with the published exhumation ages for the IC domain [*Burchart*, 1972; *Baumgart-Kotarba and Král*, 2002; *Danišìk et al*., 2008, 2010, 2011, 2012a, 2012b; *Śmigielski et al*., 2012, 2016], thus suggesting a common cooling event for these two different tectonic domains, as shown in our structural model [see also *Castelluccio et al*., 2015]. Forward modeling allowed us not only to validate the geological cross sections and contextualize the thermochronometric data sets but also to calculate the shortening rate for each step of the reconstructed tectonic evolution. According to our model, the shortening rate for the first convergent tectonic stage (Cretaceous thick-skinned inversion) was of 0.8 mm/yr. A lower rate, 0.5 mm/yr, dominated the Paleocene to early Oligocene time interval. This is in agreement with the Eocene period of relative tectonic quiescence suggested by *Książkiewicz* [1957, 1960] and *Świdziński* [1948]. A remarkable increase of the shortening rate, reaching a value of 6.5 mm/yr, characterized the late Oligocene-early Miocene time interval. This was associated with a major change in the style of thrusting, from thick skinned to thin skinned. Thrusting was then followed by middle Miocene normal faulting within the accretionary wedge, characterized by an extension rate of approximately 0.6 mm/yr.

9. Discussion

Unlike most of the works dealing with the tectonic evolution, time of deformation, and amount of shortening of the OC thrust and fold belt, the aim of this paper is to provide a comprehensive picture of the whole Carpathian orogen-foreland basin system, focusing on the relationships among the IC, PKB, and OC. Based on the reappraisal of stratigraphic and structural studies integrated with our own observations, a new scenario is proposed for the tectonic evolution of the OC thrust and fold belt. Our model involves an Early Cretaceous preshortening tectonic setting consisting of a sedimentary basin floored by thinned continental crust, on which all the preserved successions of the Inner and the Outer Carpathian domains were deposited, and an unknown—but probably limited if not null—amount of oceanic lithosphere. This paleogeographic setting is consistent with sedimentological evidences: all the successions, from the Upper Cretaceous to the Oligo-Miocene, consist of siliciclastic deposits characterized by almost the same lithology with variable sand/shale ratio. In addition, some marker levels (such as the *Globigerina Marls*, the Menilite bituminous shales, the Upper Cretaceous Puchov-type marls, and the Inoceramian-type beds) are continuous throughout the whole Carpathian depositional basin, thus indicating a similar sedimentary environment for both the IC and OC successions [*Jankowski et al*., 2012]. The lithostratigraphy of the Pieniny and the IC successions (e.g., Krížna Nappe) are also very similar, consisting of approximately 50 m thick Jurassic radiolarites overlying carbonates (Sokolica and Czajakowa Radiolarite on the Podzamcze Limestone [*Birkenmajer*, 1977]). The absence of in situ ophiolite sequence, except in Eastern Slovakia where some boreholes drilled serpentinized peridotites (so-called Iňačovce-Kriscevo Unit [*Soták et al*., 1993, 1994, Soták *et al*., 2000]) included in the volcanic province, does not suggest the presence of a so wide and continuous oceanic crust flooring the Pieniny Basin. The outcropping lithologies rather suggest subsidence and deepening of the basin in Jurassic times, as already proposed by *Kotański* [1963]. Our model is clearly at variance with various paleogeographic reconstructions proposed in the literature [e.g., *Golonka et al*., 2006; *Nemčok et al*., 2000, 2006a; *Oszczypko*, 2006; *Picha et al*., 2006], as it implies lower shortening values and no huge differences between the IC and OC original position in terms of latitude. The most obvious difference between our reconstruction and many preexisting models concerns the number of sedimentary basins originally present in the Carpathian region. Most previously proposed paleogeographic settings involve several deepwater basins, roughly NW-SE oriented, separated by ridges with almost the same orientation (from north to south: Skole and Silesian Basins, Silesian Ridge, Magura Basin, Czorsztyn Ridge, and Pieniny Basin). This subdivision derives mainly from stratigraphic observations and provenance analysis performed on pebbles and olistoliths found in the OC deposits [*Książkiewicz*, 1965; *Unrug*, 1968; *Golonka et al*., 2000, 2006; *Picha et al*., 2006; *Oszczypko*, 2006]. According to these studies, the main sources of sediments were (i) a northern massif located along the European margin for the Skole Basin, (ii) the Silesian Ridge for the inner part of the Silesian Basin and the outer Magura Basin, and (iii) the PKB for the inner part of the Magura Basin [*Książkiewicz*, 1977a, 1977b; *Oszczypko et al*., 2005]. However, the stratigraphic successions, described in detail in several works [i.e., *Ślączka et al*., 2006], suggest that all the OC tectonic units were part of a single, wide—though internally structured—foreland basin developed north to the IC belt after the emplacement of the latter onto the southern margin of the European Platform. The inferred system of deepwater basins separated by continuous, long ridges is likely to have actually consisted of an articulated and rather irregular pattern of fault-bounded blocks segmenting the basin. Accordingly, the observed distribution of turbiditic fans and the provenance of the pebbly deposits could have been controlled by the Cretaceous reactivation of basement normal faults, as a result either of foreland extension associated with the flexure of the foreland lithosphere or of early tectonic inversion predating the imbrication and stacking of thrust units on top of the thinned European Platform and the subsequent flexure of the latter. Uplift of some localized areas within the OC basin probably led to the mobilization of unconsolidated sediments whose distribution, similarly to that of the main turbidites sourced by the Late Cretaceous mountain belt, could be mainly controlled by the interaction with significant structures occurring within the basin. Confined turbidites, being characterized by long-range transport and deposition of fine-grained sediments on flank—not distal—areas of the basins, can explain most of the features observed in OC sedimentary units.

Following the Late Cretaceous phase, and the consumption of any oceanic lithosphere possibly interposed between the IC and OC continental margins, a S-SW deepening basin developed on top of the subsiding European Platform in front of the IC. The related accommodation space, forming in the proximal part of the IC chain, was filled by the Pieniny olistoliths and olistostromes coming from the erosion of the IC Mesozoic nappes. Subsequent thrust propagation into the foreland basin led to the partial tectonic superposition of Pieniny Unit on top of the Magura successions during the Eocene-early Oligocene. This scenario is at variance with the interpretation of the PKB as an oceanic basin suture characterized by abrupt lateral changes of facies reflecting different paleobathymetry, from the shallow-water marine deposits belonging to the Czorsztyn Ridge to the distal Czertezik and Niedzica successions and the basinal Branisko and Pieniny successions [e.g., *Birkenmajer*, 1960, 1986, 2008; *Birkenmajer et al*., 2008]. According to the latter interpretation, the subduction of the Pieniny Ocean during the Cenomanian, the subsequent Savian shortening event (early Miocene) [*Andrusov*, 1938], and erosion [*Birkenmajer*, 1960] led to the exhumation of the PKB. However, our new thermochronometric data indicate that exhumation of the PKB occurred later, in middle-late Miocene times. The cooling ages from the PKB are consistent with those of the surrounding thrust belt units, thus confirming that the PKB formed part of the thrust belt and did not experience a different thermal evolution. The estimated and the average cooling rates, calculated for the last 10 Ma, are of approximately 25°C/Myr. The existence of a suture zone in the PKB should have implied the presence of deposits at least reaching metamorphic temperatures, which is not the case of the Pieniny deposit [*Wójcik-Tabol*, 2003]. Our reappraisal of the PKB is consistent with the interpretation by *Roca et al*. [1995], who suggested a sedimentary origin for this unit, stacked on top of the OC, being in turn partially overthrusted by the Tatra nappes to the south. In addition, it allows reconciling the sedimentologic features of the wildflysch described by *Plašienka* [2012] with the lateral change of facies observed by *Birkenmajer* [1960]. The deposition of the Pieniny olistoliths on the flexed foreland lithosphere and its subsequent thrusting on top of the OC successions mark the end of the IC thick-skinned deformation and the closure of any oceanic domain originally present in the area. The switch in tectonic style from thick-skinned to thin-skinned thrusting due to the change in the rheology of the décollement layer was followed by in-sequence propagation of thrusting in the OC (note that our model is at variance with the interpretation of the Magura Unit as an out-of-sequence thrust sheet [e.g., *Gągala et al*., 2012; *Nemčok et al*., 2006a], for which no convincing structural evidence has ever been provided). The end of deposition on top of Magura Unit in the Upper Oligocene and the occurrence of Early

Oligocene deposits at the footwall of the Magura thrust can be interpreted both as the out-of-sequence imbrication of the Magura on top of Dukla Unit [*Gągala et al*., 2012; *Nemčok et al*., 2006a] and as the emplacement of Magura thrust during the upper Oligocene with possible removal of younger deposits at the footwall. The later activity of the Dukla and Silesian thrusts is also proved by the occurrence of synorogenic late Miocene deposits [*Gągala et al*., 2012]. The middle Oligocene-early Miocene stage was characterized by a dramatic increase in the shortening rate, which passed from 0.8 mm/yr during the Cretaceous, through a tectonically unconstrained period (oceanic subduction?) during the Paleogene (70–28 Ma), to an approximately 6.5 mm/yr during early Oligocene-early Miocene times. The Oligo-Miocene acceleration of shortening could have been triggered by internal orogen dynamics (the presence of an efficient detachment level), by external causes related to the movement of the converging plates, or by a combination of both. Lower shortening rates characterized the latest thrusting stages, when active shortening migrated at depth into to the basement. Postthrusting normal faulting affected the accretionary wedge, probably due to the extensional collapse associated with the deactivation of the sole thrust. Crustal normal faults also occur, such as the Sub-Tatra fault and the fault south of the Central Carpathian Depression [*Hrušecký et al*., 2002; *Probulski and Maksym*, 2015]; these could be related to a regional extensional regime, affecting not only the deformed wedge but also the underlying basement. This is the case for the eastern part of the Polish Carpathians, where low-angle normal faults offset the basement of the foreland [*Probulski and Maksym*, 2015]. These faults are interpreted to have played a primary role in the rapid unroofing of localized portions of the OC [*Andreucci et al*., 2013]. This regional extensional regime could have been triggered by a combination of deep lithospheric processes, also controlling the Miocene extension and development of the Pannonian Basin [*Fodor et al*., 1999; *Horváth and Cloetingh*, 1996]. Back-arc formation occurred in the absence of absolute plate motions, since shortening has been entirely accommodated by interior extension [*Horváth et al*., 2015; *Matenco et al*., 2016]. These processes are driven by the occurrence of inherited subducted slabs [*Bennett et al*., 2008; *Martin and Wenzel*, 2006; *Wortel and Spakman*, 2000], mantle upwelling inducing passive extension [*Huismans and Beaumont*, 2014], and the associated dynamic topography mechanisms [*Burov and Cloetingh*, 2009; *Horváth et al*., 2015; *Balázs et al*., 2016]. SW dipping subduction during the Miocene, with the slab having been either detached and/or rolled back to the east, was accompanied by lithosphere thinning associated with Neogene extension and heating [*Grad et al*., 2006] which are likely to be reflected by the normal faults depicted in our cross sections.

Thermochronometry allowed us to constrain our structural model, particularly for the last 15 Ma. AFT and AHe data indicate that the PKB and the IC experienced the same exhumation event during middle-late Miocene regional uplift.

10. Conclusions

In this paper we suggest a new interpretation for the tectonic evolution of the Central Western Carpathian thrust and fold belt. In particular, a new scenario has been proposed for the Cretaceous paleogeography and for the origin of the so-called Pieniny Klippen Belt which, independently of the occurrence and extent of oceanic lithosphere between the IC and OC domains, represents an intensely deformed sedimentary unit deposited in the frontal part of the IC. According to our sequential restoration, the preorogenic tectonic setting consisted of an extensional system whose architecture controlled the thickness of synrift and postrift deposits. The extent of this rifted continental area was variable. Profile I has been restored to a 135 km wide OC basin and 125 km wide IC basin, later experiencing a shortening of 54% and 57%, respectively. The shortening calculated for Profile II amounts to 63% for the OC and 26% for the IC, starting from a 270 km wide OC basin and a 38 km wide IC basin. Shortening remains almost constant (64%) in the eastern sector of the OC thrust and fold belt, increasing in the IC region. In Profile III, the OC have been restored to a 343 km wide original basin, whereas the restored IC basin has an original length of 116 km.

The Late Cretaceous Austroalpine tectonic phase affected the southern portion of the study area, causing reverse-slip reactivation of the Mesozoic normal faults and subsequent imbrication and basement uplift in the IC region. Following the complete consumption of any oceanic lithosphere originally present in the system, the flexure of the East European Platform produced by the tectonic load and the associated development of the foreland basin in the Outer Carpathian domain created the accommodation space that was filled by the Pieniny Unit north of the Inner Carpathian front. The olistoliths and olistostromes included in this basin come from the erosion of the stratigraphically and structurally higher Mesozoic successions belonging to the IC domain. Thick-skinned deformation proceeded with a shortening rate of approximately 0.8 mm/yr. Tectonic emplacement of the Pieniny Unit on top of Outer Carpathian successions marks the onset of thin-skinned thrusting. In-sequence propagation in the Outer Carpathian domain started with the high-displacement Magura Unit thrust. The subsequent development of the hinterland-dipping duplexes forming the progressively outer Dukla, Silesian, Subsilesian, and Skole units led to the present-day tectonic configuration of the OC accretionary wedge. Further displacement has been partially transferred to the OC frontal thrust by Miocene reverse-slip reactivation of preexisting basement normal faults. Crustal shortening was followed by extension, in some cases leading to significant unroofing of wide portions of the accretionary wedge. Structural observations integrated with low-T thermochronometric data suggest that postthrusting low-angle normal faults controlled the rapid exhumation of footwall units in the eastern part of the Polish Carpathians. On the other hand, the western Polish Carpathians were affected by erosion-controlled exhumation coeval with thrusting, apparently without a significant contribution by normal faulting. A middle-late Miocene exhumation of the Pieniny Klippen Belt has also been unraveled based on low-T thermochronometric data. The new cooling ages provided in this paper indicate exhumation almost coeval with that recorded in the Inner Carpathian domain and generally younger than that characterizing the Outer Carpathians. This pattern points to a regional uplift of the former domain in recent times.

Acknowledgments
Thorough and constructive reviews by two anonymous referees, together with useful comments and suggestions by Tectonics Associate Editor and Editor Claudio Faccenna, are gratefully acknowledged. The data used to produce the results of this paper are available for free from the corresponding author Ada Castelluccio at adacastelluccio@yahoo.it. Midland Valley Ltd. is gratefully thanked for providing Academic Licenses of Move software to the University of Naples and to the University of Padua. This work was supported by University of Padova (Progetto di Ateneo 2009, CPDA091987).

References

Anczkiewicz, A. (2005), Verification of maximum paleo-temperatures on the basis of smectite illitization estimated for the Tatra Mts., Podhale Basin and adjacent area of the External Carpathians using fission track method [in Polish], PhD thesis, 123 pp., Inst. Nauk Geol. Pol. Akad. Nauk, Osrodek Badawczy.

Anczkiewicz, A., M. Zattin, and J. Środoń (2005), Cenozoic uplift of the Tatras and Podhale basin from the perspective of the apatite fission track analyses, *Pol. Tow. Mineral. - Pr. Spec.*, *25*, 261–264.

Anczkiewicz, A., J. Środoń, and M. Zattin (2013), Thermal history of the Podhale Basin in the internal Western Carpathians from the perspective of apatite fission track analyses, *Geol. Carpathica*, *64*(2), 141–151, doi:10.2478/geoca-2013-0010.

Andreucci, B., A. Castelluccio, L. Jankowski, S. Mazzoli, R. Szaniawski, and M. Zattin (2013), Burial and exhumation history of the Polish Outer Carpathians: Discriminating the role of thrusting and post-thrusting extension, *Tectonophysics*, *608*, 866–883, doi:10.1016/j.tecto.2013.07.030.

Andreucci, B., A. Castelluccio, S. Corrado, L. Jankowski, S. Mazzoli, R. Szaniawski, and M. Zattin (2015), Interplay between the thermal evolution of an orogenic wedge and its retro-wedge basin: An example from the Ukrainian Carpathians, *Geol. Soc. Am. Bull.*, *127*(3–4), 410–427, doi:10.1130/B31067.1.

Andrusov, D. (1931), *Étude Géologique de la Zone des Klippes Internes des Carpathes Occidentales. I: Introduction. II: Stratigraphie (Trias et Lias)*, vol. 6, Rozpr. St. Geol. Úst, Praha.

Andrusov, D. (1938), *Etude Geologique de la Zone des Klippes Internes des Carpathes Occidentales. III: Tectonique*, vol. 9, Ibidem, Čs. Republ.

Andrusov, D. (1950), La zone des Klippes entre la Vlära et Zilina, *Geol. Sborn Slov. Akad. Vied*, *1*, 2–4.

Andrusov, D. (1974), The Pieniny Klippen Belt (the Carpathians of Czechoslovakia), in *Tectonics of the Carpathian-Balkan Region*, edited by M. Mahel', pp. 145–158, Geol. Inst. D. Štúr, Bratislava.

Bac-Moszaszwili, M. (1993), Structure on the western termination of the Tatra massif, *Ann. Soc. Geol. Pol.*, *63*, 167–193 (In Polish with English summary).

Balázs, A., L. Matenco, I. Magyar, F. Horváth, and S. Cloetingh (2016), The link between tectonics and sedimentation in back-arc basins: New genetic constraints from the analysis of the Pannonian Basin, *Tectonics*, *35*, 1526–1559, doi:10.1002/2015TC004109.

Baumgart-Kotarba, M., and J. Král (2002), Young tectonic uplift of the Tatra Mts.(fission track data and geomorphological arguments), paper presented at 17th Congress of Carpathian-Balkan Geological Association, Bratislava, Slovakia.

Behrmann, J. H., S. Stiasny, J. Milicka, and M. Pereszlenyi (2000), Quantitative reconstruction of orogenic convergence in the northeast Carpathians, *Tectonophysics*, *319*, 111–127, doi:10.1016/S0040-1951(00)00020-2.

Bennett, R. A., S. Hreinsdóttir, G. Buble, T. Bašic, Ž. Bacic, M. Marjanovic, G. Casale, A. Gendaszek, and D. Cowan (2008), Eocene to present subduction of southern Adria mantle lithosphere beneath the Dinarides, *Geology*, *36*, 3–6.

Bieda, F., S. Geroch, L. Koszarski, M. Książkiewicz, and K. Żytko (1963), Stratigraphie des Karpates externes polonaises, *Biul. Inst. Geol.*, *181*, 5–174.

Bielik, M., J. Šefara, M. Kováč, V. Bezák, and D. Plašienka (2004), The Western Carpathians—Interaction of Hercynian and Alpine processes, *Tectonophysics*, *393*, 63–86, doi:10.1016/j.tecto.2004.07.044.

Birkenmajer, K. (1953), Tectonics of the Pieniny Klippen Belt, Carpathians [in Polish], Regionalna Geol. Polski, 1, 2, (Tectonics of the Carpathians), Soc. Geol. Pol.

Birkenmajer, K. (1956), Sedimentary characteristics of the Jarmuta Beds (Maestrichtian) of the Pieniny Klippen Belt (Central Carpathians), *Bull. Acad. Pol. Sci.*, *4*, 729–735.

Birkenmajer, K. (1957), Remarks on the sedimentation of the Aalenian Flysch and the Jarmuta Beds (Senonian) of the Pieniny Klippen Belt, *Ann. Soc. Geol. Pol.*, *26*, 165–178.

Birkenmajer, K. (1958), Przewodnik geologiczny po pienińskim pasie skałkowym [in Polish], in *Pieniny Klippen Belt of Poland—Geological Guide*, Wyd. Geol., Warszawa, I (135 pp), II (74 pp.), III (88 pp.), IV (55 pp.).

Birkenmajer, K. (1960), Geology of the Pieniny Klippen Belt of Poland (A review of latest researches), *Jahrb. Geol. Bundesanst.*, *103*(1), 1–36.

Birkenmajer, K. (1977), Jurassic and Cretaceous lithostratigraphic units of the Pieniny Klippen Belt, Carpathians, Poland, *Stud. Geol. Pol.*, *45*, 1–158.

Birkenmajer, K. (1983), Strike-slip faults in the northern boundary zone of the Pieniny Klippen Belt, Carpathians, *Stud. Geol. Pol.*, *77*, 89–112.

Birkenmajer, K. (1985), Stage of structural evolution of the Pieniny Klippen Belt, Carpathians, *Stud. Geol. Pol.*, *88*, 7–31.

Birkenmajer, K. (1986), Stage of structural evolution of the Pieniny Klippen Belt, Carpathians, *Stud. Geol. Pol.*, *88*, 7–32.

Birkenmajer, K. (2003), Post-collisional Late Middle Miocene (Sarmatian) Pieniny Volcanic Arc, Western Carpathian, *Bull. Pol. Acad. Sci. Earth Sci.*, *51*, 79–89.

Birkenmajer, K. (2008), The Szopka Limestone Formation—A new lithostratigraphic name for Upper Liassic beds of the Pieniny and Branisko successions, Pieniny Klippen Belt (West Carpathians), *Stud. Geol. Pol.*, *131*, 229–235.

Birkenmajer, K., and J. Dudziak (1988), Age of Palaeogene flysch in the Pieniny Klippen Belt, Carpathians, Poland, based on calcareous nannoplankton, *Bull. Pol. Acad. Sci. Earth Sci.*, *36*, 15–24.

Birkenmajer, K., and P. Gedl (2012), Jurassic and Cretaceous strata in the Maruszyna IG-1 Deep Borehole (Pieniny Klippen Belt, Carpathians, Poland): Lithostratigraphy, dinoflagellate cyst biostratigraphy, tectonics, *Stud. Geol. Pol.*, *135*, 7–54.

Birkenmajer, K., P. Gedl, R. Myczyński, and J. Tyszka (2008), "Cretaceous black flysch" in the Pieniny Klippen Belt, West Carpathians: A case of geological misinterpretation, *Cretaceous Res.*, *29*, 535–549, doi:10.1016/j.cretres.2007.04.011.

Brandon, M. (1992), Decomposition of fission track grain-age distributions, *Am. J. Sci.*, *292*, 535–564.

Bromowicz, J. (1999), Olistoliths—A proof for the Middle Eocene mobility of the Magura Basin, paper presented at International Geological Conference "Carpathian Geology 2000", Smolenice.

Burchart, J. (1972), Fission-track age determination of accessory apatite from the Tatra Mountains, Poland, *Earth Planet. Sci. Lett.*, *15*, 418–422.

Burov, E. B., and S. A. P. L. Cloetingh (2009), Controls of mantle plumes and lithospheric folding on modes of intraplate continental tectonics: Differences and similarities, *Geophys. J. Int.*, *178*, 1691–1722.

Burtan, J., J. Chowaniec, and J. Golonka (1984), Wstępne wyniki badań nad egzotycznymi skałami węglanowymi z zachodniej części polskich Karpat fliszowych (Preliminary results of studies on exotic carbonate rocks in the western part of the Polish Flysch Carpathians), *Biul. Inst. Geol.*, *346*, 147–159.

Castelluccio, A., B. Andreucci, M. Zattin, R. A. Ketcham, L. Jankowski, S. Mazzoli, and R. Szaniawski (2015), Coupling sequential restoration of balanced cross-section and low-temperature thermochronometry: The case study of the Western Carpathians, *Lithosphere*, *7*(4), 367–378, doi:10.1130/L436.1.

Chamberlin, R. T. (1910), The Appalachian folds of Central Pennsylvania, *J. Geol. Chicago*, *18*, 228–251.

Chamberlin, R. T. (1919), The building of the Colorado Rockies, *J. Geol. Chicago*, *10*, 95–144.

Cieszkowski, M., N. Oszczypko, and W. Zuchiewicz (1987), Late Cretaceous submarine slump in the Inoceramian Beds of the Magura nappe at Szczawa, Polish Western Carpathians, *Ann. Soc. Geol. Pol.*, *57*, 189–201.

Cieszkowski, M., J. Golonka, M. Krobicki, A. Ślączka, N. Oszczypko, A. Waśkowska, and M. Wendorff (2009), The Northern Carpathian plate tectonic evolutionary stages and origin of olistolithes and olistostromes, *Geodin. Acta*, *22*(1–3), 101–126.

Csontos, L., and A. Vörös (2004), Mesozoic plate tectonic reconstruction of the Carpathian region, *Palaeogeogr. Palaeoclimatol. Palaeoecol.*, *210*, 1–56, doi:10.1016/j.palaeo.2004.02.033.

Čverčko, J. (1975), Preliminary report about results of the deep structural well Prešov-1, Mns. Geofond, Bratislava (in Slovak).

Danišìk, M., T. Pánek, D. Matýsek, I. Dunkl, and W. Frisch (2008), Apatite fission track and (U-Th)/He dating of teschenite intrusions gives time constraints on accretionary processes and development of planation surfaces in the Outer Western Carpathians, *Z. Geomorphol.*, *52*(3), 273–289.

Danišìk, M., M. Kohút, I. Broska, and W. Frisch (2010), Thermal evolution of the Malá Fatra Mountains (Central Western Carpathians): Insights from zircon and apatite fission track thermochronology, *Geol. Carpathica*, *61*, 19–27.

Danišìk, M., J. Kadlec, C. Glotzbach, A. Weisheit, I. Dunkl, M. Kohùt, N. J. Evans, M. Orvošová, and B. J. McDonald (2011), Metamorphism, exhumation and topographic evolution in orogenic belts by multiple thermochronology: A case study from the Nìzke Tatry Mts., Western Carpathians, *Swiss J. Geosci.*, *104*, 285–298.

Danišìk, M., H. D. Sinclair, F. M. Stuart, C. Persano, and P. Krzywiec (2012a), Exhumation history of the Tatry Mountains, Western Carpathians, constrained by low-temperature termochronometry, *Tectonics*, *35*, 187–207, doi:10.1002/2015TC003855.

Danišìk, M., M. Kohut, N. J. Evans, and B. J. McDonald (2012b), Eo-Alpine metamorphism and the "mid-Miocene thermal event" in the Western Carpathians (Slovakia): New evidence from multiple thermochronology, *Slovak Geol. Mag.*, *149*, 158–171.

Dumitru, T. A. (1993), A new computer-automated microscope stage system for fission-track analysis, *Nucl. Tracks Radiat. Meas.*, *21*(4), 575–580.

Dunkl, I. (2002), TRACKKEY: A Windows program for calculation and graphical presentation of fission track data, *Comput. Geosci.*, *28*(2), 3–12.

Dziadzio, P., A. Maksym, and B. Olszewska (2006), Miocene deposition in the eastern part of the Carpathian foredeep in Poland (in Polish with English summary), *Przegl. Geogr.*, *54*, 413–420.

Dziadzio, P. S. (2006), Geology of the Weglowa Oil Field, Subsilesian Unit, Polish Outer Carpathians, in *The Carpathians and Their Foreland: Geology and Hydrocarbon Resources*, *AAPG Mem*., vol. 84, edited by J. Golonka and F. J. Picha, pp. 259–291, American Association of Petroleum Geologists, Tulsa, Okla., doi:10.1306/985616m843071.

Dżułyński, S., and R. Gradziński (1960), Source of the Lower Triassic Clastics in the Tatra Mts., *Bull. Acad. Pol. Sci.*, *8*, 45–48.

Ernst, T., J. Jankowski, V. Semenov, A. Adam, M. Hvozdara, W. Jówiak, J. Lefeld, J. Pawliszyn, L. Szarka, and V. Wesztergom (1997), Electromagnetic soundings across the Tatra Mountains, *Acta Geophys. Pol.*, *45*, 33–44.

Faccenna, C., M. Mattei, R. Funiciello, and L. Jolivet (1997), Styles of back-arc extension in the central Mediterranean, *Terra Nova*, *9*, 126–130.

Faccenna, C., C. Piromallo, A. Crespo-Blanc, L. Jolivet, and F. Rossetti (2004), Lateral slab deformation and the origin of the western Mediterranean arcs, *Tectonics*, *23*, TC1012, doi:10.1029/2002TC001488.

Farley, K. A. (2002), (U-Th)/He dating: Techniques, calibrations, and applications, in *Noble Gases in Geochemistry and Cosmochemistry*, *Rev. Mineral. Geochem*., vol. 47, edited by D. Porcelli et al., pp. 819–844, Mineral. Soc. Am., Geochem. Soc., Chantilly, Va., doi:10.2138/rmg.2002.47.18.

Faryad, S. W. (1991), Pre-Alpine metamorphic event in Gemericum, *Miner. Slovaca*, *23*(5–6), 395–402.

Filo, I., and Z. Siranova (1998), Hornad and Chrast Member—New regional lithostratigraphic units of the Sub-Tatric Group, *Geol. Pr., Spravy*, *103*, 35–51.

Fleuty, M. J. (1964), The description of folds, *Geol. Assoc. Proc.*, *75*, 461–492.

Fodor, L., L. Csontos, G. Bada, I. Gyrfi, and L. Benkovics (1999), Tertiary tectonic evolution of the Pannonian Basin system and neighbouring orogens: A new synthesis of paleostress data, in *The Mediteranean Basins: Tertiary Extension Within the Alpine Orogen*, edited by B. Durand et al., *Geol. Soc. London, Spec. Publ.*, *156*, 295–334.

Földvary, G. Z. (1988), Geology of the Carpathian Region, *Geol. Mag.*, *126*(4), 443–457.

Froitzheim, N., D. Plašienka, and R. Schuster (2008), Alpine tectonics of the Alps and Western Carpathians, in *The Geology of Central Europe. II: Mesozoic and Cenozoic*, edited by T. McCann, pp. 1141–1232, Geol. Soc. Publ. House, London.

Gągala, Ł., J. Vergés, E. Saura, T. Malata, J. Ringenbach, P. Werner, and P. Krzywiec (2012), Architecture and orogenic evolution of the northeastern Outer Carpathians from cross-section balancing and forward modeling, *Tectonophysics*, *532–535*, 223–241, doi:10.1016/j.tecto.2012.02.014.

Galbraith, R. F., and G. M. Laslett (1993), Statistical models for mixed fission track ages, *Nucl. Tracks*, *5*, 3–14, doi:10.1016/1359-0189(93)90185-C.

Göğüş, O. H., R. N. Pysklywec, F. Corbi, and C. Faccenna (2011), The surface tectonics of mantle lithosphere delamination following ocean lithosphere subduction: Insights from physical-scaled analogue experiments, *Geochem. Geophys. Geosyst.*, *12*, 5.

Göğüş, O. H., R. N. Pysklywec, and C. Faccenna (2016), Postcollisional lithospheric evolution of the Southeast Carpathians: Comparison of geodynamical models and observations, *Tectonics*, *35*, 1205–1224, doi:10.1002/2015TC004096.

Golonka, J., N. Oszczypko, and A. Ślączka (2000), Late Carboniferous-Neogene geodynamic evolution and paleogeography of the circum-Carpathian region and adjacent areas, *Ann. Soc. Geol. Pol.*, *70*, 107–136.

Golonka, J., L. Gahagan, M. Krobicki, F. Marko, N. Oszczypko, and A. Ślączka (2006), Plate-tectonic evolution and Paleogeography of the Circum-Carpathian Region, in *The Carpathians and Their Foreland: Geology and Hydrocarbon Resources*, *AAPG Mem.*, vol. 84, edited by J. Golonka and F. J. Picha, pp. 11–46, American Association of Petroleum Geologists, Tulsa, Okla.

Golonka, J., K. Pietsch, and P. Marzec (2011), Structure and plate tectonic evolution of the northern Outer Carpathians, in *Tectonics*, pp. 65–92, INTECH Open Access Publ, Kraków, Poland.

Golonka, J., M. Krobicki, A. Waśkowska, M. Cieszkowski, and A. Ślączka (2015), Olistostromes of the Pieniny Klippen Belt, Northern Carpathians, *Geol. Mag.*, *152*(2), 269–286, doi:10.1017/S0016756814000211.

Grabowski, J. (1995), Palaeomagnetic studies in the High Tatra series, southern Poland, *Przegl. Geogr.*, *43*, 113–116.

Grabowski, J. (1997), Paleomagnetic results from the Cover (High Tatric) unit and Nummulitic Eocene in the Tatra Mts (Central West Carpathians, Poland) and their tectonic implications, *Ann. Soc. Geol. Pol.*, *67*, 13–23.

Grabowski, J. (2005), New Berriasian palaeopole from the Central West Carpathians (Tatra Mountains, southern Poland): Does it look Apulian?, *Geophys. J. Int.*, *161*(1), 65–80, doi:10.1111/j.1365-246X.2005.02539.x.

Grabowski, J., and M. Nemčok (1999), Summary of paleomagnetic data from the Central West Carpathians of Poland and Slovakia: Evidence for the late cretaceous-early tertiary transpression, *Phys. Chem. Earth Part A*, *24*(8), 681–685, doi:10.1016/S1464-1895(99)00099-X.

Grabowski, J., J. Michalik, R. Szaniawski, and I. Grotek (2009), Synthrusting remagnetization of the Krizna nappe: High resolution palaeo- and rock magnetic study in the Strazovce section, Strazovske vrchy Mts, Central West Carpathians (Slovakia), *Acta Geol. Pol.*, *59*(2), 137–155.

Grabowski, J., J. Haas, E. Márton, and A. Pszczółkowski (2010), Magneto-and biostratigraphy of the Jurassic/Cretaceous boundary in the Lókút section (Transdanubian Range, Hungary), *Stud. Geophys. Geod.*, *54*(1), 1–26, doi:10.2478/v10096-010-0018-z.

Grad, M., A. Guterch, G. Randy Keller, T. Janik, E. Heged⊠s, J. Vozár, A. Ślącka, T. Tiira, and J. Yliniemi (2006), Lithospheric structure beneath trans-Carpathian transect from Precambrian platform to Pannonian Basin: CELEBRATION 2000 seismic profile CEL05, *J. Geophys. Res.*, *111*, B03301, doi:10.1029/2005JB003647.

Gross, P., E. Köhler, and O. Samuel (1984), A new lithostratigraphical division of the Inner-Carpathian Paleogene, *Geol. Pr.*, *81*, 103–117 [In Slovak with English summary].

Gross, P., E. Köhler, J. Mello, J. Hasko, R. Halouzka, and A. Nagy (1993), *Geology of Southern and Eastern Orava, Bratislava*, 292 pp., D. Stur Inst. Geol, Bratislava.

Handy, M. R., S. M. Schmid, R. Bousquet, E. Kissling, and D. Bernoulli (2010), Reconciling plate-tectonic reconstructions with the geological-geophysical record of spreading and subduction in the Alps, *Earth Sci. Rev.*, *102*, 121–158.

Hayward, A. B., and R. H. Graham (1989), Some geometrical characteristic of inversion, in *Inversion Tectonics*, *Spec. Publ. Classics*, edited by M. A. Cooper and G. D. Williams, pp. 17–39, Geol. Soc., London.

Hók, J., P. Siman, W. Frank, J. Krá, J. Kotulová, and M. Rakús (2000), Origin and exhumation of mylonites in the Lúčanská Malá Fatra Mts. (Western Carpathians), *Slovak Geol. Mag.*, *6*, 325–334.

Homza, T. X., and W. K. Wallace (1994), Geometric and kinematic models for detachment folds with fixed and variable detachment depths, *J. Struct. Geol.*, *17*(4), 575–588, doi:10.1016/0191-8141(94)00077-D.

Horváth, F., and S. A. P. L. Cloetingh (1996), Stress-induced late-stage subsidence anomalies in the Pannonian Basin, *Tectonophysics*, *266*(1), 287–300.

Horváth, F., B. Musitz, A. Balázs, A. Végh, A. Uhrin, A. Nádor, B. Koroknai, N. Pap, T. Tóth, and G. Wórum (2015), Evolution of the Pannonian Basin and its geothermal resources, *Geothermics*, *53*, 328–352.

Houseman, G. A., and L. Gemmer (2007), Intra-orogenic extension driven by gravitational instability: Carpathian-Pannonian orogeny, *Geology*, *35*, 1135–1138, doi:10.1130/G23993A.1.

Hrušecký, I., L. Pospíšil, and M. Kohút (2002), Geological interpretation of the reflection seismic profile 753/92, in *Hydrocarbon Potential of the Eastern Slovakian Basin and Adjacent Areas*, *Open File Rep.*, edited by I. Hrušecký, Geol. Surv. Slovak Republic, Bratislava (in Slovakian).

Hrušecký, I., D. Plašienka, and L. Pospíšil (2006), Identification of the North European platform below the eastern part of the Western Carpathian Flysch belt, in *The Carpathians and Their Foreland: Geology and Hydrocarbon Resources*, *AAPG Mem.*, vol. 84, edited by J. Golonka and F. J. Picha, pp. 717–727, American Association of Petroleum Geologists, Tulsa, Okla.

Huismans, S. R., and C. Beaumont (2014), Rifted continental margins: The case for depth dependent extension, *Earth Planet. Sci. Lett.*, *407*, 148–162

Jaglarz, P., and J. Szulc (2003), Middle Triassic evolution of the Tatricum sedimentary basin: An attempt of sequence stratigraphy to the Wierchowa Unit in the Polish Tatra Mountains, *Ann. Soc. Geol. Pol.*, *73*, 169–182.

Jankowski, L., R. Kopciowski, and W. Ryłko (2004a), *Geological Map of the Outer Carpathians: Borderlands of Poland, Ukraine and Slovakia*, Pol. Geol. Inst., Warszawa.

Jankowski, L., R. Kopciowski, and W. Ryłko (2004b), *Geological Map of the Outer Carpathians: Borderlands of Ukraine and Romania*, Pol. Geol. Inst., Warszawa.

Jankowski, L., R. Kopciowski, and W. Ryłko (2012), The state of knowledge of geological structures of the Carpathians between Biała and Risca River—Discussion, *Biul. Państw. Inst. Geol.*, *449*, 203–216 (In Polish with English summary).

Janočko, J., M. Pereszlényi, D. Vass, V. Bezák, S. Jacko Jr., S. Jacko, M. Kohút, M. Polák, and J. Mello (2006), Geology and hydrocarbon resources of the Inner Western Carpathians, Slovakia, and Poland, in *The Carpathian and Their Foreland: Geology and Hydrocarbon Resources*, *AAPG Mem.*, vol. 84, edited by J. Golonka and F. J. Picha, pp. 569–603, American Association of Petroleum Geologists, Tulsa, Okla.

Jolivet, L. (2001), A comparison of geodetic and finite strain pattern in the Aegean, geodynamic implications, *Earth Planet. Sci. Lett.*, *187*, 95–104.

Jurewicz, E. (2000a), Tentative reconstructions of the stress axes from the thrust-folding stage in the Tatra Mts. on the basis of slickensides in the granitoid core, southern Poland [in Polish with English summary], *Przegl. Geol.*, *48*, 239–246.

Jurewicz, E. (2000b), Tentative correlation of the results of structural analysis in the granitoid core and nappe units of the Tatra Mts., southern Poland [in Polish with English summary], *Przegl. Geol.*, *48*, 1014–1018.

Jurewicz, E. (2005), Geodynamic evolution of the Tatra Mts. and the Pieniny Klippen Belt (Western Carpathians): Problems and comments, *Acta Geol. Pol.*, *55*(3), 295–338.

Jurewicz, E., and B. Bagiński (2005), Deformation phases in the selected shear zones within the Tatra Mts granitoid core, *Geol. Carpathica*, *56*, 17–28.

Ketcham, R. A. (2005), Forward and inverse modelling of low-temperature thermochronology data, *Rev. Mineral. Geochem.*, *58*, 275–314.

Ketcham, R. A., R. A. Donelick, and W. D. Carlson (1999), Variability of apatite fission-track annealing kinetics: III. Extrapolation to geological time scales, *Am. Mineral.*, *84*, 1235–1255, doi:10.2138/am.2006.464.

Kiriakidis, L. G. (1989), The Vardar ophiolite: A continuous belt under the Axios basin sediments, *J. Geophys. Int.*, *98*, 2, doi:10.1111/j.1365-246X.1989.tb03345.x.

Kohút, M., and S. C. Sherlock (2003), Laser microprobe Ar^{40}-Ar^{39} analysis of pseudotachylyte and host-rocks from the Tatra Mountains, Slovakia: Evidence for late Palaeogene seismic/tectonic activity, *Terra Nova*, *15*, 417–424, doi:10.1046/j.1365-3121.2003.00514.x.

Korab, T., and T. Durkovic (1978), *Geology of the Dukla Unit (East Slovakian Flysch)* (in Slovakian with English summary), 194 pp., Geologicky Ustav D. Stura, Bratislava.

Koszarski, L., and A. Ślączka (1976), The Outer (Flysch) Carpathians: The Cretaceous, in *Geology of Poland*, *Stratigr. Part 2*, vol. I, edited by S. Cieslinski, pp. 495–498, 657–679, 740–748, Inst. Geol., Warszawa.

Kotański, Z. (1961), Tectogénèse et reconstitution de la paléogéographie de la zone haut-tatrique dans les Tatras [in Polish with English summary], *Acta Geol. Pol.*, *11*, 187–467.

Kotański, Z. (1963), On the character of the Western Carpathian Mesozoic geosyncline and the Podhale epimiogeosyncline [in Polish with English summary], *Acta Geol. Pol.*, *13*, 13–25.

Kotlarczyk, J. (1978), Stratigraphy of the Ropianka Formation in the Skole unit of the Flysch Carpathians (in Polish with the English summary), *Pol. Akad. Nauk Oddział Krakowie, Kom. Nauk Geol. Pr. Geol.*, *108*, 1–82.

Kotlarczyk, J. (1985), An outline of the stratigraphy of marginal tectonic units of the Carpathian orogen in the Krakow-Przemysl area: Guide to Excursion 4, paper presented at the 13th Congress of Carpatho-Balkan Geological Association, Krakow, Poland.

Král', J. (1977), Fission track ages of apatites from some granitoid rocks in West Carpathians, *Geol. Zb. Geol. Carpathica*, *28*, 269–276.

Králiková, S., R. Vojtko, P. Andriessen, M. Kováč, B. Fügenschuh, J. Hók, and J. Minár (2014a), Late Cretaceous-Cenozoic thermal evolution of the northern part of the Central Western Carpathians (Slovakia): Revealed by zircon and apatite fission track thermochronology, *Tectonophysics*, *615–616*, 142–153, doi:10.1016/j.tecto.2014.01.002.

Králiková, S., R. Vojtko, L. Sliva, J. Minár, B. Fügenschuh, M. Kováč, and J. Hók (2014b), Cretaceous-Quaternary tectonic evolution of the Tatra Mts. (Western Carpathians): Constraints from structural, sedimentary, geomorphological, and fission track data, *Geol. Carpathica*, *65*(4), 307–326, doi:10.2478/geoca-2014-0021.

Krs, M., M. Krsova, and P. Pruner (1996), Paleomagnetismand paleogeography of the Western Carpathians from the Permian to the Neogene, in *Paleomagnetism and Tectonics of the Mediterranean region*, *Spec. Publ.*, vol. 105, edited by A. Morris and D. H. Tarling, pp. 175–184, Geol. Soc., Prague.

Kruczyk, J., M. Kądziałko-Hofmokl, J. Lefeld, P. Pagač, and I. Túnyi (1992), Paleomagnetism of Jurassic sediments as evidence for oroclinal bending of the InnerWest Carpathians, *Tectonophysics*, *206*, 315–324.

Kruglov, S. S. (2001), The problems of tectonics and paleogeodynamics of western Ukraine (a critical survey of the new publications) [in Ukrainian], paper presented at Ukrainian Interdisciplinary Committee for Tectonics, L'viv.

Krzywiec, P. (2001), Contrasting tectonic and sedimentary history of the central and eastern parts of the Polish Carpathian foredeep basin—Results of seismic data interpretation, *Mar. Pet. Geol.*, *18*, 13–38, doi:10.1016/S0264-8172(00)00037-4.

Książkiewicz, M. (1957), Geology of the Northern Carpathians, *Geol. Rundsch.*, *45*, 369–411.

Książkiewicz, M. (1960), Palaeogeographic outline of the Polish Flysch Carpathians, *Pr. Inst. Geol.*, *33*, 209–231.

Książkiewicz, M. (1962), Geological atlas of Poland: Stratigraphic and facial problems, Inst. Geol., Wyd. Geol., Warsaw, Poland, 16 maps.

Książkiewicz, M. (1965), Les Cordilléres dans les mers crétacées et paleogenes des Carpthes du Nord, *Bull. Soc. Geol. Fr.*, *7*, 443–455.

Książkiewicz, M. (1977a), Tectonics of the Carpathians, in *Geology of Poland, Tectonics*, *Wyd. Geol.*, vol. 4, edited by W. Pozaryski, pp. 476–604, Publ. House, Warsaw, Poland.

Książkiewicz, M. (1977b), Plate movement hypothesis and Carpathian development [in Polish], *Ann. Soc. Géol. Pol.*, *47*, 321–353.

Leško, B., and O. Samuel (1968), *Geology of the Eastern Slovakian Flysch* [in Slovakian with English summary], 256 pp., Slovenska Akad. Ved., Bratislava.

Leško, B., et al. (1985), *Oporny vrt Hanusovce-1*, *Reg. Geol. Zapadn. Karpat*, vol. 20, 205 pp., GUDS, Bratislava.

Lexa, J., V. Bezák, M. Elečo, J. Mello, M. Polák, M. Potfaj, and J. Vazár (2000), *Geological Map of Western Carpathians and Adjacent Areas 1:500000*, Geol. Surv. of Slovak Republic, Bratislava.

Ludwiniak, M. (2010), Multi-stage development of the joint network in the flysch rocks of western Podhale (InnerWestern Carpathians, Poland), *Acta Geol. Pol.*, *60*(2), 283–316.

Mahel', M. (1981), Island character of Klippen Belt: Vahicum—Continuation of Southern Penninicum in West Carpathians, *Geol. Zb. Geol. Carpathica*, *32*, 293–305.

Mahel', M. (1986), *Geologická stavba Československỳch Karpat: 1. Paleoalpínske jednotky*, 503 pp., Veda, Bratislava.

Mahel', M., and T. Buday (1968), *Regional Geology of Czechoslovakie: Part 2. The West Carpathians*, 723 pp., Geol. Surv. of Czechoslovakia, Praha.

Malata, T., and K. Żytko (2006), *Kuźmina-1*, *Profile Głębokich Otworów Wiertniczych* [in Polish], vol. 110, 68 pp., Państwowego Instytutu Geologicznego, Warszawa.

Maliverno, A., and W. B. F. Ryan (1986), Extension in the Tyrrhenian Sea and shortening in the Apennines as a result of arc migration driven by sinking of the lithosphere, *Tectonics*, *5*, 227–245, doi:10.1029/TC005i002p00227.

Marchegiani, L., G. Bertotti, G. Cello, G. Deiana, S. Mazzoli, and E. Tondi (1999), Pre-orogenic tectonics in the Umbria-Marche sector of the Afro-Adriatic continental margin, *Tectonophysics*, *315*, 123–143, doi:10.1016/S0040-1951(99)00277-2.

Marciniec, P., and Z. Zimnal (2006), *Borzęta IG-1*, *Profile Głębokich Otworów Wiertniczych* [in Polish], vol. 109, 66 pp., Państwowego Instytutu Geologicznego, Warszawa.

Martin, M., and F. Wenzel (2006), High-resolution teleseismic body wave tomography beneath SE-Romania-II. Imaging of a slab detachment scenario, *Geophys. J. Int.*, *164*, 579–595.

Márton, E., and P. Márton (1996), Large scale rotations in North Hungary during the Neogene as indicated by paleomagnetic data, in *Paleomagnetism and Tectonics of the Mediterranean Region*, edited by A. Morris and D. H. Tarling, *Geol. Soc. London, Spec. Publ.*, *105*, 153–173.

Márton, E., L. Mastella, and A. K. Tokarski (1999), Large counterclockwise rotation of the Inner West Carpathian Paleogene flysch—Evidence from paleomagnetic investigations of the Podhale Flysch (Poland), *Phys. Chem. Earth Part A*, *24*(8), 645–649.

Márton, E., M. Rauch-Włodarska, O. Krejčí, A. K. Tokarski, and M. Bubík (2009), An integrated palaeomagnetic and AMS study of the Tertiary flysch from the Outer Western Carpathians, *Geophys. J. Int.*, *177*(3), 925–940.

Márton, E., J. Grabowski, D. Plašienka, I. Túnyi, M. Krobicki, J. Haas, and M. Pethe (2013), New paleomagnetic results from the Upper Cretaceous red marls of the Pieniny Klippen Belt, Western Carpathians: Evidence for general CCW rotation and implications for the origin of the structural arc formation, *Tectonophysics*, *592*, 1–13.

Matenco, L., G. Bertotti, K. Leever, S. Cloetingh, S. M. Schmid, M. Tărăpoancă, and C. Dinu (2007), Large scale deformations at a locked collisional boundary: Coeval Pliocene-Quaternary differential tectonic movements in the foreland of the SE Carpathians, *Tectonics*, *26*, TC4011, doi:10.1029/2006TC001951.

Matenco, L., I. Munteanu, M. ter Borgh, A. Stanica, M. Tilita, G. Lericolais, C. Dinu, and G. Oaie (2016), The interplay between tectonics, sediment dynamics and gateways evolution in the Danube system from the Pannonian Basin to the western Black Sea, *Sci. Total Environ.*, *543*, 807–827, doi:10.1016/j.scitotenv.2015.10.081.

Matyszkiewicz, J., and T. Słomka (1994), Organodetrital conglomerates with ooids in the Cieszyn Limestone (Tithonian-Berriasian) of the Polish Flysch Carpathians and their paleogeographic significance, *Ann. Soc. Geol. Pol.*, *63*, 211–248.

Mazzoli, S., and A. M. Algarra (2011), Deformation partitioning during transpressional emplacement of a “mantle extrusion wedge”: The Ronda peridotites, western Betic Cordillera, Spain, *J. Geol. Soc.*, *168*(2), 373–382, doi:10.1144/0016-76492010-126.

Mazzoli, S., L. Jankowski, R. Szaniawski, and M. Zattin (2010), Low-T thermochronometric evidence for post-thrusting (<11 Ma) exhumation in the Western Outer Carpathians, Poland, *C. R. Geosci.*, *342*, 162–169, doi:10.1016/j.crte.2009.11.001.

McClusky, S., et al. (2000), Global Positioning System constraints on plate kinematics and dynamics in the eastern Mediterranean and Caucasus, *J. Geophys. Res.*, *105*(B3), 5695–5719, doi:10.1029/1999JB900351.

Meijer, P. T., and M. J. R. Wortel (1997), Present-day dynamics of the Aegean region: A model analysis of the horizontal pattern of stress and deformation, *Tectonics*, *16*(6), 879–895.

Milička, J., M. Pereszlényi, and A. Nagy (2011), Hydrocarbon potential of Northern promontories of the Pannonian Basin System in Slovakia, *Miner. Slovaca*, *43*, 351–364.

Morley, C. K. (1996), Models for relative motion of crustal blocks within the Carpathian region, based on restorations of the Outer Carpathian thrust sheets, *Tectonics*, *15*, 885–904, doi:10.1029/95TC03681.

Myśliwiec, M., et al. (2006), Hydrocarbon resources of the Polish Carpathian Foredeep: Reservoirs, traps, and selected hydrocarbon fields, in *The Carpathians and Their Foreland: Geology and Hydrocarbon Resources*, *AAPG Mem*., vol. 84, edited by J. Golonka and F. J. Picha, pp. 351–393, American Association of Petroleum Geologists, Tulsa, Okla., doi:10.1306/985613M843073.

Nemčok, J. (1980), Nontraditional view of East-Slovakian Klippen Belt, *Geol. Carpathica*, *31*(4), 563–568.

Nemčok, J., and D. Poprawa (Coords.) (1988–1989), *Geological Atlas of Western Outer Carpathian and Their Foreland*, Państw. Inst. Geol., Warszawa.

Nemčok, J., et al. (Eds.) (1994), *Geologická Mapa Tatier 1: 50 000*, MŽP SR-GÚDŠ, MOSZNL, PIG, Bratislava.

Nemčok, M., M. P. Coward, W. J. Sercombe, and R. A. Klecker (1999), Structure of the West Carpathian accretionary wedge: Insights from cross-section construction and sandbox validation, *Phys. Chem. Earth*, *24*, 659–665, doi:10.1016/S1464-1895(99)00096-4.

Nemčok, M., J. Nemčok, M. Wojtaszek, L. Ludhová, R. A. Klecker, W. J. Sercombe, M. P. Coward, J. Franklin, and J. Keith (2000), Results of 2D balancing along 20° and 21°30′ longitude and pseudo-3D in the Smilno Tectonic Window: Implications for shortening mechanisms of the West Carpathian accretionary wedge, *Geol. Carpathica*, *51*, 281–300.

Nemčok, M., J. Nemčok, M. Wojtaszek, L. Ludhová, N. Oszczypko, W. J. Sercombe, M. Cieszkowski, Z. Paul, M. P. Coward, and A. Ślączka (2001), Reconstruction of Cretaceous rifts incorporated in the Outer West Carpathian wedge by balancing, *Mar. Pet. Geol.*, *18*, 39–64, doi:10.1016/S0264-8172(00)00045-3.

Nemčok, M., P. Krzywiec, M. Wojtaszek, L. Ludhová, R. A. Klecker, W. J. Sercombe, and M. P. Coward (2006a), Tertiary development of the Polish and eastern Slovak parts of the Carpathian accretionary wedge: Insights from balanced cross sections, *Geol. Carpathica*, *57*, 355–370.

Nemčok, M., L. Pospíšil, I. Hrušecký, and T. Zsíros (2006b), Subduction in the remnant Carpathian Flysch Basin, in *The Carpathians and Their Foreland: Geology and Hydrocarbon Resources*, *AAPG Mem*., vol. 84, edited by J. Golonka and F. J. Picha, pp. 767–785, American Association of Petroleum Geologists, Tulsa, Okla., doi:10.1306/985628M843083.

Olszewska, B. W., and J. Wieczorek (1998), The Paleogene of the Podhale Basin (Polish Inner Carpathians)—Micropaleontological perspective, *Przegl. Geol.*, *46*(8/2), 721–728.

Oszczypko, N. (1991), Stratigraphy of the Palaeogene deposits of the Bystrica subunit (Magura nappe, Polish Outer Carpathians), *Bull. Pol. Acad. Sci. Earth Sci.*, *39*, 415–431.

Oszczypko, N. (2006), Late Jurassic-Miocene evolution of the Outer Carpathian fold-and-thrust belt and its foredeep basin (Western Carpathians, Poland), *Geol. Quart.*, *50*(1), 169–194.

Oszczypko, N., P. Krzywiec, M. Lemberger, M. Stefaniuk, K. Pietsch, and H. Trygar (1998), Integrated geological-geophysical interpretation of the Rzeszó w-Smilno profile (Western Carpathians), Abstract 446 presented at Carpath.-Balkan Geol. Assoc., XVI Congress, Vienna.

Oszczypko, N., M. Oszczypko-Clowes, J. Golonka, and F. Marko (2005), Oligocene-Lower Miocene sequences of the Pieniny Klippen Belt and adjacent Magura Nappe between Jarabina and Poprad River (East Slovakia and South Poland): Their tectonic position and paleogeographic implications, *Geol. Quart.*, *49*(4), 379–402.

Oszczypko, N., P. Krzywiec, I. Popadyuk, and T. Peryt (2006), Carpathian foredeep basin (Poland and Ukraine): Its sedimentary, structural, and geodynamic evolution, in *The Carpathians and Their Foreland: Geology and Hydrocarbon Resources*, *AAPG Mem*., vol. 84, edited by J. Golonka and F. J. Picha, pp. 293–350, doi:10.1306/985612M843072.

Oszczypko-Clowes, M. (2001), The nannofossil biostratigraphy of the youngest deposits of the Magura nappe (east of Skawa river, Polish Flysch Carpathians) and their paleoenvironmental condition, *Ann. Soc. Geol. Pol.*, *71*, 139–188.

Paul, Z., and D. Poprawa (1992), Budowa geologiczna płaszczowiny magurskiej w strefie przypienińskiej w świetle badań uzyskanych z wiercenia Nowy Targ PIG 1, *Przegl. Geol.*, *7*, 404–409.

Peszat, C. (1967), The lithological development and condition of sedimentation of the Cieszyn Limestones (with English summary), *Pr. Geol. Oddzial Krakowie*, *44*, 1–111.

Petrik, I., P. Nabelek, M. Janák, and D. Plašienka (2003), Condition of formation and crystallization kinetics of highly oxidized pseudotachylytes from the High Tatras (Slovakia), *J. Petrol.*, *44*, 901–927.

Picha, F., J. S. Zdeněk, and O. Kreci (2006), Geology and hydrocarbon resources of the Outer Western Carpathians and their foreland, Czech Republic, in *The Carpathians and Their Foreland: Geology and Hydrocarbon Resources*, *AAPG Mem*., vol. 84, edited by J. Golonka and F. J. Picha, pp. 49–175, American Association of Petroleum Geologists, Tulsa, Okla., doi:10.1306/985607M843067.

Pieńkowski, G., et al. (2008), Jurassic, in *The Geology of Central Europe: 2. Mesozoic and Cenozoic*, edited by T. McCann, pp. 823–922, Geol. Soc., London.

Plašienka, D. (1995a), Passive and active margin history of the northern Tatricum (Western Carpathians, Slovakia), *Geol. Rundsch.*, *84*, 748–760, doi:10.1007/BF00240565.

Plašienka, D. (1995b), Mesozoic evolution of Tatric units in the Malé Karpati and Považský Inovec Mts.: Implications for the position of the Klape and related units in western Slovakia, *Geol. Carpathica*, *46*, 101–112.

Plašienka, D. (Ed.) (1999), *Tektonochronolögia a Paleotektonicky Model Jursko-Kriedoveho Vyvoja Centrälnych Zäpadnych Karpät (Tectonochronology and Paleotectonic Evolution of the Central Western Carpathians During the Jurassic and Cretaceous)* [English summary], 127 pp, Veda, Bratislava.

Plašienka, D. (2003), Dynamics of Mesozoic pre-orogenic rifting in the Western Carpathians, *Mitt. Österr. Geol. Ges.*, *94*, 79–98.

Plašienka, D. (2011), The Pieniny Klippen Belt–structure, evolution and position in the Carpathian tectonic framework, *Geologické výzkumy na Moravě a ve Slezsku*, *1*, 39–44.

Plašienka, D. (2012), Early stage of structural evolution of the Carpathian Klippen Belt (Slovakian Pieniny sector), *Miner. Slovaca*, *44*, 1–16.

Plašienka, D., and M. Mikuš (2010), Geological structure of the Pieniny and Šariš sectiors of the Klippen Belt between the Litmanová and Drienica villages in Eastern Slovakia. Bratislava, *Miner. Slovaca*, *42*(2), 155–178 (In Slovak, English summary).

Plašienka, D., P. Grecula, M. Putiš, M. Kováč, and D. Hovorka (1997), Evolution and structure of the Western Carpathians: An overview, in *Geological Evolution of the Western Carpathians*, edited by P. Grecula, D. Hovorka, and M. Putiš, pp. 1–24, Min. Slovak, Bratislava.

Plašienka, D., J. Soták, M. Jamrichová, E. Halásová, D. Pivko, S. Jozsa, J. Madzin, and V. Mikuš (2012), Structure and evolution of the Pieniny Klippen Belt demonstrated along a section between Jarabina and Litmanová villages in Eastern Slovakia, *Miner. Slovaca*, *44*, 17–38.

Polák, M. (2008), General geological map of the Slovak Republic, Map sheet 27 - Poprad, Śtatny Geologickỳ ústav Dionýza Štúra.

Probulski, J., and A. Maksym (2015), Methodology of building a synergic velocity model for deep seismic surveys in terms of geological interpretation in parts of the Carpathian profile-POLCRUST, in *NAFTA-GAZ*, vol. 51, pp. 9, Oddział Geol. i Ekspl. PGNiG SA, Warsawa.

Prokešová, R., D. Plašienka, and R. Milovský (2012), Structural pattern and emplacement mechanisms of the Krížna cover nappe (Central Western Carpathians), *Geol. Carpathica*, *63*(1), 13–32, doi:10.2478/v10096-012-0001-y.

Putiš, M. (1994), South Tatric-Veporic basement geology: Variscan nappe structure; Alpine thick-skinned and extensional tectonics in the Western Carpathians (Eastern Low Tatra Mountains, Northwestern Slovak Ore Mountainis), *Mitt. Österr. Geol. Ges.*, *86*, 83–99.

Putiš, M., F. Wolfgang, D. Plašienka, and L. A. Biron (2009), Progradation of the Alpidic Central Western Carpathians orogenic wedge related to two subductions: Constrained by Ar/Ar ages of white micas, *Geodin. Acta*, *22*(1–3), 31–56, doi:10.3166/ga.22.31-56.

Rakús, M., M. Misík, J. Michalík, R. Mock, T. Durkovic, T. Koráb, R. Marschalko, J. Mello, M. Polák, and J. Jablonsky (1990), Paleogeographic development of the West Carpathians: Anisian to Oligocene, in *Evolution of the Northern Margin of Tethys*, *Mém. Soc. Géol. Fr. 154*, vol. 3, edited by M. Rakús et al., pp. 39–62, Paris.

Ratschbacher, L., W. Frisch, H. G. Linzer, and O. Merle (1991a), Lateral extrusion in the Eastern Alps. Part 2: Structural analysis, *Tectonics*, *10*, 257–271, doi:10.1029/90TC02623.

Ratschbacher, L., O. Merle, P. Davy, and P. Cobbold (1991b), Lateral extrusion in the eastern Alps. Part 1: Boundary conditions and experiments scaled for gravity, *Tectonics*, *10*, 245–256, doi:10.1029/90TC02622.

Reiners, P. W., T. L. Spell, S. Nicolescu, and K. A. Zanetti (2004), Zircon (U-Th)/He thermochronometry: He diffusion and comparisons with ^{40}Ar/^{39}Ar dating, *Geochim. Cosmochim. Acta*, *68*, 1857–1887, doi:10.1016/j.gca.2003.10.021.

Roca, E., G. Bessereau, E. Jawor, M. Kotarba, and F. Roure (1995), Pre-Neogene evolution of the Western Carpathians: Constraints from the Bochnia-Tatra Mountains section (Polish Western Carpathians), *Tectonics*, *14*, 855–873, doi:10.1029/95TC00828.

Roniewicz, P. (1959), Sedimentary characteristics in the High-Tatra Series. (In Polish, English symmary), *Acta Geol. Pol.*, *9*, 301–317.

Roure, F., E. Roca, and W. Sassi (1993), The Neogene evolution of the Outer Carpathian flysch units (Poland, Ukraine and Romania): Kinematics of a foreland/fold-and-thrust belt system, *Sediment. Geol.*, *86*, 177–201, doi:10.1016/0037-0738(93)90139-V.

Royden, L. H. (1993), Evolution of retreating subduction boundaries formed during continental collision, *Tectonics*, *12*(3), 629–638.

Samuel, O., and O. Fusan (1992), Reconstruction of subsidence and sedimentation of Central Carpathian Paleogene, *Zapadne Karpaty, Ser. Geol.*, *16*, 7–46.

Săndulescu, M. (1988), Cenozoic tectonic history of the Carpathians, in *The Pannonian Basin: A Study in Basin Evolution*, *AAPG Mem.*, vol. 35, edited by L. Royden and F. Horvath, pp. 17–25, American Association of Petroleum Geologists, Tulsa, Okla.

Santantonio, M. (1993), Facies associations and evolution of pelagic carbonate platform/basin systems: Examples from the Italian Jurassic, *Sedimentology*, *40*, 1039–1067, doi:10.1111/j.1365-3091.1993.tb01379.x.

Santantonio, M. (1994), Pelagic carbonate platform in the geologic record: Their classification, and sedimentary and paleotectonic evolution, *Am. Assoc. Pet. Geol. Bull.*, *78*, 122–141.

Schmid, S. M., D. Bernoulli, B. Fügenschuh, L. Matenco, S. Schefer, R. Schuster, M. Tischler, and K. Ustaszewski (2008), The Alpine-Carpathian-Dinaridic orogenic system: Correlation and evolution of tectonic units, *Swiss J. Geosci.*, *101*, 139–183, doi:10.1007/s00015-008-1247-3.

Semyrka, G. (2009), Vitrinite reflectance and types of kerogen in well sections in the eastern part of the Polish Carpathians, *Geologia*, *35*(2/1), 49–59.

Ślączka, A. (1971), Geology of the Dukla unit [in Polish with English summary], *Pr. Inst. Geol.*, *1*, 1–63, Polski Instytut Geologiczny, Warszawa.

Ślączka, A., S. Krugłov, J. Golonka, N. Oszczypko, and I. Popadyuk (2006), Geology and hydrocarbon resources of the Outer Carpathians, Poland, Slovakia, and Ukraine: General geology, in *The Carpathians and Their Foreland: Geology and Hydrocarbon Resources*, *AAPG Mem.*, vol. 84, edited by J. Golonka and F. J. Picha, pp. 221–258, American Association of Petroleum Geologists, Tulsa, Okla., doi:10.1306/985610M843070.

Śmigielski, M., F. M. Stuart, P. Krzywiec, C. Persano, H. D. Sinclair, K. Pisaniec, and K. Sobien (2012), Neogene exhumation of the Northern Carpathians revealed by low temperature thermochronology, *Geophys. Res. Abstr.*, *14*, EGU2012-12063.

Śmigielski, M., H. D. Sinclair, F. M. Stuart, C. Persano, and P. Krzywiec (2016), Exhumation history of the Tatry Mountains, Western Carpathians, constrained by low-temperature thermocrhronometry, *Tectonics*, *35*, 187–207, doi:10.1002/2015TC003855.

Sokołowski, S. (1973), Geology of Palaeogene and Mesozoic basement of the Podhale Trough southern limb in then column of the Zakopane deep borehole (in Polish with English summary),, *Biul. Inst. Geol.*, *265*, 5–103.

Soták, J. (1998a), Sequence stratigraphy approach to the Central Carpathian Paleogene (Eastern Slovakia): Eustasy and tectonics as controls of deep sea fan deposition, *Slovak Geol. Mag.*, *4*(3), 185–190.

Soták, J. (1998b), Central Carpathian Paleogene and its constrains, *Slovak Geol. Mag.*, *4*(3), 203–211.

Soták, J., D. Plašenka, J. Spišiak, and P. Uher (1993), Neptunian carbonate dykes hosted by basic volcanic rocks in the Považsky Inovec Mts.—Western Carpathians, *Miner. Slovaca*, *25*, 193–201 [In Slovak with English summary].

Soták, J., J. Spišiak, and A. Biroo (1994), Metamorphic sequences with Bündnerschiefer lithology in the pre-Neogene basement of the East Slovakian Basin, *Mitt. Österr. Geol. Gesell.*, pp. 111–120.

Soták, J., A. Vozárová, and J. Ivanická (1999), New microfossils from the early Paleozoic formations of Gemericum (Foraminiferida), *Geol. Carpathica*, *50*, 72–74.

Soták, J., A. Biroň, R. Prokešova, and J. Spišiak (2000), Detachment control od core complex exhumation and back-arc extension in the East Slovakian Basin, *Slovak Geol. Mag.*, *6*(2–3), 130–132.

Soták, J., M. Pereszlenyi, R. Marschalko, J. Milicka, and D. Starek (2001), Sedimentology and hydrocarbon habitat of the submarine-fan deposits of the Central Carpathian Paleogene Basin (NE Slovakia), *Mar. Pet. Geol.*, *18*, 87–114.

Sperner, B. (1996), *Computer Programs for the Kinematic Analysis of Brittle Deformation Structures and the Tertiary Evolution of the Western Carpathians (Slovakia)*, *Tubinger Geowiss. Arbeiten, A27*, pp. 1–81.

Sperner, B., L. Ratschbacher, and M. Nemčok (2002), Interplay between subduction retreat and lateral extrusion: Tectonics of the Western Carpathians, *Tectonics*, *21*(6), 1051, doi:10.1029/2001TC901028.

Spiegel, C., B. Kohn, D. Belton, Z. Berner, and A. Gleadow (2009), Apatite (U–Th–Sm)/He thermochronology of rapidly cooled samples: The effect of He implantation, *Earth Planet. Sci. Lett.*, *285*, 105–114, doi:10.1016/j.epsl.2009.05.045.

Stampfli, G. M., and C. Hochard (2009), Plate tectonics of the Alpine realm, in *Ancient Orogens and Modern Analogues*, edited by J. B. Murphy, J. D. Keppie, and A. J. Hynes, *Geol. Soc. London Spec. Publ.*, *327*, 89–111.

Stefaniuk, M. (2006), Some results of a new magnetotelluric survey in the area of the Polish Outer Carpathians, in *The Carpathians and Their Foreland: Geology and Hydrocarbon Resources*, *AAPG Mem*., vol. 84, edited by J. Golonka and F. J. Picha, pp. 707–716, American Association of Petroleum Geologists, Tulsa, Okla., doi:10.1306/985624M843081.

Struzik, A. A., M. Zattin, and R. Anczkiewicz (2002), Apatite fission track analyses from the Polish Western Carpathians, *Geolines*, *14*, 87–89.

Świdziński, H. (1948), Stratigraphical index of the Northern Flysch Carpathians, *Bull. Panstw. Inst. Geol.*, *37*, 1–128.

Szaniawski, R., M. Ludwiniak, and J. Rubinkiewicz (2012), Minor counterclockwise rotation of the Tatra Mountains (Central Western Carpathians) as derived from paleomagnetic results achieved in hematite-bearing Lower Triassic sandstones, *Tectonophysics*, *560–561*, 51–61, doi:10.1016/j.tecto.2012.06.027.

Szaniawski, R., S. Mazzoli, L. Jankowski, and M. Zattin (2013), No large-magnitude tectonic rotations of the Subsilesian Unit of the Outer Western Carpathians: Evidence from primary magnetization recorded in hematite-bearing Węglówka Marls (Senonian to Eocene), *J. Geodyn.*, *71*, 14–24, doi:10.1016/j.jog.2013.07.001.

Túnyi, I., and E. Marton (1996), Indications for large Tertiary rotation in the Carpathian-Northern Pannonian region outside the North Hungarian Paleogene Basin, *Geol. Carpathica*, *47*(1), 43–50.

Uchman, A. (2004), Tatry, ich skały osadowe i badania sedymentologiczne, in *Geologia Tatr: Ponadregionalny Kontekst Sedymentologiczny*, edited by M. Kędzierski, S. Leszczyński, and A. Uchman, pp. 5–21, VIII Krajowe Spotkanie Sedymentologów, Zakopane.

Uhlig, V. (1890), Ergebnisse geologischer Aufnahmen in den westgalizischen Karpathen: II. Th. Der pieninische Klippenzug, Jb. geol. B.-A., Bd. 40, H. 3–4.

Uhlig, V. (1907), LJberdie Tektonik der Karpa-then: Wien, *Acad. Wiss. Mater. Nat.*, *116*, 871–982.

Unrug, R. (1968), Kordyliera śląska jako obszar źródłowy materiału klastycznego piaskowców fliszowych Beskidu Śląskiego i Beskidu Wysokiego (Polskie Karpaty zachodnie), *Rocz. Pol. Tow. Geol.*, *38*(1), 81–164.

Ustaszewski, K., S. M. Schmid, B. Fügenschuh, M. Tischler, E. Kissling, and W. Spakman (2008), A map-view restoration of the Alpine–Carpathian–Dinaridic system for the Early Miocene, *Swiss J. Geosci.*, *101*(1), 273–294.

Vermeesch, P. (2009), RadialPlotter: A Java application for fission track, luminescence and other radial plots, *Radiat. Meas.*, *44*, 409–410, doi:10.1016/j.radmeas.2009.05.003.

Vermeesch, P., D. Seward, C. Latkoczy, M. Wipf, D. Guenther, and H. Baur (2007), Alpha-emitting mineral inclusions in apatite, their effect on (U-Th)/He ages, and how to reduce it, *Geochim. Cosmochim. Acta*, *71*, 1737–1746, doi:10.1016/j.gca.2006.09.020.

Voigt, S., et al. (2008), Cretaceous, in *The Geology of the Central Europe. II: Mesozoic and Cenozoic*, edited by T. McCann, pp. 923–998, Geological Society, London.

Vozárová, A., and J. Vozár (1988), *Late Paleozoic in Western Carpathians*, Geol. Ústav, Dionýza Śtúra, Bratislava.

Wagreich, M. (1995), Subduction tectonic erosion and Late Cretaceous subsidence along the northern Austroalpine margin (Eastern Alps, Austria), *Tectonophysics*, *242*, 63–78.

Wdowiarz, S. (1985), Some problems of the geological structure and oil/gas productivity of the Central Carpathian Synclinorium in Poland [in Polish], *Biul. Inst. Geol.*, *350*, 5–45.

Wdowiarz, S., T. Wieser, J. Szczurowska, and J. Morgiel (1974), Geological structure of the Skole Unit and basement in the column of the Cisowa IG-1 borehole (In Polish with English summary), *Biul. PIG*, *273*, 5–94.

Wójcika, A., P. Marciniec, and P. Nescieruk (2006), *Tokarnia IG-1*, *Profile Głębokich Otworów Wiertniczych* [in Polish], vol. 108, 58 pp., Państwowego Instytutu Geologicznego, Warsawa.

Wójcik-Tabol, P. (2003), Reflectance of disperced organic matter particles in shales of the Magierowa Member in the Pieniny Klippen Belt compared with clay crystallinity and isotopical data, *Miner. Soc. Pol. Spec. Pap.*, *22*, 236–239.

Wortel, M. J. R., and W. Spakman (2000), Subduction and slab detachment in the Mediterranean-Carpathian Region, *Science*, *290*, 1910, doi:10.1126/science.290.5498.1910.

Zattin, M., B. Andreucci, L. Jankowski, S. Mazzoli, and R. Szaniawski (2011), Neogene exhumation in the Outer Western Carpathians, *Terra Nova*, *00*, 1–9, doi:10.1111/j.1365-3121.2011.01011.x.

Zieliński, J. J. (1963), The discovery of buried flysch fold in yhe Region of Przemyśl [in Polish], *Rocz. PTG*, *33*, 387–397.

Zuchiewicz, W., and N. Oszczypko (2008), Topography of the Magura floor thrust and morphotectonics of the Outer West Carpathians, Poland, *Ann. Soc. Geol. Pol.*, *78*, 135–149.

Żytko, K. (1997), Electrical conductivity anomaly of the Northern Carpathians and the deep structure of the orogen, *Ann. Soc. Geol. Pol.*, *67*, 25–43.